

©Copyright 2016

Jeffrey A. Herron

Closed-Loop Deep Brain Stimulation:
Bidirectional Neuroprosthetics for Tremor and BCI

Jeffrey A. Herron

A dissertation
submitted in partial fulfillment of the
requirements for the degree of

Doctor of Philosophy

University of Washington

2016

Reading Committee:

Howard J. Chizeck, Chair

Andrew L. Ko

Jeffrey G. Ojemann

Program Authorized to Offer Degree:
Electrical Engineering

University of Washington

Abstract

Closed-Loop Deep Brain Stimulation:
Bidirectional Neuroprosthetics for Tremor and BCI

Jeffrey A. Herron

Chair of the Supervisory Committee:
Professor Howard J. Chizeck
Department of Electrical Engineering

Deep brain stimulation (DBS) has become a widely adopted method for treating a variety of neurological and movement disorders. However, current clinically deployed systems are open-loop and do not take into account the potentially intermittent nature of symptoms. By closing the loop with wearable sensors to directly sense symptoms such as tremor, we can determine not only when stimulation may be necessary but also estimate what intensity of stimulation should be used. By limiting stimulation to only the level needed, we can increase the battery life of the implanted devices and reduce exposure to unintended side-effects.

To accomplish this, I have developed a mobile and wireless platform for investigating closed-loop DBS applications in ambulatory patients. The platform consists of a set of worn sensors communicating over Bluetooth to a host application running on a smartphone or PC. By taking advantage of sensed data including inertial measurements, electromyography(EMG) and local field potentials, host applications built on my research platform are capable of performing digital signal processing and data fusion in order to make control decisions. These control decisions can include enabling or disabling stimulation or modifying individual stimulation parameters (voltage, pulse width, frequency) in response to changes in neurological symptoms. These control decisions are then sent over Bluetooth to a Medtronic Nexus system which relays packets and control decisions to an implanted Activa PC or PC+S

neurostimulator. By taking advantage of this real-time command link between the implanted device and the host application we can create a closed-loop DBS system for testing in human patients.

To test this research platform, I have performed vanguard experimental work to use these closed-loop systems with both Essential Tremor and Parkinson's Disease patients. In Essential Tremor patients, I have used wearable inertial and EMG sensors to suppress kinetic tremor as the patient repeatedly performed a task that produced tremor. Two control methods were used with a patient at the University of Washington, one using an inertial-based tremor estimate to manipulate the stimulation amplitude and the second used EMG to selectively determine when clinical stimulation should be delivered. Additionally, by making use of the sensed neural data available from the Aactiva PC+S, we have been able to prototype brain-computer interface(BCI) tasks to teach the patient how to use motor imagery to control a cursor. In Parkinson's patients, I have developed systems to suppress rest tremor using both an inertial sensor and the beta-band sensed from the patient's subthalamic nucleus. Both of these systems were tested at Stanford University. This work represent some of the first experiments using where wearable sensors or neural-sensed signals have been used in this way with a fully implanted neural interface.

As this project has moved forward it will allow for investigations into the clinical performance of long-term closed-loop deep brain stimulation and brain-computer interfaces. This future work will include developing system-identification experiments to develop models of symptom-stimulation relationships. This system modeling work will enable new patient-specific algorithms to be developed to improve the closed-loop DBS performance with either wearable sensor or neural sensing in the future. There is also a future opportunity to design a system that uses a BCI-triggered DBS algorithm to allow patients to use their BCI cursor control to manipulate their own stimulation level.

The significance of this work will be in improving DBS patient quality of life through

enabling DBS systems to provide selective therapeutic stimulation. This will allow implanted batteries to last longer or to be made smaller, and patients will only experience side-effects when they need their symptoms treated. The mobile systems I have developed will also be useful in expanding our understanding of neurological movement disorders treatable with DBS by providing consistent data collection and monitoring while patients continue their lives outside of the clinic or hospital. As these systems are clinically deployed, we anticipate that a large amount of valuable data will be obtained. This will facilitate dynamical modeling that will give new insight into the neurological basis of tremor and will expand the understanding of the underlying neural control problems that give rise to tremor disorders.

TABLE OF CONTENTS

| | Page |
|--|------|
| List of Figures | iii |
| Chapter 1: Introduction | 1 |
| 1.1 Specific Research Aims | 4 |
| 1.2 Document Outline | 6 |
| Chapter 2: Clinical DBS Overview | 8 |
| 2.1 History of DBS | 8 |
| 2.2 System Overview | 9 |
| 2.3 Current clinical usage | 9 |
| 2.4 DBS for Essential Tremor | 10 |
| 2.5 DBS for Parkinson’s Disease | 13 |
| Chapter 3: Closed-Loop DBS Overview | 16 |
| 3.1 Open Loop versus Closed Loop | 16 |
| 3.2 Components of a Closed-Loop System | 17 |
| 3.3 Prior Closed-Loop DBS Work | 23 |
| Chapter 4: Interfacing with Implantable Neurostimulators | 25 |
| 4.1 Foundational Code Development: The Nexus C# DLL | 26 |
| 4.2 Modified for mobile use: the Nexus-D Extension | 32 |
| 4.3 Closed-Loop System Framework for System Integration | 38 |
| Chapter 5: Sensing Tremor | 41 |
| 5.1 Inertial Sensing | 42 |
| 5.2 Electromyographic Sensing | 45 |
| 5.3 Neural Signals | 48 |

| | |
|--|-----|
| Chapter 6: Control Paradigms | 52 |
| 6.1 When to Take Action: Direct and Indirect Markers | 52 |
| 6.2 How to Take Action: Static and Dynamic Stimulation | 54 |
| 6.3 The Patient’s Role: Non-Volitional and Volitional Systems | 56 |
| 6.4 Comparing Algorithms: Performance Metrics | 58 |
| Chapter 7: Closed-Loop DBS Prototypes | 61 |
| 7.1 On-line Movement Intentions for Real-Time Stimulation | 62 |
| 7.2 Real-Time Activa PC+S Sensing and Stim Validation | 68 |
| Chapter 8: Wearable Closed-Loop DBS | 72 |
| 8.1 PD CLDBS with Wearables | 72 |
| 8.2 ET CLDBS with Wearables | 89 |
| 8.3 Future Work: Improving Closed-Loop Performance | 96 |
| Chapter 9: Chronic Neural Sensing and Brain Computer Interfaces | 99 |
| 9.1 Sensing of Movement and Intention | 100 |
| 9.2 Constant Velocity Cursor Task | 105 |
| 9.3 Future Work: Improving BCI Performance | 111 |
| Chapter 10: Bidirectional Neuroprosthetics | 112 |
| 10.1 Beta-Modulated Stimulation in PD Patients | 113 |
| 10.2 Future Work: Cortical Sensing for Essential Tremor Patients | 117 |
| Chapter 11: Conclusion | 121 |
| 11.1 Significance of this Work | 123 |
| 11.2 The Importance of Neural Security and Privacy | 124 |
| 11.3 The Role of Ethics in Closed-Loop DBS Design | 126 |
| 11.4 Final Thoughts | 129 |
| Bibliography | 131 |

LIST OF FIGURES

| Figure Number | Page |
|---|------|
| 2.1 Deep Brain Stimulation System | 8 |
| 3.1 A Generic CLDBS System | 17 |
| 4.1 Aactiva PC+S | 25 |
| 4.2 Nexus-D Block Diagram | 26 |
| 4.3 Nexus C# Architecture | 28 |
| 4.4 NexDEx Block Diagram | 33 |
| 4.5 NexDEx Hardware | 34 |
| 4.6 NexDEx Firmware | 35 |
| 4.7 Closed-Loop System Framework | 39 |
| 5.1 IMU Watches | 43 |
| 5.2 PD Inertial Sensing | 44 |
| 5.3 PD Spectral Analysis | 45 |
| 5.4 PD Forearm EMG | 46 |
| 5.5 EMG Armband | 47 |
| 5.6 EMG Front End Housing | 47 |
| 5.7 PD Inertial and LFP | 49 |
| 5.8 PD LFP Bandpower | 50 |
| 6.1 Wired Demo: Wrist IMU | 55 |
| 6.2 Wired Demo: EMG | 56 |
| 7.1 Generic Closed-loop DBS | 61 |
| 7.2 EEG Experimental Setup | 64 |
| 7.3 EEG Electrode Positions | 65 |
| 7.4 EEG Results | 66 |
| 7.5 Wired Prototype | 69 |
| 7.6 Wired Demo: Neurostimulator Electrode Signals | 70 |

| | | |
|------|--|-----|
| 8.1 | Deep Brain Stimulation System | 72 |
| 8.2 | Basic Structure of a wearable CLDBS System | 74 |
| 8.3 | Threshold Overview | 75 |
| 8.4 | Baseline Overview | 77 |
| 8.5 | Experiment Application | 78 |
| 8.6 | Trial RHand | 82 |
| 8.7 | Trial LHand | 83 |
| 8.8 | Baseline Trial 1 | 84 |
| 8.9 | Baseline Trial 2 | 85 |
| 8.10 | Prompting PSD Results | 94 |
| 9.1 | BCI with a DBS | 99 |
| 9.2 | Prompting Time-Domain Results | 101 |
| 9.3 | Prompting PSD Results | 102 |
| 9.4 | PSD Over Time | 103 |
| 9.5 | BCI Task Overview | 105 |
| 9.6 | Unity Based BCI System | 106 |
| 9.7 | Overt Task Results | 108 |
| 9.8 | Imagined Task Trial 1 | 109 |
| 9.9 | Imagined Task Results | 110 |
| 10.1 | PD Neuro-CLDBS Results | 115 |

ACKNOWLEDGMENTS

The dissertation that follows is the result of years of work and at this point in my thesis, I would like to thank those who have helped me along the way. This thesis would not have been possible without the support and help from many people, and I will be forever thankful for their aid.

Firstly, my deepest gratitude goes to my wife Tami who has put up with all of my PhD-related stress and responded with nothing but patience and care. Her support as I transitioned back into academia to pursue my PhD has enabled all of the work in this thesis.

Additionally, I have been supported by many family and friends who I would like to thank. This includes my parents Andrew and Jennifer Herron, my sisters Jessica and Sarah, and my grandparents Donald Moore, Patsy Moore, James Herron, and Kathy Herron. I would also like to thank and acknowledge the impact of Tom Blank who has been a key mentor in my early career and encouraged my return to graduate school.

I would like to acknowledge and thank my advisor Howard Chizeck for all of the guidance he has given me on this project. Thank you to all members of the UW BioRobotics Laboratory. In particular, Tamara Bonaci deserves many thanks for her constant advice and guidance while navigating grad school.

I would also like to thank the various students, graduate and undergraduate, that have directly collaborated with me on various aspects of this project including Margaret Thomp-

son, Tim Brown, Brady Houston, Andrew Haddock, and Katherine Pratt. Students who I have mentored as they work on parts of the research covered by this document include Emma Vidarsson, Alan E Casallas, Francisco Garcia, and Paula Cieszkiewicz. Another thank you to all of my faculty mentors and student peers within the NSF Engineering Research Center for Sensorimotor Neural Engineering.

I would like to thank and acknowledge our clinical collaborators for the ongoing work we are doing. Special credit goes to our UW clinical team Andrew Ko and Jeff Ojemann. I would also like to thank our clinical collaborators at Stanford including Helen Bronte-Stewart, Anca Velisar, Mahsa Malekmohammadi, and Zack Blumenfeld.

I'd also like to give many thanks to Tim Dennison of Medtronic for his ongoing support of this project and my research. He has been a great mentor and one I hope to stay in close contact with in the future. Many thanks also goes out to Duane Bourget, also from Medtronic, for all of his technical support while I was developing code for the Nexus-D and Activa PC+S.

Finally, I need to acknowledge the financial support that has helped me along the way. This work has been supported by a donation from Medtronic and by Award Number EEC-1028725 from the National Science Foundation for the Center for Sensorimotor Neural Engineering. The content of this thesis is solely my responsibility does not necessarily represent the official views of the National Science Foundation or Medtronic.

DEDICATION

to the love of my life, Tami

Chapter 1

INTRODUCTION

Neurological movement disorders are among some of the most debilitating diseases that have a dramatic effect on the quality of life of patients. While medication can be used for treatment for a time, often as the disease progresses these treatments become ineffective at suppressing symptoms. Over the last decade, deep brain stimulation (DBS) has rapidly become one of the most important tools in the treatment of medication-resistant neurological disorders. DBS has proven to be a safe and effective clinical method of treating Parkinson's disease [1], Essential Tremor [2] [3], and Dystonia [4]. When pharmacological methods are not sufficient to dampen the worsening symptoms in these progressive neurological movement disorders, DBS is used as a last resort despite the fact that it requires brain surgery [5]. A DBS system delivers therapy by electrical stimulation of target locations in the brain far enough below the surface that a depth electrode is required. Current DBS systems consist of implanted electrodes in the brain connected to an implanted neurostimulator in the chest through a wire routed under the skin down the neck. The exact location of the implanted electrodes determines which neurological disorders can be treated. This includes movement disorder symptoms such as tremor, but DBS has also been shown to potentially help treat non-motor disorders such as chronic pain [6].

While these "brain pacemakers" can have a dramatic positive impact on the symptoms of patients with neurological disorders, there is still considerable room for improvement in current clinically deployed systems. For instance, the stimulation of brain tissue can cause a variety of unintended side effects, for example some patients experience difficulty while speaking [7]. Another consideration is that the power requirements of the stimulation are

the largest factor in the decreased overall expected lifetime of the device. This is important due to the fact that surgery is required for battery replacement. A more clinical concern is how there is considerable difficulty for the clinician in selection of stimulation parameters [7]. A clinician programming a deep brain stimulator needs to manually minimize power usage and severity of any side-effects while also maximizing tremor suppression. Furthermore, even when the correct parameters are chosen, many neurological movement disorders are very intermittent and constant stimulation is not needed.

This gets to the heart of the most pressing issue with current deep brain stimulation: modern DBS systems do not take into account the intermittent and variable nature of neurological movement disorders [8]. Instead these systems simply stimulate deep brain structures at a constant level and consistent rate. This open-loop approach is fundamentally in conflict with the closed-loop nature of the nervous system where sensory feedback plays a major role in performing every action and movement.

The solution to addressing these shortcomings of DBS is to create a feedback loop where stimulation parameters are adjusted based on the severity of symptoms that a patient is experiencing at a given moment. This requires the development and exploration of various sensors and control algorithms that can measure, identify, and act upon the various symptom states. It also requires wearable systems with the ability to communicate and update stimulation parameters in an implanted neurostimulator. Developing closed-loop methods for DBS leads to two questions: first how do we engineer the systems I have described, and second how can we experimentally validate the designed systems?

There are several important design requirements of such a system to consider while designing prototype experimental platforms. The most basic requirement includes the ability to detect or predict the onset tremor. This detection or prediction must be done in such a way as to reduce potential burden on the patient and needs to be localized specifically to the tremoring region of the body. Secondly, the system needs the ability to respond with stimulation within strict time limits. This requires real-time telemetry links between computational elements and implantable hardware. Finally, appropriate stimulation patterns

need to be utilized that will effectively treat the incipient tremor, including stimulation-on-ramping which aids in avoiding undesirable side-effects.

The platform that I have built is prototype mobile system for future studies in ambulatory patients that leverages an investigational implant built by an industrial collaborator. The system utilizes the Medtronic Activa PC+S, an implantable deep brain neurostimulator that can perform simultaneous sensing and stimulation from the implanted electrodes [9]. The Activa PC+S sense neural signals using either a traditional DBS electrodes or a cortical strip for surface electrocorticography (ECoG). Using the Activa PC+S is a shortcut to chronic implants in our patients with a straightforward regulatory process to follow in the form of an FDA Investigational Device Exemption (IDE). This has allowed us to demonstrate a closed-loop DBS system capable of utilizing sensed data from worn sensor systems and the implanted electrodes to update stimulation parameters in response to changes in the symptoms experienced by patients.

To test closed-loop systems built upon this platform, I am working closely with neurosurgeons and neurologists to improving the treatment of Essential Tremor (ET) and Parkinson's disease (PD). While the current understanding of the mechanisms that cause these disorders and the symptoms they generate is still quite limited, they both have distinctive physical symptoms that can be observed through wearable sensors [10] [11]. This makes them a plausible disorders to target for initial closed-loop DBS investigations due to the variety of sensors that can be used to close the loop. These sensors can include measuring limb kinematics through inertial sensors, muscle activity through surface electromyography (EMG), or neural signals from the implanted electrodes themselves. Furthermore, the experienced symptoms are often intermittent and can change in intensity from moment to moment due to a wide array of physiological or environmental factors [5]. A future closed-loop DBS system would limit the output stimulation to only the time and level needed by either measuring the current symptom intensity or by a biosignal that predicts symptoms. This is expected to give patient benefits by both increasing the device's lifetime through lowering power usage and also limiting patient exposure to side-effects.

By including neural-sensing components into the real-time experimental environment, we may discover that triggering stimulation based off of a neural signal may be advantageous as well. This would have the advantage of potentially being a system that could be embedded in a future device without the need of communication to external devices. Alternatively, the neural signals we can stream from our implanted Aactiva PC+S may allow for the testing of a chronic brain-computer interface (BCI). A fully implanted BCI system has the advantage of being able to do long term invasive sensing without risk of either the electrodes shifting or additional infection.

Given that the field of closed-loop DBS systems is so new, and the breadth of the possible research projects is large, I have selected three aims to focus on for this thesis. Firstly, I will demonstrate closed-loop DBS using wearable sensors. Secondly, I will use an investigational neuromodulation implant with the ability to sense neural data to perform experiments to evaluate the device for future BCI and closed-loop DBS opportunities with a chronic platform. Finally, I will use neural signals from the implant to close the loop for neural-triggered DBS. These three aims are covered in detail in the next section.

1.1 Specific Research Aims

1.1.1 Aim 1: Demonstrate Closed-Loop DBS using Wearable Sensors

Closed-loop deep brain stimulation can potentially be enabled by utilizing external wearable sensors and/or readings directly from the cortex. I hypothesize that by applying closed-loop control paradigms to essential tremor and Parkinson’s patients we can lower the average power of the stimulation while maintaining the same level of tremor mitigation as well as reducing the side-effects that the patient experiences.

Initially, worn sensors will be used to titrate when therapy is required and the electrical stimulation will be turned on and off as needed. This will be done both by monitoring the amount of tremor the patient is actually experiencing as well as attempting to stop tremor before it physically manifests by determining when they are making movements that may

result in tremor. Next, stimulation parameters will be dynamically adjusted in response to the sensed tremor. In this case, tremor characteristics (such as amplitude or tremor frequency) will be dynamically mapped to stimulation parameters such as amplitude, pulse width and stimulation frequency.

Using data collected from these trials, I will compare how algorithms perform across different patients and symptoms. By investigating how variable symptom responses are to a closed-loop system, it may be possible to determine how we should focus future efforts to improve closed-loop systems. If these systems result in highly variable responses across patients, it may be that more patient-specific methods will be required in the future. However, this work will require an investigation into quantifying closed-loop algorithm performance. For this, we will evaluate our systems based upon both symptom suppression efficiency and stimulation power efficiency.

1.1.2 Aim 2: Demonstrate Chronic Neural Sensing and BCI

The closed-loop system platform used in the first aim will then be used to investigate the neural signals we can collect from our patients. Additionally, we will demonstrate fully implanted BCI control of a computer cursor using this chronic interface. This will provide a platform for long-term studies for investigating a patient's ability to learn novel BCI tasks without risk of electrodes shifting or infection. Furthermore, this platform can be used to test how well patients can learn to use their deep brain electrical signals for BCI over longer time frames than current ECoG studies allow.

This will be done by leveraging the neural sensing capabilities of the Activa PC+S. Characteristics of the signals will be mapped to a one-dimensional cursor task. Demonstrating effective patient control of will be done by monitoring the time to completion of the tasks which will lend itself to future Fitzian-styled proficiency investigations. Furthermore, this platform will enable long-term learning studies on how a patient modulating their brain signals to generate commands performs these tasks over the course of many months or years.

1.1.3 Aim 3: Demonstrate and evaluate a near-term bidirectional neuroprosthetic

I will also utilize the sensed neurological data from the Aactiva PC+S implanted electrodes to modulate therapeutic stimulation parameters in real time. This will be first done as a means of incipient tremor intervention to eliminate tremor before it ever physically manifests. To stop incipient tremor we will investigate using both deep brain neural signals that may be related to tremor and cortical electrodes that indicate a subject's intent to move. These tremor and movement markers will then be used to trigger or modify stimulation parameters to improve the power-efficiency and reduce treatment side-effects.

1.2 Document Outline

The next chapter will cover the current state of the art of current open-loop DBS practices. In particular, I will focus on the treatment of Parkinson's Disease and Essential Tremor. Following that will be an overview of closed-loop DBS and the prior work in the field.

Chapters Four through Seven cover the engineering and system integration needed before beginning human experiments. These chapters will explore the hardware, firmware, and software algorithms that I have developed while also defining different classes of closed-loop DBS systems that need to be considered. Results from testing the various systems that have been prototyped and tested on the bench-top are presented as proof of concepts before human trials.

Chapters Eight through Ten are where I present the results of human testing with these closed-loop systems in order to fulfill the research aims of this thesis. The chapters are ordered by aim, with wearable closed-loop DBS results being presented first, neural sensing and BCI will be presented second, and chapter ten will cover bidirectional neuroprosthetics in the form of neural-triggered DBS stimulation. Given the preliminary nature of these results, each chapter will also have a future work section detailing my view of the next steps to push the research even farther.

The final chapter is where I will review the research that has been presented and discuss

non-technical aspects of the research. In particular, I will present ethical and security considerations that my work raises which will be an important avenue for further research in the future.

Chapter 2

CLINICAL STATE OF THE ART: DEEP BRAIN STIMULATION FOR NEUROLOGICAL DISORDERS

2.1 *History of DBS*

Electrical stimulation of the brain has a long history and it has played an instrumental role in the mapping of the brain and brain functions. Electrical stimulation of neural tissue was used to identify various brain structures deep within the brain and it was not long before the tremor-mitigating effect of high-frequency stimulation was discovered [6]. However, it is only relatively recently that this has translated into a method for treating chronic conditions. In the early 1990s, neuroscientists were finally able to demonstrate the long-term benefit of deep brain stimulation (DBS) for the treatment of tremor for essential tremor and Parkinson's disease patients [12]. Since that time, deep brain stimulation has been shown to be an effective and highly beneficial treatment for patients that exhibit a wide variety of neurological disorders. DBS has not only had tremendous success in the treatment of neurological movement disorders such as Essential Tremor (ET), dystonia, and Parkinson's disease (PD) but has also been shown to aid in the treatment of Tourette syndrome, pain, and depression [6]. There has even been studies into applying DBS to aid in the treatment of addiction, obesity, dementia, and stroke recovery [13]. For our work, we have focused on building closed-loop DBS proof of concepts for

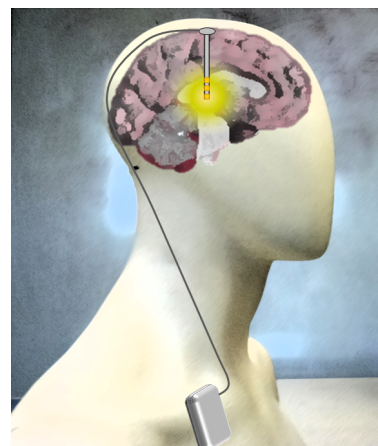


Figure 2.1: An implanted deep brain stimulation system

two common neurological movement disorders: Essential Tremor and Parkinson’s Disease, but first I will review DBS in general before looking at how DBS is used in ET and PD specifically.

2.2 System Overview

Deep brain stimulation systems consist of one or two electrode leads placed deep in the brain connected to an implanted pulse generator (IPG) placed subcutaneously in the upper torso of a patient. The leads can be placed in a large variety of locations to electrically stimulate different structures deep within the brain. The pulse generator in the torso houses the system’s controller, battery, and communication channel to external programming devices. After the system is implanted, the device’s stimulation parameters are configured in a follow up visit where a clinician explores how the various parameters modify treatment and side-effects.

2.3 Current clinical usage

Due to the invasive nature of brain surgery, deep brain stimulation is often used as a last resort when all other treatment options fail [3]. DBS implanted pulse generators (IPGs) are implanted underneath the clavicle, similar to a cardiac pacemaker, with wires routed up the neck under the skin to the surface of the skull where the leads are then implanted into the brain [13]. Some common targets include the ventral intermediate (VIM) nucleus of the thalamus for essential tremor [12] [14], the globus pallidus for dystonia [4], or subthalamic nucleus for Parkinson’s disease [1]. This allows the entire system to be fully under the skin barrier which reduces the risk of long-term infections.

2.3.1 Parameter Tuning

After implantation, there are a series of clinical visits to enable the DBS therapy and select stimulation parameters. Currently however, this parameter tuning is still an ”ad hoc empirical process” where clinicians attempt to choose stimulation amplitude, pulse-width and

frequency to effectively mitigate tremor by trial and error which frequently leads to patients experiencing side effects or not realizing the full benefit of the DBS therapy [7].

This can be a difficult process and clinicians sometimes have to reduce treatment effectiveness to bring unintended side-effects to acceptable levels. Clinicians also must consider average power usage while choosing stimulation parameters. Most clinical DBS systems are not rechargeable and must be replaced when the battery runs out. The lifetime of these devices is not only dependent on the implanted battery size but also the stimulation parameters selected. This leads to a highly variable battery life when comparing across different patients. For example, with the Medtronic Activa PC the battery life can be anywhere from 11 years to just several months [15].

2.3.2 Potential Side-effects

A wide variety of side-effects can be experienced by patients, which is perhaps unsurprising when one considers the wide variety of sensory and muscle commands relayed through the deep brain. Common unintended side-effects can include paresthesias (burning or tingling sensations), trouble speaking, or even eye closure [7]. The intensity and location of these side-effects can and will vary with stimulation parameters, so a clinician can try to tune the system to reduce them and preserve treatment effectiveness.

2.4 DBS for Essential Tremor

Essential tremor is characterized by an uncontrollable rhythmic motion due to oscillatory muscle contractions [16]. While tremor symptoms are often first observed localized to a single limb or part of the body, the progressive nature of this neurological disorder often results in the tremor slowly spreading and growing in amplitude with time [5]. Most commonly, it manifests as a high amplitude 4-12Hz oscillatory disturbance whenever a patient attempts to use an effected limb [14]. Essential tremor is the most common neurological movement disorder within the United States with more than 5 million Americans affected [17]. Furthermore, it has been estimated that essential tremor develops in .4% to 3.9% of the general

population [18]. The disorder is far more common in the elderly population, with an estimated incidence of at least 13% for those over the age of 60 [18]. While essential tremor was considered a benign disorder in the past, the potential impact on a patient's daily of life has changed the characterization of this disorder. Not only do essential tremor patients have a much harder time completing everyday tasks, but they are also at a heightened risk of tripping since tremor has been correlated to an increased likelihood of missteps while walking [17]. For the elderly population affected by this disorder, trips and falls pose a real danger to their long-term ability to stay mobile and healthy.

Essential Tremor: Symptoms and Diagnosis

There are several types of tremor that can arise in a patient with essential tremor. These are rest, postural, intention, and kinetic tremors [16]. The most commonly diagnosed form is kinetic tremor, which corresponds to uncontrollable tremors whenever a patient performs voluntary movement with the effected limb or body part. However, it is also common for the other forms of tremor to arise as the disease progresses and worsens. Rest tremor occurs while the arm is at rest and not actively being used. This form of tremor is more commonly associated with Parkinson's disease, but can arise in essential tremor patients as well. Postural tremor is triggered when holding a limb against the force of gravity, such as when one is holding a hand out in front to shake hands. Finally, intention tremor is characterized by patients experiencing tremors when they are performing a visually guided task, such as pointing to something they can see.

Diagnosing essential tremor can be difficult due to the multitude of other movement disorders that exhibit similar symptoms. For instance, somewhere between 30-50% of patients are initially misdiagnosed with a different movement disorder such as Parkinsons disease, hyperthyroidism, or dystonia [16]. However, skilled clinicians are able to precisely diagnose and characterize essential tremor utilizing EMG and accelerometers strapped to the affected body part [5]. Examining periods of significant coherence between the EMG and accelerometry ensures that the measurements of movement are due to the extensors and flexors activating

periodically out of phase due to tremor and not due to some outside influence [14].

Essential Tremor: Mechanism

The causes of essential tremor are still poorly understood. While genetic causes have been implicated through studies on twins [19] others have pointed to a variety of environmental causes that may explain how tremor arises in patients [20]. Regardless of the specific cause, it seems that the symptoms are due to the emergence of one or more neural oscillatory circuits [21]. The possibility of multiple oscillators potentially arising is due to the fact that tremors across different parts of the body often are not coherent [22]. Even the location where these oscillators arise is currently under debate, but the brainstem, thalamus and cerebellum have been identified as strong candidates [23] [24].

Essential Tremor: Pharmaceutical Treatment

Being a progressive disorder with no cure, treating essential tremor focuses almost entirely on lessing symptoms. In the early stages of the progressive disorder, tremor is commonly treated solely with pharmaceutical medication. Treatment often starts with propranolol which improves tremor in two thirds of patients and usually reduces the experienced tremor accelerations by 50% [5]. However, after two years only a quarter of patients still respond well to this treatment. It is not uncommon for essential tremor patients to proceed through a gauntlet of other drugs with varying levels of effectiveness and side-effects such as primidone, nadolol, gabapentin or others [16]. Common side-effects from these pharmacological agents can include anything from fatigue, nausea, dizziness, or even confusion. Furthermore, it is estimated that pharmaceutical treatment will be eventually ineffective for between 25-55% of essential tremor patients [25].

Essential Tremor: Surgical Treatment

While surgical methods are reserved only for those patients who have medication-resistant tremor, surgical methods are a highly effective treatment and result in between 75-100% suppression of tremor in 70-90% of patients [5]. There are two surgical methods that are used for these cases of otherwise untreatable tremor, both of which target the ventral intermediate (VIM) nucleus of the thalamus. The first of these surgical methods is a thalamotomy: a surgical lesioning of the VIM thalamic nucleus. However, the removal or destruction of tissue from the brain is by definition permanent and there is a significant incidence of long-term side-effects associated with the procedure [26]. The second surgical therapy is thalamic stimulation using a chronically-implanted deep brain neurostimulator. While a more complicated and expensive procedure, DBS has become the far more attractive surgical treatment due to the reduced number of adverse events and because the stimulator settings can be periodically tuned and modified after implantation by clinicians [5] [25]. Similar to how the exact mechanisms and causes of essential tremor are poorly understood, the mechanism by which DBS treats tremor is also unclear. Interestingly, DBS not only suppresses the magnitude of the tremor, but modifies the frequency peak as well [14]. This potentially suggests a more complicated mechanism than simply suppressing a neural oscillator circuit. Regardless, the fact remains that DBS has a dramatic improvement in tremor symptoms for many essential tremor patients [12].

2.5 DBS for Parkinson's Disease

Like essential tremor, Parkinson's disease (PD) is also a progressive neurological disorder that results in a physically manifested tremor. However patients with Parkinson's disease are differentiated by exhibiting rigidity (a resistance to movement), postural instability and bradykinesia (slowness while executing movements) [27]. Due to difficulty of diagnosing PD it is difficult to determine the overall prevalence of the disease, but at least 0.3% of the overall population (and 1% of those over 60) or 6.3 million adults have been estimated to

be affected by PD [28] [29]. The incidence rate of PD is significantly higher for patients over the age of 60 and only 4% of new cases affect those under 50 [30]. Furthermore, the incidence rate seems to be 91% higher for men than women (19 per 100,000 versus 9.9 per 100,000) [30]. The disease is highly debilitating and patients report a definitive lower quality of life than the general population [31].

2.5.1 Parkinson's Disease: Symptoms and Diagnosis

While essential tremor patients most commonly experience tremor during volitional movement, PD is characterized instead by a rest tremor between 4-6Hz [32]. Parkinson's disease is also often accompanied by gait impairment, freezing during motor tasks and speech problems. Other forms of tremor (such as kinetic, intention or postural) may also be observed. Non-motor symptoms such as cognitive decay or depression are also common [33]. There is no definitive diagnostic test for PD, clinical diagnosis is based on the presence of the four "cardinal" motor features (rest tremor, rigidity, postural instability and bradykinesia) and how the patient responds to levodopa [32]. In fact, currently the only way to definitively confirm the presence of Parkinson's disease is during patient autopsy [28].

2.5.2 Parkinson's Disease: Mechanism

The primary cause of symptoms in Parkinson's disease has been identified to be the death of neurons in the substantia nigra pars compacta (SNpc) [34]. These neurons are known to be instrumental in the brain's dopamine system and their loss leads to a substantial dopamine deficiency. This dopamine deficiency is responsible for all of the major symptoms present in Parkinson's patients [34].

2.5.3 Parkinson's Disease: Pharmaceutical Treatment

No drug has had a more dramatic effect on the treatment of PD than levodopa. Levodopa produces a dramatic reduction in PD symptoms by being able to directly act upon dopamine

receptors due to a chemical similarity to dopamine [35]. However, in long term care levodopa is known to cause dyskinesia, which in extreme cases can outweigh any benefit given by the drug [36]. Within the first five years of treatment with levodopa, approximately 40% of PD patients will experience dyskinesias related to levodopa therapy, although this number varies with age of onset [37]. These dyskinesias are unpredictable and can often include loss of mobility or involuntary movements [35] [36].

Other than levodopa, there are a series of other synthetic dopamine agonists that can be used in the treatment of PD [35]. However, in the early treatment of PD, before dyskinesia onset, no other drug rivals the effectiveness of levodopa [36]. Unfortunately, nothing can stop the progression of the disease and as the symptoms worsen dosages are continually ramped up in an attempt to manage the disease.

2.5.4 Parkinson's Disease: Surgical Treatment

The two approaches to the surgical treatment of Parkinson's disease consist of surgical lesioning or deep brain stimulation. However, due to common and often irreversible complications, surgical lesioning has become a rare practice in the current treatment of Parkinson's disease [38]. The surgical sites for DBS electrode implantation for PD often target the ventral intermediate nucleus of the thalamus (VIM), the subthalamic nucleus (STN) and the internal globus pallidus (GPi) [39]. While VIM stimulation is known to be effective at treating all tremors (and is the site used in essential tremor), STN and GPi stimulation have been shown to aid in the treatment of other motor symptoms present in PD patients and have become the most common sites used for treatment [13]. While STN stimulation has been shown to be more effective than medication alone [1], GPi stimulation is an important alternative for patients with PD-related speech or cognitive symptoms [13]. DBS also allows for a more consistent level of treatment when compared to levodopa [6], which loses effectiveness between doses due to being absorbed [36].

Chapter 3

CLOSED-LOOP DBS OVERVIEW

In this chapter, I review open-loop and closed-loop systems in regards to neuromodulation platforms. Definitions and descriptions of various system components are over-viewed, and prior closed-loop DBS work is referenced and discussed. This chapter is to clearly define the scope and terminology used in the upcoming chapters that discuss specific methods for closed-loop DBS system development.

3.1 Open Loop versus Closed Loop

As discussed earlier in this document, currently clinical neurostimulators are considered *open-loop* systems. This means that the parameters of these systems are set to a pre-determined level and left at a static setting while delivering therapy. Many of the current shortcomings of DBS therapy come from the open-loop nature of current clinical devices [8]. For instance, in the cases of the disorders with intermittent symptoms, such as those we have discussed so far, patients are subjected to constant stimulation regardless if the patient is actually experiencing tremor or bradykinesia.

Closing the loop refers to a system that uses sensors to determine when and how to take action. In this case, closed-loop systems will use sensors to estimate symptom severity and decide what level of stimulation is needed at a given time, resulting in less power being used and reduced exposure to side-effects. For a patient that needs DBS to treat tremor, an example of such a sensor may include a smartwatch that can track when a patients limb tremors. This watch could then communicate with the neurostimulator to start, stop, or modify stimulation parameters in response to a patients tremor. The stimulation would then change in such a way as to reduce the patients tremor as needed. This interaction

between sensor, actuator, and patient is referred as a closed-loop system due to the fact that each system is directly interacting with the other components as to reduce the undesirable symptom. When closing the loop for a system, one can expect that the system will act more efficiently and effectively. The desire to close the loop for neural stimulation systems is to make implantable devices more power efficient so the battery does not run out as fast and for improved effectiveness in treating neurological disorders.

3.2 Components of a Closed-Loop System

We have based our system design on a generic closed-loop DBS system shown in Figure 3.1. Current implanted systems only make use of an open-loop device providing stimulation to the brain of a patient to provide treatment. In our work, physiological sensors of symptoms are used to determine when and how this treatment is provided. The mapping of sensed data to stimulation parameter changes, in our case worn inertial measurements mapped to voltage amplitude settings, is handled by extracting symptom biomarkers through signal processing and using a configurable control algorithm to determine new settings.

We can split up this diagram into three separate external components that are required for

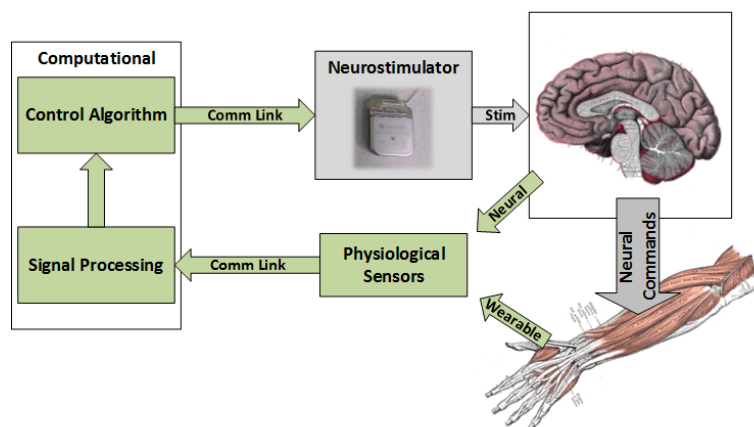


Figure 3.1: A generic closed-loop DBS system.

closed-loop therapy. First, there is the deep brain stimulator and implanted electrodes, which are the system's actuator, which provides the therapeutic electrical stimulation. Second, sensors are required to collect data related to a patient's symptoms. In our case, we are considering two classes of sensors: worn devices on an affected limb and neural recordings of signals from the brain. Finally, signal processing and control algorithms are required to map raw sensed data to an appropriate response for the actuator to take.

3.2.1 Actuators: Implantable Neurostimulators

In the systems I will be discussing in this thesis, the actuator is exclusively a deep brain stimulator. Implantable DBS systems often have several tunable parameters that clinicians use when programming the devices to ensure effective therapy. Electrical stimulation can be configured to either occur between several electrodes in a bipolar configuration or between a single electrode and the implanted device's case in what is considered a monopolar configuration. When determining the shape of a regular stimulation wave form the minimum parameters required to be specified are amplitude, pulse width, and frequency. Stimulation amplitude can be in either voltage or current depending on the device or setup. Stimulation pulses are most commonly biphasic to ensure a zero sum-total current through the electrodes. This helps to negate or slow the corrosion of the electrodes due to ionic chemical reactions on the surface of the electrode due to the currents involved with stimulation. All three parameters can have effects on the patient's treatment and side-effects, and as discussed earlier, the sheer breadth of the control parameter space present a difficult problem for clinicians to work through to find an optimal treatment.

In our work a clinician will determine, through current standard programming techniques, the electrode configuration and a set of waveform parameters that meet a clinical standard of care for a given indication. Then the clinician will identify a safe range for a specific waveform parameter that we can freely modulate in using an automated system. This safe parameter space is programmed into the device separately and can not be overwritten without using the clinical programmer. This will provide our closed-loop systems a base standard of care

that we can compare our performance against and many of the concerns for patient safety are mitigated by the clinician's involvement in programming hard-coded safety limits into the device separately.

An additional important sub-component of the implanted neurostimulator is the need for a transcutaneous communication link between external components and the implanted device. The closed loop systems proposed in this work are not possible without a real-time link that can change stimulation parameters in response to sensed neurological symptoms. One important consideration for this communication link is the total data to be transmitted between the implanted device and the external communication unit. Transmitting data from the implant to the outside world is "expensive" due to the power cost to the implanted battery. This is less of an issue for rechargeable implants, due to the lack of surgery required to change the battery, but it may dramatically impact how long the patient can go between battery charges. Since batteries can easily be changed for external devices, it is less of a concern about the power cost of transmitting data into the implant.

3.2.2 Sensors: Wearable and Invasive Sensing

Closed loop DBS systems require sensors to monitor the patient for signs that correspond to symptoms of the neurological disorders being treated. The sensors I am interested in investigating for these closed-loop systems fall into two categories: wearable and invasive neural sensing. An example of wearable sensors could be worn watches with inertial sensing to monitor the presence of tremor. Invasive neural sensing would make use of data recorded from implanted electrodes either from the surface of the brain or from the deep brain stimulation recording sites.

Wearable sensing techniques to record the presence of tremor are relatively straightforward. There are two avenues for wearable sensing that I am considering: inertial methods and electromyography. The widespread use of accelerometers, gyroscopes, and magnetometers in consumer electronics have given rise to many devices that can sense their movement in 3D space. As a patient tremors, the inertial sensor would move in 3D space at the same

frequency as the limb, and tremor can easily be estimated using spectral methods. However, one drawback with inertial methods is that it is impossible to ensure that the measured signals were generated by the patient and not the environment. For example, if a patient were in a car on a bumpy road and oscillating at a similar frequency, it would be possible that the system would mistake the car's motions as tremor. Surface electromyography (EMG) is a solution to this problem. EMG is the measurement of electrical potentials on the skin to estimate muscle activity. By measuring not the movements of the limb, but instead the activation of the muscles that cause the limb to move, it is possible to guarantee that estimated tremor is coming from the patient and not from an external source. However, surface EMG can be difficult to use due to a large number of possible artifacts that come from the physical interface between the device and the skin. Additionally, the electrodes can shift and move over the course of a day making calibration difficult.

Invasive neural systems have some distinct advantages over wearable sensing. First, wearable sensors are good at estimating the tremor a patient is already experiencing, but it may be difficult to extending this to predicting when in the future a patient will have tremor. By tracking movement intentions or other neural signals, it may be possible to determine when a patient is in a state that will cause tremor before any symptoms are manifested. Additionally, the electrodes do not shift over time so the systems do not need to necessarily be recalibrated over time. One downside of this approach however, is it requires new implantable hardware with the ability to sense from the nervous tissue as well as stimulate. This new implantable hardware will also need the ability to either classify the data on the device and take predefined actions, or will need to stream the data out of the body to an external processing unit. Sensing, classifying, and the streaming of data all will take additional power from the already limited implanted battery, potentially lessening the power efficiency gains that the closed-loop paradigm provides.

3.2.3 Control Algorithms: Dynamics, Parameter Adjustment, and Volition

Arguably the most difficult part of designing a closed-loop system is the creation of the algorithms to transform raw data from sensors into actions that need to be taken by the actuators. The aim of the signal processing and control algorithms is to create a feedback loop using the system's sensors to produce a stable and beneficial output. However, depending on the underlying system dynamics this can be a tremendously difficult problem. Each component in the system, whether it be the neural tissue, sensors, or the implant, have an effect on the overall system through modifying the loop-gain, time lag, and frequency response. It is the responsibility of the algorithm designer to compensate for the other components in the system in order to deliver effective treatment. Considering the fact that so little is understood about the underlying dynamics of the neural circuitry these systems are interfacing to and the sheer scale of variability between patient to patient it is likely that much of the signal processing and control system design will have to be created specifically for an individual. Similarly, the sensors and treatment method will have to be selected in order to give adequate closed-loop system performance.

Signal processing is required to transform the raw sensed data into usable features that correspond to the presence or absence of neurological symptoms. The exact signal processing required depends on both the signal source and control scheme. For instance, a wearable sensor that measures the physical presence of tremor by tracking the movements of the limb lends itself easily to a spectral analysis. In this case, the bandpower estimate in the tremor band could be used as an estimate of the total tremor a patient is experiencing. However, the filter or digital fourier transform parameters selected to make this assessment will have an impact on the system lag, resolution, and specificity of the estimate.

When it comes to modifying the stimulation waveform in response to sensed symptom changes, there are two general approaches to a control algorithm should modify the implanted device's parameters. Firstly, the control algorithm can simply turn on or off the clinical stimulation parameters depending on the presence of symptoms. In this case the

stimulation parameters would be at a "static" level and all power savings or side-effect reductions would be the result of just enabling or disabling the stimulation at the right time. In contrast, a "dynamic" stimulation response would instead have the control algorithm tune the parameters directly to tune the delivered therapy to a specific level. For example, a control algorithm could adjust the stimulation amplitude in direct response to the amplitude of the sensed tremor. Such a system's power efficiency would not just be a function of total time on versus off, but would also be driven by a reduction in the average power used for stimulation when the device is enabled.

Designing control algorithms can also follow one of two overarching paradigms: they can either be non-volitional or volitionally controlled. A non-volitional system would be similar to the earlier example using a wearable inertial sensor to trigger stimulation based on the presence of tremor. In this case, the system responds if tremor is sensed regardless of the patient's desire for treatment. While this is potentially advantageous over an open-loop system, the fact remains that patients have no control over their potentially unpleasant side-effects. The patient's only option for making a choice between treatment and side-effects requires taking off of the watch or disabling the closed-loop system. A volitionally-based control system on the other hand, would trigger stimulation not on the presence of tremor, but instead on the patient's desire to be treated. In such a system, a patient needs to have the ability to generate commands for the implanted device. Such systems exist today in the form of hand-held patient programmers, but these can be difficult to use for those with neurological movement disorders. A more advanced system would be one that allows a patient to use a brain-computer interface to make a moment-to-moment adjustment of their stimulation by volitionally modulating their neural signals. The ability for people to learn to volitionally control their neural signals to control external devices is well established in BCI literature. Furthermore, such a feature could potentially be fully integrated into the implanted device if such an implant was to have the ability to sense from the patient's cortex. This would have the additional advantage of not requiring power-intensive communication with external devices.

3.3 Prior Closed-Loop DBS Work

3.3.1 Tremor Sensing

Other labs and researchers have already been developing sensing methods to build closed-loop DBS systems. Sensors have been used to estimate if a patient is sleeping for the express purpose of turning off DBS stimulation to save battery life [40]. For Parkinson's disease, beta-band activity has been used as an indicator of tremor [27] and EMG and inertial measurements have been used in identifying periods where an essential tremor patient needed stimulation [41]. There has also been work from the medical device industry to include neural sensing capabilities within their implantable devices [9]. Closed-loop neuromodulation platforms with sensing capabilities have also been identified as a potential platform for brain-computer interface research [42].

3.3.2 Human Studies

There have been few prior studies that actually built proof of concept systems and tested them in vivo. It has been shown in Primate models of Parkinson's disease that closed-loop DBS is a more effective method for treatment [43]. Closed-loop neuromodulation systems have also been shown suppressing seizures in ovine models [44]. More recently this work has begun to transfer into human trials. Using cortically sensed beta-band information to turn on and off stimulation, closed-loop DBS in PD patients has been shown to dramatically reduce the amount of stimulation a patient needs to treat their tremor [45]. In fact, the study of eight patients found that the closed-loop DBS system actually improved patient's motor scores when compared to even the continuous DBS stimulation control. A closed-loop DBS system for ET patients that determines and triggers stimulation has been shown with four male essential tremor patients that exhibited severe intention tremor in Japan [11]. In this case, muscle activity driven by voluntary movement in the affected limb triggered stimulation and successfully suppressed the tremor. Both experiments were using a static preset stimulation pattern determined by a clinician to be effective at suppressing tremor.

Neither study attempted to use their sensors to determine stimulation parameters in real-time. Real-time adjustment of stimulation parameters may prove to further reduce the total power required to suppress the tremor and adjust for any day-to-day variability in the disorders [8]. Researchers have used computer simulations to show that stimulation dynamic control with local field potentials (LFPs) is potentially possible [46], however this work has not been applied to human experiments yet.

Chapter 4

INTERFACING WITH IMPLANTABLE NEUROSTIMULATORS

Current clinical neurostimulators are implanted and configured to treat neurological movement disorders in an open-loop manner with static stimulation patterns. In order to achieve the research aims of this dissertation, current clinical neurostimulators are not sufficient as a research platform due to the lack of real-time stimulation parameter control and no ability to sense neural data. For this reason, in our preliminary work we will be using the Medtronic Activa PC+S system, an investigational implantable device. The PC+S is modified version of the Activa PC, a FDA approved deep brain stimulator. The Activa PC+S system expands upon neurostimulator functionality with advanced sensing capabilities. Medtronic has built the Nexus-D system to enable real-time communication



Figure 4.1:
**The Activa PC+S
Implantable
Neurostimulator
(Credit: Medtronic)**

between a desktop computer and the implant over a standard USB interface. This allows the desktop computer to log data from the implanted electrodes or fuse data from various sensors and update stimulation parameters on command. The modifiable stimulation parameters of primary interest include stimulation current, frequency and duty cycle. This real-time modification of the DBS stimulation parameters will allow the device to act as an actuator in the fully closed-loop systems mentioned earlier to be developed and deployed. Furthermore, bioelectrical measurements can be made across any of the electrode sites allowing for a dynamic and configurable set of measurements to be made. This will allow us

to estimate neural states and measure features that may correlate to activity or symptoms of interest. These neural states and features may also be potentially used as a signal source for a brain-computer interfaces, which is a long-term focus of our research.

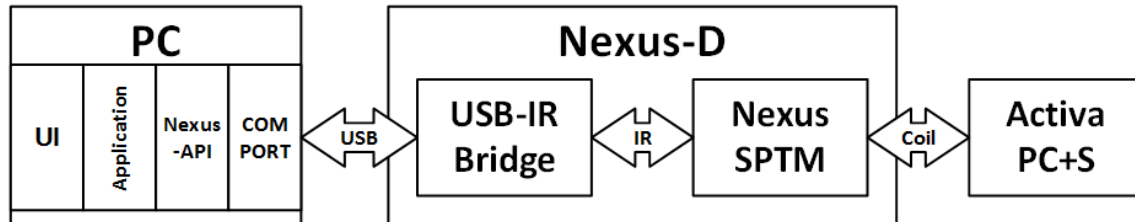


Figure 4.2: The Nexus-D System

A block diagram illustrating the usage of the Nexus-D system is shown in Figure 4.2. The Nexus-D consists of a reprogrammed Medtronic sensing programmer telemetry module (SPTM) to create a communication channel to the implanted Activa neurostimulator. A host application on a desktop computer can access this communication channel through a commercially available USB to IrDA (infrared data association) bridge (an Actisys IR224UN).

4.1 Foundational Code Development: The Nexus C# DLL

While Medtronic has provided a specification for the communication interface to the Nexus-D system, it is a very low-level interface requiring a developer to generate their own packets, CRCs, and protocol acknowledgments in order to create a system that uses the Nexus-D. Furthermore, one shortcoming of the Medtronic communication interface to the implanted neurostimulator was the inability to specify stimulation parameters. Instead, the system must implement an increment or decrement parameter command and the Nexus system will return what the new stimulation level is.

While Nexus now has a JAVA API to enable developers easy use of the Nexus-D, it was not released when work was started on this project. As such, it was required to develop our own code base for using the Nexus-D. Since a Java API was under development at

Medtronic, C# was selected to use for this project in order to diversify the available tools for future development. The Nexus C# DLL we have developed completely handles all low-level communication with the system and maintains all knowledge of the implanted system state. Furthermore, it allows users to directly set stimulation parameters and define the ramping to the new value.

4.1.1 Nexus C# DLL Component Architecture

The C# DLL I developed for use in our experiments is a multi-threaded code library that provides an abstraction layer for the Nexus-D and Aactiva PC+S so that closed-loop applications can easily be developed. The API provided by this DLL exposes several different types of function calls in order to interact with underlying components that directly control the Aactiva PC+S with the Nexus-D. A general block diagram of the architecture of the full DLL is shown in figure 4.3.

Expanding upon the packet specification given to us by Medtronic, the following software components were developed to allow a developer easy access to the underlying functions of the system: a serial communication link management, a keep-alive watchdog system, a stimulation parameter controller subsystem, and a sensing data management subsystem. In addition to these functional components, a local copy of the implanted device's state is implemented to minimize unneeded and power-intensive communication. The functionality and use of each of these subcomponents is detailed in the following section with a description of all coding functions and class afterward.

Communication Link Management

This API provides full link management of the serial to Nexus-D link. The link management works for both the normal Nexus-D connected via USB or for the NexDEX Bluetooth interface to the Nexus system. The link management subcomponent handles all communication through the serial COM port including packet header construction, retransmissions in the case of system NACKs, and resynchronization of data in the case of system timeouts.

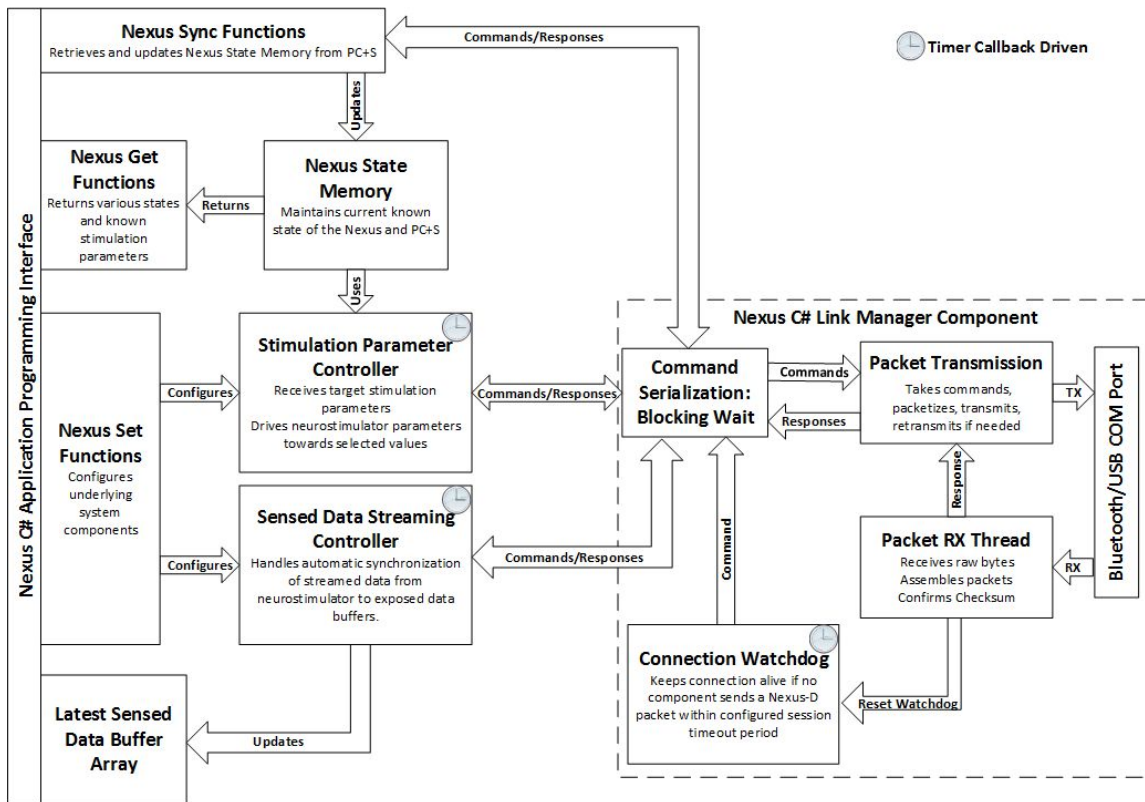


Figure 4.3: Nexus C# DLL Component Block Diagram

It automatically reassembles received packets from the serial interface and returns packet responses to the rest of the system.

Keep-Alive Watchdog Timer

The Nexus-D allows real-time command and control of the Activa PC+S in a supervisory session that will timeout if no packet is sent over the interface over a predetermined period of time. While this can save battery life, it is in fact a barrier to developing ambulatory systems and experiments that may potentially allow for longer periods of time between commands than originally designed. The Nexus C# API's link management component automatically creates a watchdog timer that will request the Nexus status at a shorter interval than the

timeout period to ensure that the connection stays alive. Every time a packet is sent by other components or the user, the watchdog timer is reset to stop unneeded packets from being sent.

Stimulation Parameter Controller

The Medtronic Nexus-D does provide a user or developer the ability to modify stimulation parameters in real time. However, this control is limited to only increment or decrement commands. After receiving an inc or dec for the parameters, the system then responds with the new level of stimulation. Instead of forcing users to perform this process repeatedly to reach the stimulation level they want, our system instead uses a stimulation parameter controller that allows users to have the system automatically ramp to a stimulation level. The stimulation parameter controller can ramp parameters at a configurable rate by controlling both the step size and step interval. This paradigm enables a developer to focus on determining stimulation set-points and our system will take care of the actual ramping between stimulation levels. Additionally, it automatically tracks parameter limits to reduce the number of unnecessary packets.

Sensing Synchronization

The Nexus-D system provides access to data sensed by an Activa PC+S. Our API simplifies the process by automatically syncing data from the Activa PC+S and providing an event-driven wait method that can be used to wait for new data to arrive. This allows multi-threaded programs that need to wait on sensed data from the Activa PC+S to be easily written.

Nexus State Memory

Since communication to the implanted device is both slow and consumes power, it is important to minimize the number of commands and requests to the implanted device. For this

reason, at system start up a single synchronization of the Aactiva PC+S and Nexus-D configuration is performed. This state memory is then updated whenever a command is executed, allowing users instant access to state information without having to wait on communication delays. This memory is separated into three categories: general information, stimulation group configuration, and sensing channel configuration. General information contains all system wide data about the devices that are not stimulation or sensing specific. This includes firmware versions and session timeout periods. The stimulation group configuration data includes all of the information about how the system can stimulate. The Aactiva PC+S can have up to four different "groups" of stimulation modalities configured, with each group able to have different stimulation leads, amplitudes, frequencies, or pulse widths used to treat the patient. The Nexus-D can be used switch between these groups in real-time, but that means it is necessary to save in memory the state the system left each stim. group in before switching back to it. The final set of saved data is the sensing configuration which keeps track of which channels are enabled, sampling rates, and the format of returned data packets.

4.1.2 Enabling Bidirectional Behavior: How the DLL handles concurrent sense and stim

One important issue to discuss for the closed-loop systems covered in this thesis is how to optimize communication performance when there may be a significant demand of data to be sent through the Nexus-D. This concern arises from the fact that commands need to be sent to the Nexus-D one at a time and the DLL needs to wait for a response from the Nexus-D before the next packet can be sent. Additionally, the Nexus-D's communication channel to the Aactiva PC+S is half-duplex, meaning that data can only be transmitted in a single direction at a time. The link-management code was designed to enforce this serialization of packets, and blocks new commands from being sent to the Nexus-D unless the resource is free or a previous command times-out.

Given these concerns, special attention needs to be given to the exact timing of packets when both sensing and stimulation are enabled. While the stimulation controller and sensing

synchronization components can operate at whatever timing is needed on their own, when both are enabled at once, sensing data can easily be lost. This difficulty arises from the fact that sensing packets must be sent with precise timing in order to not miss data, and a stimulation packet may interrupt this timing.

There are several reasons why the exact timing of sensing and stimulation packets can cause missed data. It is important to first discuss the timing of individual packets themselves. New sensed data is available on request every 400ms on the Nexus-D, and the command to retrieve the data has a 500ms timeout period. Most often, retrieving a sensing packets can take as little as 110ms, but it can take longer (up to 400ms) depending on the time interval between when the get data packet is sent and when the data is actually ready for transmission. On the stimulation side, most stim parameter changes usually take around 115ms to complete a transaction, but there is a timeout period of up to 300ms for these types of packets. Another consideration is that using the NexDEx Bluetooth interface adds around 50ms to the transaction delay for each packet due to the Bluetooth stack on both the Windows machine and on the NexDEx.

If stimulation and sensing packets need to be sent concurrently, then every 400ms a get data packet and a stimulation update need to be sent. While the average transaction times indicate that there is enough time to complete both actions in a single 400ms window, there is very little room for the error. Additionally, the timeout periods already indicate that we are over-saturating the communication channel with a total of 800ms of packet timeout duration to accomplish both a sense and stim action. If these packets take too long to complete, or if multiple stimulation commands are attempted between sensing packets, the sensed data may be overwritten with new data before the DLL has the opportunity to download it.

This means that while sensing, we can only ever possibly send out a single stimulation command in between sensing packets unless we want to lose data. While the stimulation parameter controller was designed to be able to ramp stimulation arbitrarily, when sensing is enabled it is locked at a single update per 400ms time period. Additionally, the DLL triggers this stimulation update immediately after the sensing data transaction ends because

the communication time-budget is already in timeout-deficit.

This design choice has several closed-loop system implications. Firstly there is the already mentioned forced ramping rate, which may require the use of non-ideal ramps to be used with patients. A more nuanced implication though is the fact that the system as described does not allow for time for the most recent data to be processed before a stimulation update goes out. Instead, the stimulation update will be based on the data packet that arrived before the most recent one. In theory, the most recent data may indicate a change in state that is different that would require a control action to be taken. This in-effect adds an additional closed-loop system lag of 400ms to our algorithms where both sensing and stimulation are needed.

4.2 Modified for mobile use: the Nexus-D Extension

The Nexus system allows for many new explorations into deep brain stimulation systems and other neural interfaces. The problem is that this system only enables tethered experiments. Considering that many of the patients being treated with deep brain stimulation are those with neurodegenerative movement disorders, it will be difficult to design comprehensive experiments that can examine the effect of these closed-loop systems in real world scenarios with a tethered system. Instead of relaying data only to and from a PC, I have modified the Nexus-D to enable Bluetooth communication to a smartphone. The Nexus-D system is comprised a combination of the reprogrammed SPTM and the commercially available USB to IrDA bridge. It is important to note that the bridge is purely a translator between the USB interface from the PC and the infrared communication interface. No command generation, interpretation or parsing of data is performed in the bridge of any kind. It simply passes any data communicated over USB directly to/from the Nexus SPTM. To achieve our goal of interfacing to the Nexus-D wirelessly, custom hardware was required to take the place of the USB to IrDA bridge. I began the design of the Nexus-D Extension (NexDEx) as a means of implementing this vision of a mobile battery-powered Nexus interface that could communicate wirelessly with a desktop computer, a smartphone, or even directly to sensors.

A block diagram of this new system and its intended uses are shown in Figure 4.4.

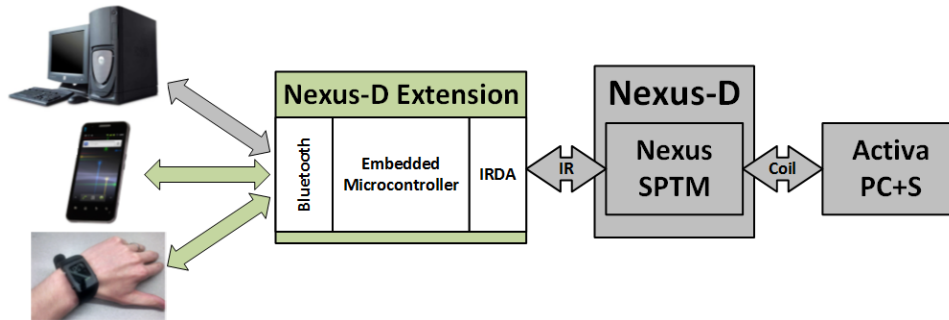


Figure 4.4: The Nexus-D Extension (NexDEx) System

In order to test the practicality of such a system, I first disassembled the commercially available USB-to-IrDA bridge used in the Nexus-D. I observed that the bridge makes use two key components: a USB-serial chip and a serial-IrDA chip. By removing the USB-serial and exposed the raw serial interface to the IrDA interface, I could then easily integrate a separate serial-Bluetooth module and battery recharging circuit that I had used in a different prototyping project. This prototype system is shown in the middle of figure 4.5. By configuring the Bluetooth module's serial interface, I was able to successfully make a wireless connection to the Nexus-D. By only modifying the USB to IrDA interface, I was able to preserve all of the safety and interface features of the Nexus-D. Through testing this prototype with Nexus-D C# DLL code I had developed, I confirmed that this modification added acceptable delay such that the timeouts defined in the Nexus-D specification were still valid due to the speed of Bluetooth communication.

For the second generation system, a custom printed circuit board was designed in Altium PCB designer to integrate a Bluetooth interface, TI MSP430 microcontroller, and an IrDA transceiver. This allowed us to cut out the commercially available USB to IrDA bridge used in the Nexus and instead communicate directly to the Nexus SPTM over the infrared interface. Since the USB to IrDA component was only a translational bridge, removing it



Figure 4.5: **The Nexus-D Extension (NexDEx) System Hardware:** Top - Normal Nexus-D System. Middle - Prototype Wireless Interface. Bottom - Final NexDEx Implementation.

has no impact on the overall functionality that the Nexus-D system provides. This means that once again in this new modified system all of the safety mechanisms and functionality of the Nexus-D are maintained. The board consists of a typical four layer stack-up with signals on the outer layers and power planes on the inner layers, with the final fully assembled project shown in the bottom figure of 4.5. This NexDEx system gives us the advantage of having a mechanically robust and fully mobile embedded system that will allow for studies on ambulatory patients untethered from a PC for the duration of the experiments.

By including an embedded microcontroller in the loop, we are able to move much of the lower-level functionality required to run the Nexus-D out of the application environment and onto the wearable implant communication system. This means we can move the hard real-time code that manages stimulation and sensing into embedded code, however it also

means we need to implement a local copy of all Nexus/Activa PC+S state information to keep track of the implanted device. A block diagram showing the system components of the NexDEx firmware are shown in figure 4.6.

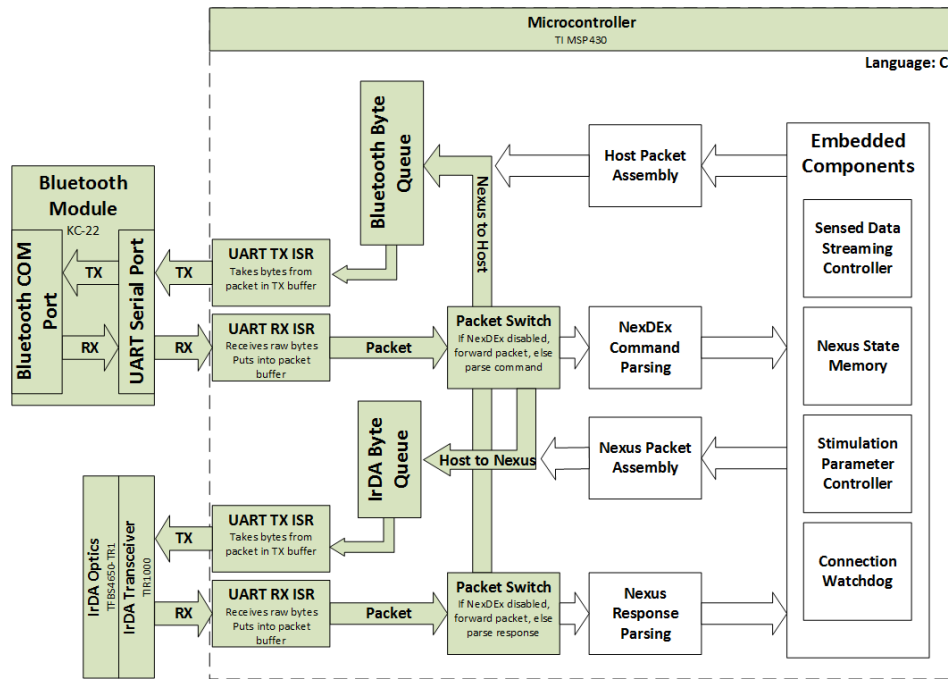


Figure 4.6: **The Nexus-D Extension (NexDEx) System Firmware:** Green components are used as a serial pass-through when NexDEx embedded functionality is disabled. This gives the hardware compatibility to with Nexus C# DLL and the Medtronic Java interfaces. When making use of the expanded command set, embedded components can be enabled that take over low-level functionality like stimulation ramping and automating the streaming of sensed data. In this case, direct host access to the Nexus-D is disabled via the packet switches.

Many of the same software components that were built into the C# DLL are repeated in the NexDEx. For instance, in the current Activa PC+S system architecture, stimulation parameters can only be incremented or decremented, there is no way to dictate a stimulation setpoint or target. This means that a closed-loop system requires a significant amount of code on the host application dedicated to simply managing the timing required to ramp the

various stimulation parameters to each new setpoint determined by the system controller. By including firmware components in this embedded microcontroller, the low-level stimulation adjustments and ramping can instead be offloaded from the smartphone or wearable sensors. This will reduce the load on the mobile processor and reduce the power and bandwidth of the Bluetooth communication. In addition, the new sensed data can be buffered using a first-in-first-out (FIFO) method that would allow for the bursting of data in a way that the Nexus-D cannot currently accommodate. These sorts of optimizations allow our test applications to be focused on the larger and more power hungry signal processing algorithms required to determine how and when stimulation should be delivered. Transitioning hard real-time code into the embedded platform is particularly important due to the fact that mobile operating systems have indeterminable response times due to system interrupts and sharing the processor with many other processes and programs.

One important note, is that while implementing systems that interface with human patients, it is of dire importance to not have multiple controllers for stimulation. This is because there may be disagreement between the controllers on what the output stimulation could be, which may lead to dangerous race conditions or other undesirable behavior. For this reason, when a host enables the NexDEx embedded functionality the internal “packet switches” shown on figure 4.6 disable all host access to the underlying Nexus-D and Acliva PC+S. To enable the NexDEx is to remove all real-time control from the host, who is regulated to asynchronously modifying the embedded controller set-points and receiving streamed data from the NexDEx if sensing is enabled. This means that for a user of the desktop Nexus-D C# DLL will then have less visibility of command timing. This is acceptable because the NexDEx embedded functionality is meant for resource-scarce mobile platforms (smartphones and smartwatches) and not as a replacement for the Nexus C# DLL when using a desktop computer as a controller in the loop.

4.2.1 Mobile Application Opportunities

Since we have moved many of the hard real-time software components into the embedded firmware running on our mobile communication interface, a smartphone has the bandwidth to perform higher-level signal processing and make control decisions based on sensed data. Due to the fact that the embedded stimulation control system manages parameters based on given setpoints, the signal processing and control decisions can be batch processed on a much more lenient time scale. If new setpoints and control decisions are only being calculated a couple times a second, which is reasonable given the frequency range of tremor, then sensed data can be buffered until it is processed when a control decision is being made. In the multi-threaded operating systems that run on modern smartphones, these lenient timing requirements greatly reduce system complexity and ease application development. To further limit the load on the smartphone processor it is possible to offload initial data filtering and processing back onto the worn sensors. However, this may not be desirable if one wants to do long term monitoring and logging of the symptoms, which may require access to the raw data. For our demonstrations and prototypes, we have developed an Android application that allows the testing of various control algorithms. The application can receive data directly from Bluetooth-enabled worn sensors or can be relayed data from a desktop if the prototype sensors are unable to directly connect to the smartphone.

Adding persistent neurostimulator to network connections can enable practical functionality that is not directly related to closed-loop DBS. Some identified advantages of these systems could include using the smartphone's data connection to enable the neurostimulator to communicate to servers within the cloud. The neurostimulator could send sensed data or usage reports for long-term clinician-patient monitoring. The data logged to the cloud could include sensor data from any worn sensors that can sense any exhibited symptom states. The cloud servers could retain this historical data to refine future treatment for the patient.

Smartphone to neural implant connections could also enable new alert and alarm functionality. Utilizing this mobile communication channel, neurostimulators will have an enhanced

ability to act upon dangerous situations. If the device senses an emergency situation, such as a seizure, it could automatically use the channel to make a 911-call to emergency services or notify family members that help is needed. Furthermore, any additional sensors used to monitor the neurological disorder’s symptoms may be used to trigger these alerts and alarms.

4.3 Closed-Loop System Framework for System Integration

Given the exploratory nature of this thesis’ research aims, it is important to be able to quickly create and deploy new algorithms, sensing methods, or experimental tasks. In order to enable easy and fast system integration for each new experiment, I set out to create a generic code-base that make use of standardized interfaces in order to be reconfigured as desired. The approach that I took was to split a closed-loop program into four distinct layers that would have standardized interfaces to allow for easy modification of internal requirements. The block diagram of the generic system framework is shown in Figure 4.7.

Working from the bottom up of the figure, the physical layer is composed of the actual hardware devices that need to be interfaced with in order to perform the sensing or control outputs required for the system to work. In a wearable closed-loop DBS system, this may be composed of worn inertial or electromyographic sensors providing data on limb movement. The neural data collected from the Aactiva PC+S sensing channels are another important sensor to consider. On the actuator side, in a BCI experiment the system’s output may be a cursor on a screen, but in a closed-loop DBS experiment it will be the Aactiva PC+S stimulation settings.

Given that every physical sensor or actuator have their own communication protocols and formatting, it is impossible to design a uniform interface for system integration without an intermediate step. This is the purpose behind the Parsing Layer, where raw communication with the devices is performed for the purpose of collecting data into a standardized buffer interface for later algorithm processing, or allowing the program to easily control system outputs. Each sensor has it’s own unique “Sensor Parser” that inherits from a generic parsing class that defines how data will be stored and accessed. This simplifies the requirements for

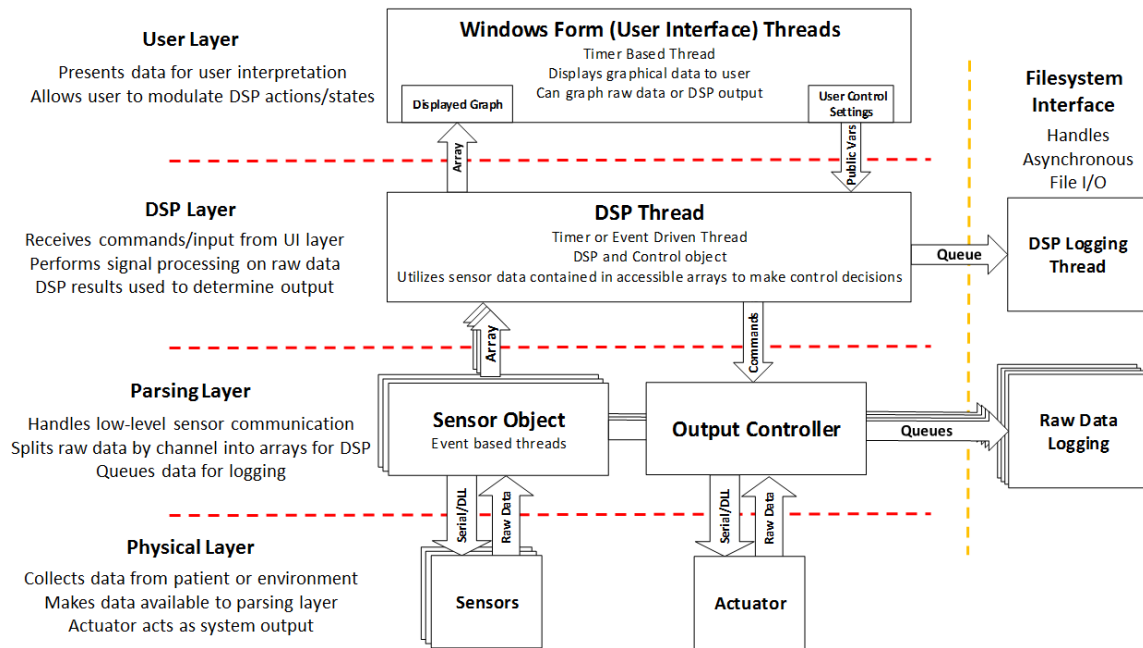


Figure 4.7: **Generic Closed-Loop System Framework:** Block diagram illustrating the general form of our closed-loop programs. This framework was designed to allow for fast and iterative development of exploratory code for experiments in human patients. A layered approach allows for standardized interfaces that lower development times and ease testing.

integrating a new sensor into the framework through standardization.

After data has been collected and stored in time-shifting buffers of the latest data, digital signal processing and control decisions need to be made in order to close the loop between sensing feedback and output control. This is the functionality implemented by the digital signal processing (DSP) layer, which needs to perform the processing needed to accomplish this in real-time. Often in this work, the DSP requires a spectral analysis to be performed on data collected, so often we need to perform a fast-fourier transform (FFT) as part of this processing. However, using an FFT is not required and a user could define any control algorithm by writing an event-driven callback function. These events can be generated either through a regular timer, or by an event from a sensor parser that indicates that data is ready for processing. By centralizing the DSP functionality into a single function, adjusting control algorithms becomes a simple and standardized process with distinct requirements for

an application developer.

The final layer is the user interface layer, which has been coded to allow for easy displaying of real-time data to users. Additionally, it allows for users to change states or variables used in the DSP functionality to run more complicated experiments or tune settings. Since this code interfaces with users, the real-time responsiveness of the code has a much lower requirement, and runs asynchronously to all the DSP and sensing functionality in order to ensure that issues like frame update rate or user's actions don't accidentally interfere with the real-time responsiveness of the system as a whole.

However, there is one additional component that needs to be addressed. On the right side of the block diagram is a code segment that cuts across the layers. This is the logging interface that needs to interact with the computer's filesystem. Since transaction times to system disk are not predictable, this allows the real-time closed-loop system to not get slowed down with writing data to the disk. Instead, logging data can be queued up into threads that are written to the file separate from the real-time control loop.

Going forward from this chapter, all of the closed-loop demonstration and experimental systems used this structure for the PC-side code. Given the spread of sensing methods, control algorithms, and signal processing needed, this demonstrates the functional and flexible nature of the designed framework.

Chapter 5

SENSING TREMOR

The fundamental requirement to close the loop for any system is that there needs to be observable signals that indicate the state of the underlying system. These observed signals can then be used to determine what actions need to be taken through feedback. In our case, we need to be able to observe signals from symptoms related to essential tremor and Parkinson's disease. There are three different sensing modalities we are investigating in our wireless systems development that may be able to fulfill this role. These three sensing modalities include measuring the physical movement of the limb, the electrical signals from the muscles, and the neural signals commanding the muscles to activate in an oscillatory manner. We can measure the tremor's physical movement and muscle activity using a wrist mounted inertial measurement unit (IMU) and electromyography (EMG). The ability to use these signals to predict tremor onset has been shown [41]. Sensing the oscillating neural circuits commanding the muscles is far more difficult and requires invasive biopotential measurements. This can be accomplished by utilizing neurological readings from the cortex or thalamus through the DBS electrodes. By fusing relevant data from these sensors, we will estimate the instantaneous level of tremor that the patient is experiencing. From this estimate, we can use the Medtronic Nexus system to trigger stimulation or to modify stimulation parameters.

It is important to note that throughout this chapter we present tremor-related data collected from human subjects. Much of this data was collected by or in collaboration with Helen Bronte-Stewart from Stanford University from Parkinson's patients. Data was selected that illustrate sensing of symptoms through these modalities. Throughout this chapter we will be reviewing these sensing methods and using this collected data to illustrate their capabilities in monitoring tremor.

5.1 *Inertial Sensing*

Inertial sensing can consist of several different types of modalities including acceleration, gyroscopic or orientation measurements. Due to the rise of microelectromechanical systems (MEMS), the size and power required to perform these forms of sensing have dropped dramatically over the last decade and inertial sensing methods have become common enough to make their way into smartphones and wearable systems such as smart watches.

For our research, we have begun developing a series of IMU watches. The IMU watches we have built are battery-powered devices that directly measure the tremor that a patient is experiencing by sensing the accelerations and position of the affected arm. The first of these watches was a modified MSP430 Chronos watch which uses a proprietary RF link to communicate to a desktop PC. It features a full nine axis IMU, which consists of a three axis accelerometer, gyroscope, and compass. Each axis provides an orthogonal and independent data source for us to use in tremor state classification. This is probably more information than is necessary but we plan to determine the minimum number of axes needed to accurately sense tremor state. A picture of this watch is shown below in figure 5.1A.

Due to the fact that this watch can only communicate over a proprietary link to a desktop, we began development of a second watch that would instead use Bluetooth to enable communication to a smartphone or the NexDEx system (4.2). Due to no longer fitting within the Chronos form-factor, a 3D printed enclosure was created by mentored student Francisco Garcia to house the device. A picture of the fully assembled second prototype is shown below in figure 5.1B.

However, once we began collaborating with other research sites, this prototype watch became impractical due to the required maintenance and difficulty reprogramming the device at other sites. We began developing applications for Android smartwatches so other research sites could buy their own watches commercially. Additionally, with Android studio, it became trivial to update software on the watch over USB. For our experiments we made use of the LG G Watch as our inertial sensor. The G Watch has a 9 axis inertial measurement unit

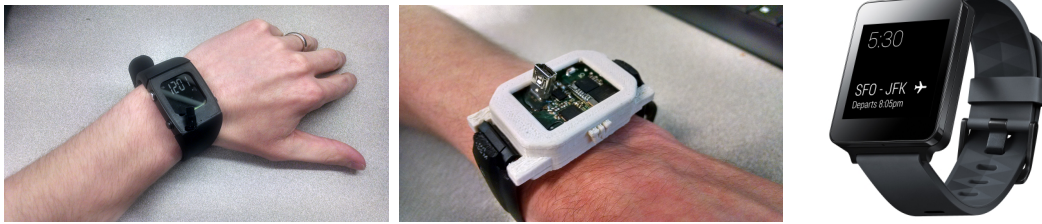


Figure 5.1: **Prototype Inertial measurement watches:** The left watch (A) is a modified MSP430 Chronos watch to support a full nine-axis IMU. Middle (B) is a custom designed Bluetooth enabled version. On the right (C), is the commercially available LG G Watch, which was used for final wearable experiments

(IMU) that is able to measure 3 axes each of acceleration, gyroscopic, and magnetic field data [47]. We wrote an Android Wear application that is able to stream the raw data, sampled at 100Hz, to a desktop computer. One difficulty with this system is the fact that the Android Wear API does not allow incoming Bluetooth connections. This proved to be a minor obstacle as we could instead host a Bluetooth service on the desktop PC or the NexDEX. The smartwatch now initiates a connection to the remote device by making a direct connection based on Bluetooth radio MAC address. The downside of this approach is that it requires hard-coding the Bluetooth MAC address into the Android Wear application. This means that the Android Wear application requires a software update every time a different Bluetooth radio needs to be used. Once the watch has been appropriately programmed, it is capable of streaming real-time 9axis inertial data to a computer or any other Bluetooth enabled device.

Inertial sensing of limb kinematics is a well-established method of identifying tremor. Inertial sensing allows for monitoring of the limb's movement through space over time. It is straightforward to identify periods of tremor due to an increase in spectral power at the frequency of the tremor. However, it is impossible to tell if the sensed movement is the patient's tremor or caused by an outside source, such as a patient riding in a car on a bumpy road. An example of raw gyroscope data estimate for a Parkinson's patient experiencing rest tremor is shown in figure 5.2. Signal processing must be performed on the sensed data

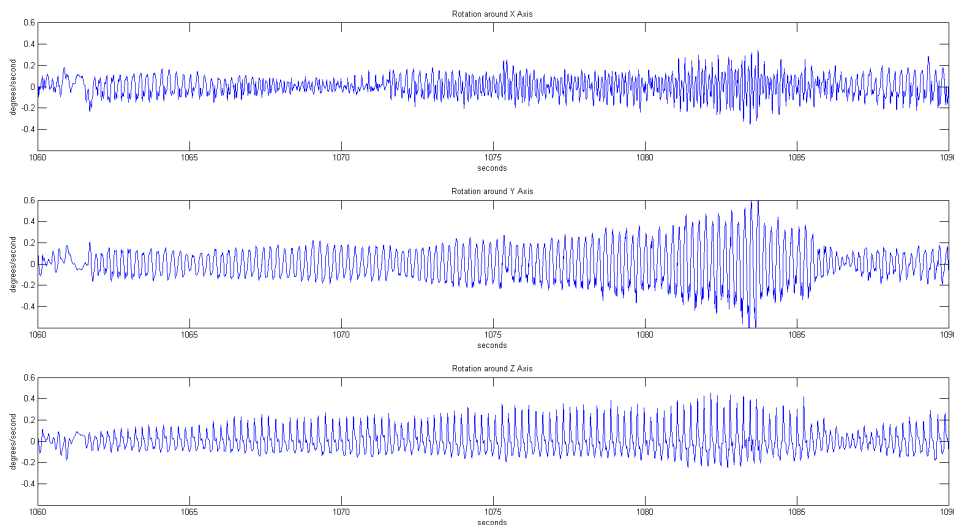


Figure 5.2: **Gyroscopic measurement of rest tremor:** Three axis of gyroscopic measurements from the LG G Watch worn on the wrist. Signals recorded while a PD subject is at rest and their left hand begins to tremor.

in order to estimate the tremor that a patient is experiencing at a given moment. Since tremor can manifest differently on each axis of rotation, it is important to use a method that captures the total tremor band power across all three gyroscope axes.

The oscillatory nature of tremor lends itself to a spectral analysis, based upon examination of the power of oscillations within different frequency bands. An example of such an analysis is shown in figure 5.3. This analysis was performed on the same slice of data shown in figure 5.2, with the top graph being the Y-axis data for reference. Each axis of raw gyroscope data is then transformed into the frequency domain using a Fast-Fourier Transform (FFT), illustrated as a spectrogram in the middle graph of figure 5.3. An estimate of the patient's tremor can be calculated by summing the band power of the bins corresponding to the tremor frequency range. While PD rest tremor is typically considered to have a peak between 4-6Hz [32], I summed the bins corresponding to 4-8Hz in order to collect the entire band power of the fundamental tremor frequency. This final tremor estimate of figure 5.2 is shown in the bottom graph of figure 5.3.

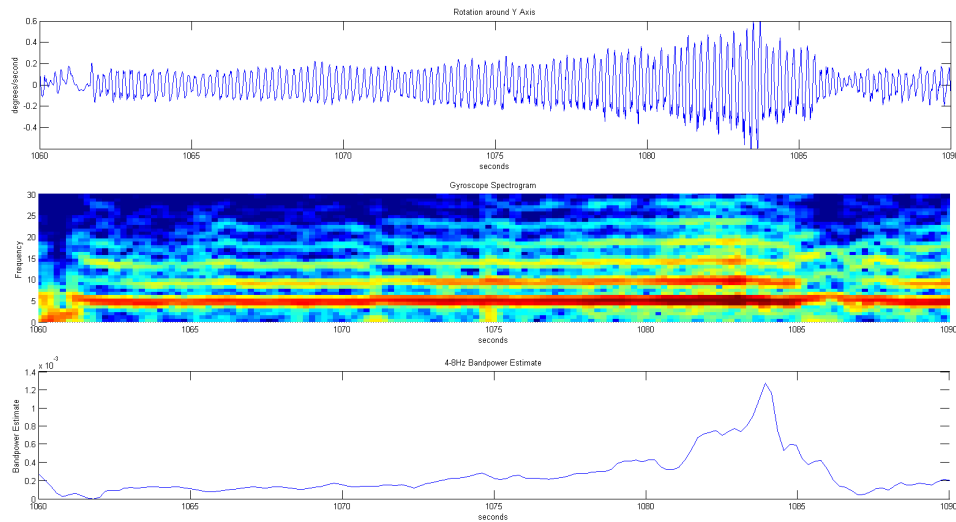


Figure 5.3: **Tremor Analysis:** Signal processing on raw data shown in figure 5.2. Top: Gyroscopic measurement of tremor. Middle: Spectrogram displaying the sum output of separate FFTs on X, Y, and Z axis data calculated offline. Bottom: Real-time tremor estimate based on summing the 4-8Hz output bins from FFTs during experimental data collection.

5.2 Electromyographic Sensing

Electromyography is the sensing of the electrical activation of muscle tissue. Whenever a muscle contracts, electrical activity can be measured from the surface of the skin. The magnitude of this signal is in direct proportion to the force that the muscle is applying. Whereas inertial measurements indicate the position of the limb in space, the EMG instead measures the force that muscles are applying. However, when only using EMG it is impossible to know the external forces on the limb, so it is impossible to estimate the actual position of the limb or the speed with which it is moving with just EMG sensing. Due to this fact, it is common to include inertial sensing on any EMG-based hardware.

To illustrate how tremor appears on a patient's EMG, I will once again use data collected from Parkinson's disease patients. Two EMG traces are shown below in figure 5.4, each on a different muscle group on a forearm during tremor. The physical cause of tremor in this case is due to the fact that the muscle activations are oscillatory and completely out of phase

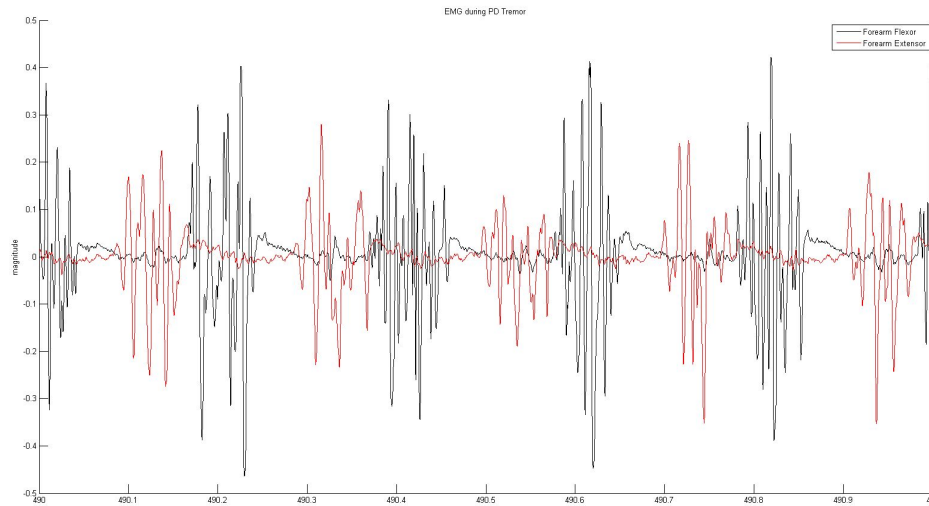


Figure 5.4: **Parkinson's Disease Tremor EMG:** electrical activity from out of phase activating muscles during tremor. The black trace is the forearm flexor and the red trace is an extensor. The rhythmic and out of phase activation causes a physically manifested and observable tremor.

with each other. This leads to the rhythmic movements known as tremor. In this case the tremor is close to five times a second.

For initial EMG sensing, I am using the gTec Mobilab. The device has eight sensing channels that are attached to the arm utilizing disposable adhesive gel electrodes. The electrodes are distributed around the arm over various motor groups of interest. Furthermore, the sensed data can be wirelessly streamed via a Bluetooth connection to a local computer. This device requires a specific API that runs on the Windows desktop platform, so as such it is unable to directly send data to a mobile system. While the gTec is mobile and battery powered, we have begun developing various mobile EMG hardware for our smartphone work.

There are a multitude of difficulties in building EMG-based systems. Firstly, positioning the electrodes on top of the correct muscles can be difficult for a naive user, and differences in electrode placement could result in requiring a recalibration of the system. While wet gel electrodes provide an excellent signal-to-noise ratio, they are limited use and some patients

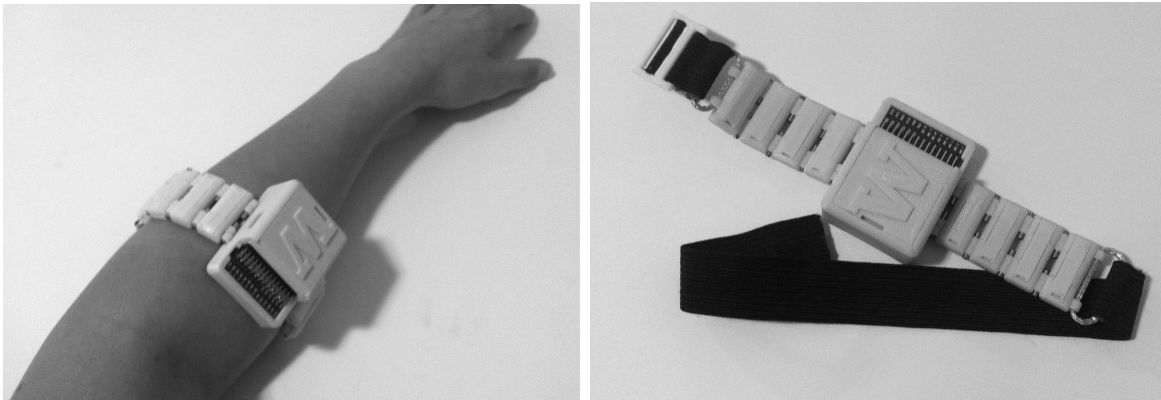


Figure 5.5: **Mechanical EMG Armband Prototype** Designed by collaborator Emma Vidarsson. Shown both worn and not worn. Enclosures built from 3D printed components

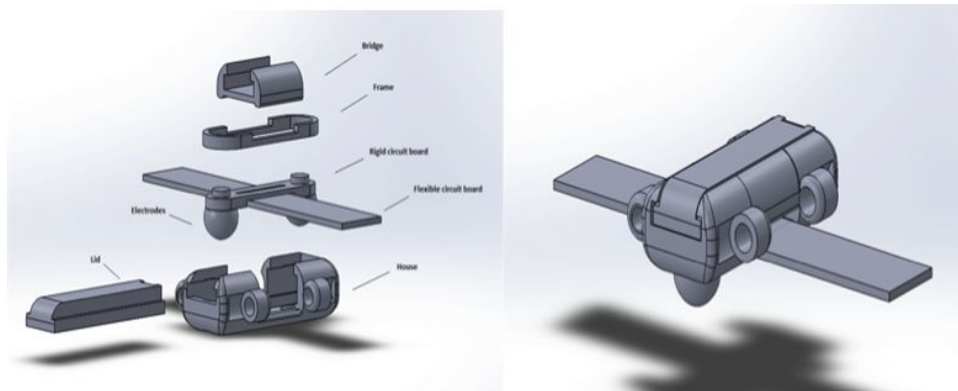


Figure 5.6: **Prototype EMG Electrical Front End Housing:** The final housing for the electrical components of our EMG analog front end. On the left is an exploded view and the right is a fully assembled version. Designed by collaborator Emma Vidarsson.

may be allergic to the gel compounds. For a robust and reusable system dry electrodes seem to have numerous advantages but the quality of the EMG recordings is not one of them. The tremendously high impedance of dry electrodes often introduce more problems than they solve. Not only does it make designing the analog front end more difficult but they are also prone to slippage causing artifacts and invalidating any calibration.

These difficulties have not dissuaded us from pursuing designs that may address these

issues however. The difficulties in dry electrode EMG armbands are mechanical in nature. Reducing slippage and maintaining good contact pressure for ensuring a consistent electrical impedance are paramount. To address these concerns, we collaborated with a mechanical engineering graduate student, a visiting scholar from Sweden, Emma Vidarsson to design an EMG armband that may improve device performance. Pictures and renderings of various components of her work are shown in figures 5.5 and 5.6.

The device currently uses the Microsoft Research Biopotential board. This board has a Bluetooth wireless interface, is battery powered, and a TI ADS1298 biopotential amplifier for analog to digital conversions of biologically-derived electrical signals such as EKG and EMG. The board uses a fully programmable MSP430 microcontroller and is currently being used to evaluate the performance of our analog front end and mechanical design. Unfortunately it seems that our latest design still has too low of an input impedance to be effective.

Given how difficult it is to design custom EMG devices, we investigated other commercial devices that show promise for armband EMG acquisition. In particular, I focused some effort on integrating the Thalmic Labs Myo armband into our real-time processing environment. The Myo can wirelessly stream raw EMG data from eight dry electrodes spaced equally around the arm. While the system performs much better than the in-house armband that was designed, for our experiments we made use of the gTec wet electrode system. This was primarily in response to the increased risk of dry electrode movement artifacts that are unavoidable while using dry electrodes.

5.3 Neural Signals

Of particular interest is the possibility of utilizing the implanted lead electrodes of the DBS system for neural sensing. While one electrode pair is configured to provide stimulation, a secondary pair could be used for neural sensing of the tremor, allowing a single implanted system to perform closed-loop mitigation of tremor. This has the advantage of not requiring any additional worn sensors or utilizing precious battery power on packet transmission. Since electrical stimulation at the electrode sites is able to mitigate tremor, it seems plausible that

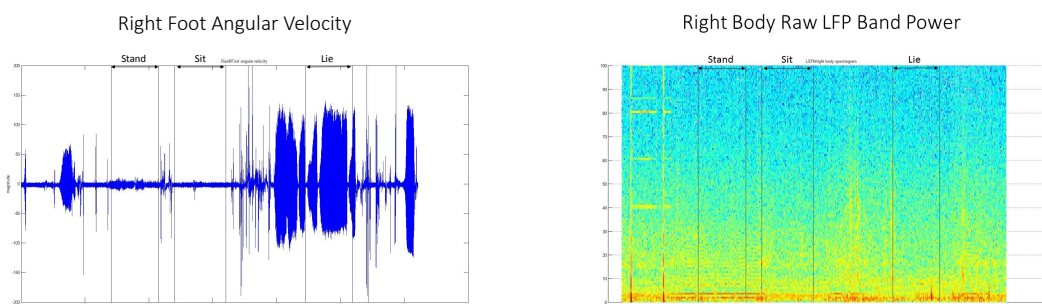


Figure 5.7: **Parkinson's Disease Raw Accelerometry and LFP Spectrogram:**

Top: Raw data from an accelerometer during a PD patient stand-sit-lie task. Durations of each task are denoted by black lines and labelled. A mild tremor of 10 deg/sec was observed while standing and a severe 100 deg/sec tremor was observed while lying down.

Bottom: LFP during this task

there may be a biological signature of tremor that we can sense from the electrodes as well. Fortunately, the Medtronic PC+S has the ability to sense and transmit electrically sensed data to the same outside communication system thus allowing us to demonstrate neural signals modifying stimulation parameters in real-time.

Tremor symptoms can show up in a variety of ways in the patient's neural signals. Beta band activity at the stimulation sites have already been shown to be related to Parkinson's disease symptoms for instance. Shown in figure 5.7 is an example of how this can manifest. In this case we see the accelerometer readings from the inertial sensing section and spectrogram of the sensed DBS electrode LFPs. We break down the spectrogram into power bands over time in figure 5.8.

In this example it would appear that the beta-band of the patient is lower during the tremor. From here, there are a variety of classification methods we can investigate but it is likely that whichever classification system is used will need to be heavily tailored to the needs of the patient.

The Activa PC+S allows sensing of neurally-modulated local field potentials (LFPs) that indicate various brain activity near the electrode sites. This will allow us to estimate

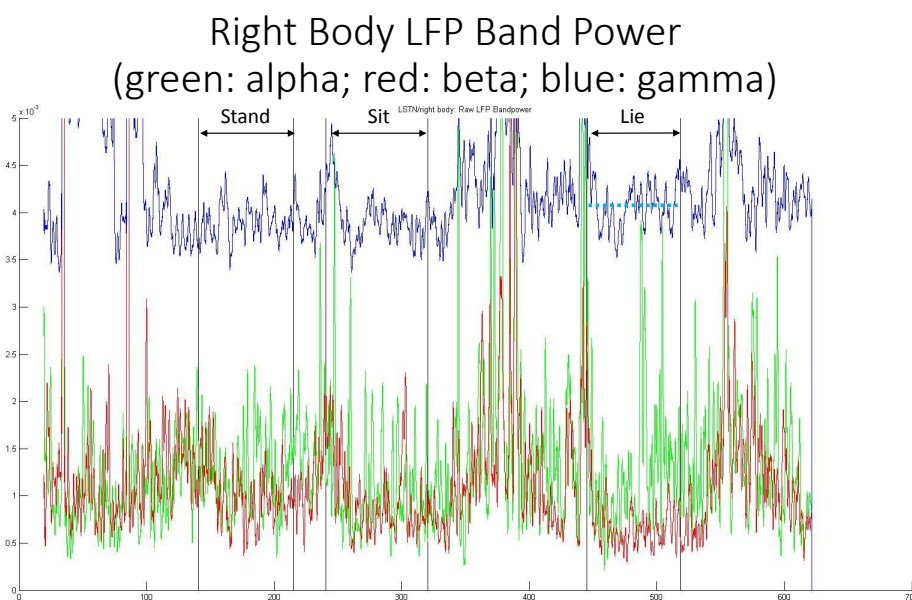


Figure 5.8: **Parkinson's Disease LFP Bandpower:** LFP bandpower during this stand-sit-lie task. Patient experienced large rest tremor during the lying portion of the task.

neural states and measure features that may correlate to activity or symptoms of interest. The Medtronic Activa PC+S system also has the option of utilizing a cortical strip of four electrocorticography (ECOG) electrodes. This allows collecting signals from many additional sites on the brain such as the motor or sensory cortex. These additional sites may contain information useful for tremor mitigation. For instance, for an essential tremor patient that experiences kinetic tremor when they move their hand, we could sense data from the motor cortex to determine when they intend to use their hand. By stimulating whenever the patient initiates movement, tremor may potentially be dramatically reduced.

These sensed neural states and features may also be used as a signal source for a brain-computer interfaces, which is a long-term focus of our research in this area. However, it is still unknown how effectively a subject could learn to consciously modulate the signals of their deep brain structures that are the targets of DBS, like the thalamus, for brain computer interface purposes. The ECOG electrodes can be placed in target areas traditionally associ-

ated with BCI research such as the motor cortex which will allow us to explore ECOG-based BCI applications in a fully implanted system in a mobile patient. This DBS platform will enable us to explore ECOG-based BCI applications on timescales currently unavailable and give us greater insight into the way the brain learns to utilize the extra control channels we are creating.

Chapter 6

CONTROL PARADIGMS

It should be readily apparent by this point that given the array of sensing hardware, data processing techniques, and the available actions able to be taken by the implanted device, that there is an incredibly large space for designing novel closed-loop DBS systems. Additionally, the control algorithms that need to govern the system integration of the components I've discussed so far, is potentially an even broader space of possible methods of various levels of complexity.

Performing a review of the possible algorithms that could be used would be counterproductive due to the preliminary nature of this work and how the system was purposefully designed to be a generic and extensible platform for future work. Instead, in this chapter I will strive to define terms that can be used to discuss the space of possible control strategies one could employ in describing or designing a closed-loop DBS system for a patient.

6.1 When to Take Action: Direct and Indirect Markers

The first design question while assembling a closed-loop DBS system is what biomarkers or signals the algorithm will use to determine control actions. One example of an important signals for use in a feedback loop could be a measurement of symptom intensity, such as tremor band-power. Alternatively, a biomarker could be found that doesn't represent a symptom, but instead indicates a high probability of a patient experiencing the effects of their disorder. To distinguish between these two different classes of triggering action, I will be using the term "*Direct*" to indicate a system that uses a measured symptom to make control actions and the term "*Indirect*" to indicate that a system is using a non-symptom measure to trigger stimulation.

Using direct measurements of symptoms provides a straightforward method of designing closed-loop systems. An example of such a system is one that uses a worn inertial sensor to measure rest tremor in a PD patient, and then dynamically adjusts the stimulation based on how strong the tremor is. The simplest form of such a system is one that turns on stimulation when tremors are present, and turn the stimulation off when the tremors recede. However, as will be seen in coming chapters, such systems can have poor performance due to the fact that they require symptoms to be present in order to react. This means that no matter how quickly a direct system reacts, the patient will already be in the bad state that the system should prevent. However, these systems are often more power efficient due to a low false-positive rate, and the stimulation that the system delivers can be tuned to just the level needed to treat the symptoms that the patient are experiencing at a given moment.

Indirect control methods approach the closed-loop problem from a different angle, instead relying on a signal that is merely associated with a heightened risk of symptoms. An example of an indirect signal would be using movement intention signals taken from the cortex to determine when an ET patient is actively moving their limb. Since ET patients often tremor when they move, a closed-loop DBS system could turn stimulation on whenever the patient's signals indicate that they are moving their limb, regardless if tremor is present or not. The effectiveness of an indirect method depends on the signal's usefulness in predicting symptoms. In the case of movement-intention based DBS for an ET patient, this could be considered a conservative approach since the system would likely have a high true-positive and false-positive rate, resulting in more stimulation being delivered than necessary. This is because the tremor only happens during movement, but not all movements result in tremor. Additionally, since the signal may not modulate based on symptom intensity, it may be more difficult to tune the output stimulation for a specific episode. This may result in a system being less power-efficient due to an "all-or-nothing" treatment approach.

It should be noted of course, that hybrid approaches exist as well. While not investigated as a part of this thesis, a hybrid system that uses both direct and indirect signals to determine control actions could provide great results. For instance, a system that triggered

stimulation based off of indirect measures of movement intention and then tuned the stimulation amplitude based on a direct measure of tremor may provide better results than either direct or indirect method used by itself. However, the sensor fusion required to do so makes this a much larger design space that I did not have time to examine for this thesis. However, using sensor fusion techniques will undoubtedly provide ample room for work in the future.

6.2 How to Take Action: Static and Dynamic Stimulation

Once a system has determined that action is necessary, the simplest form of response is to trigger a pre-stored “*Static*” stimulation pattern. In this situation, a clinician determines the appropriate electrical stimulation parameters to use but the closed-loop system is responsible for determining when the stimulation is being delivered. This can be triggered by either sensing tremor as it is being experienced by the patient or after sensing the intention to move in an effort to stop tremor before any oscillation manifests. As discussed in 3.3.2, others have used signal sources to perform this functionality.

An example of a static control action paradigm would be to use the IMU watch described above and our Nexus C# API to build a program that triggers a pre-set stimulation pattern when a tremor is sensed. When the tremor recedes for a long enough duration, the stimulation could then be turned back off. An example time-synchronized plot such a algorithm is shown in Figure 6.1. In addition to triggering stimulation from directly sensing tremor, we also hope to be able to initiate treatment of incipient tremor before symptoms have physically or neurally manifested. One strategy for performing this form of tremor mitigation would be to place the cortical strip over the motor cortex for the effected limb. Whenever there is significant activity or signals of an intention to move are identified, we could preemptively trigger stimulation to avoid any tremor symptoms from appearing.

The second control method is the “*Dynamic*” modification of stimulation parameters in response to attributes of sensed signals, such as magnitude and spectral components of the sensed tremor. In this case, a clinician defines a range of parameters and stimulation limits. This permits the design of a control loop using sensed tremors to adjust stimulation param-

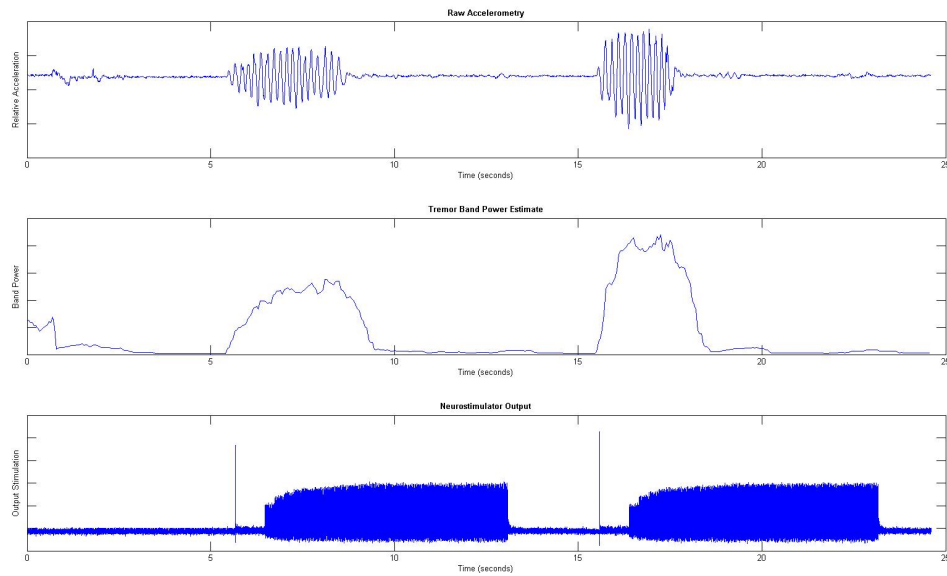


Figure 6.1: **Inertial triggering of static stimulation patterns:** In the top plot, the raw acceleration magnitude is plotted with two tremoring motions made at approximately $t = 5\text{s}$ and $t = 15\text{s}$. These tremors increased the spectral power within the tremor band shown in the middle plot. When this power rises above a threshold, it triggers a pre-set stimulation pattern until tremor subsides. Note that the sensed data is from a healthy individual emulating a rhythmic tremor while wearing the IMU watch, so it may not be representative of pathological tremor.

eters. Initial experimental proof-of-concepts were limited to the use of proportional control, where an estimate of tremor power is directly mapped to the stimulation intensity with a single gain modifier. This was done for ease of implementation while also demonstrating the platform’s ability to prototype dynamic forms of control.

An example of this form of control would be to dynamically adjust the stimulation amplitude proportionally to the sensed tremor. A demonstration of such a system was built that uses a limb EMG. In this experiment, I performed a FFT on a single biopotential EMG channel which was collected through the commercial bioamplifier with a wet electrode. WI then mapped the total power within an identified tremor band to the stimulation voltage with a static gain. A time-synchronized plot of the collected EMG, band power estimation,

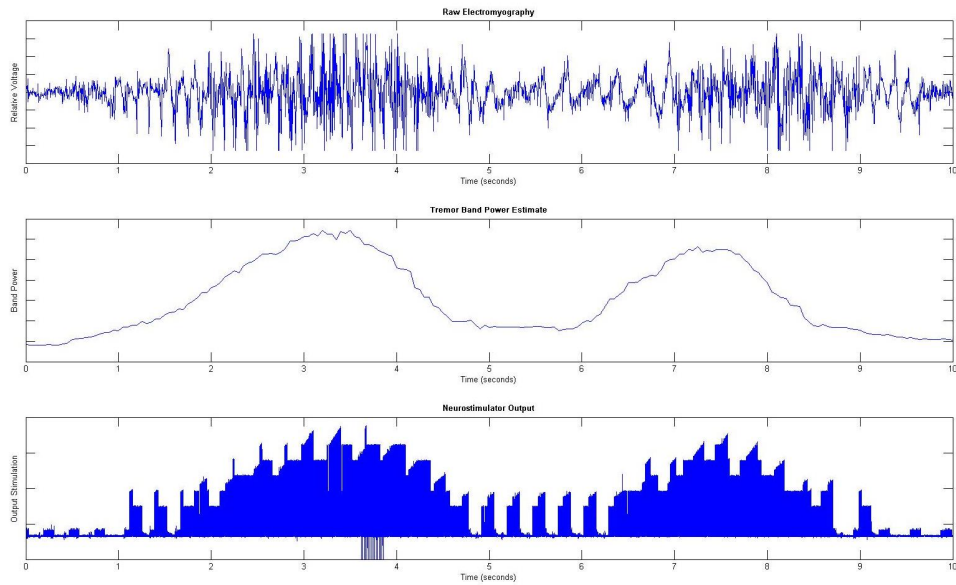


Figure 6.2: **Electromyography mapped proportionally to stimulation voltage:** In the top plot, the raw EMG is plotted with two tremoring motions initiated at approximately $t = 1$ s and $t = 6$ s. These tremors increased the spectral power within the tremor band shown in the middle plot. This power estimation is proportionally mapped to the stimulation voltage level, plotted in the bottom graph. Note that the sensed data is from a healthy individual emulating a rhythmic tremor while wearing the EMG sensor, so it may not be representative of pathological tremor.

and resulting stimulator output is shown in Figure 6.2. The total power that the neurostimulator is consuming is clearly proportionally driven by the level of measured spectral power density within the identified tremor band.

6.3 *The Patient's Role: Non-Volitional and Volitional Systems*

The most fundamental distinction for a closed-loop stimulation system is defining the role of the patient. For this reason, the first defining feature of any DBS system is whether a system is volitional or non-volitional.

Most current open-loop treatment available today to patients could be considered non-volitional control of tremor. Unless equipped with a patient-programmer made available

by their clinician, many patients receiving DBS treatment can't change their stimulation settings without consulting with a clinician. This lack of control of when or how they are or not being stimulated is what classifies systems as non-volitional.

A non-volitional closed-loop neurostimulation system refers to using sensors to automatically trigger the therapeutic stimulation without any patient involvement. For a patient that needs DBS to treat tremor, an example of such a sensor may include a smartwatch that can track when a patient's limb tremors. This watch could then communicate with the neurostimulator to start, stop, or modify stimulation parameters in response to a patient's tremor. The stimulation would then change in such a way as to reduce the patient's tremor as needed. This interaction between sensor, actuator, and patient is referred to as a closed-loop system due to the fact that each system is directly interacting with the other components as to reduce the undesirable symptom. When closing the loop for a system, one can expect that the system will act more efficiently and effectively. The desire to close the loop for neural stimulation systems is to make systems more power efficient so the implanted battery doesn't run out as fast and for the system to be more effective in treating neurological disorders.

Patient volitional control in current clinically deployed systems usually takes the form of a physical patient-programmer that an implanted individual can use to turn on or off their stimulation, or possibly to manually adjust up or down the stimulation they're receiving. Often these devices can be difficult to use, as they require the patient, with a movement disorder, to physically place the programmer on top of the implant and press buttons to make the changes that they want.

More advanced volitional systems may be feasible using investigational neuromodulation platforms. An interesting subset of potential closed-loop neural stimulation systems is one where we are not measuring external signals to determine when stimulation should be required. Instead, it is possible to use signals measured from the brain itself to determine when stimulation is or is not necessary. Such systems can be referred to as bidirectional neuroprosthetics. This refers to an implanted neural device that can both sense electrical brain activity and electrically stimulate the brain tissue. In a closed-loop neurostimulation

system context, these systems would use neural signals generated by the brain to determine when therapeutic stimulation is needed. What is particularly interesting with these systems is that the brain may learn how to take advantage of them in such a way that a patient learns how to volitionally control their own stimulation. Essentially the brain may learn to control the device as if it was a part of their body and the patient can consciously modify the stimulation level at will. There is already a significant body of literature that supports the fact that the brain can learn how to manipulate its own electrical signals to control artificial devices using brain-computer interface (BCI) technology. This same BCI technology could be leveraged by DBS system researchers to allow a person to control their stimulation level.

6.4 Comparing Algorithms: Performance Metrics

For the experiments that follow in the next chapters, we will compare how effective therapy is when we map features in our sensed data to stimulation amplitude. For PD patients, this will include mapping inertial signals and beta-band deviations to stimulation amplitude. For ET patients, we will use both the IMU and EMG worn sensors to identify tremor and trigger automatic response. In general, increasing the total stimulation power increases the tremor mitigation effects. These experiments will take advantage of this fact and increase the power level to just what is needed to eliminate tremor. Effectiveness of these methods will be analyzed by examining the sensor data after the closed-loop experiments, video-taping the effected limb, and having patients report perceived side-effects during the experiments. The aim will be to experimentally determine how we can maximize therapeutic outcomes while minimizing power and side-effect incidence.

One issue that we have observed while developing closed-loop algorithms for PD rest tremor [48], is that any given algorithm can produce dramatically different results across patients or even for the same patient on different limbs. In this section I will propose metrics for closed loop algorithm evaluation based upon results from patient trials using wearable sensors and the several example control algorithms used with our PD patients.

6.4.1 Important Parameters

The metric that I am proposing captures the trade-off between power efficiency and symptom suppression. The purpose of this metric is to compare the effectiveness of different dynamic systems across various patients. It bases this comparison by normalizing the closed-loop algorithm performance to the patient’s clinical open loop tremor suppression and stimulation power used.

I first calculate an “average tremor” value for both open-loop and closed-loop trials by summing the total band power in the tremor band (4-8Hz) and dividing by the total tremor band power while the patient received no stimulation. From this, the additional tremor the patient experiences due to using the closed-loop DBS system is determined by subtraction as shown:

$$Trem = \frac{BP_{CL}}{BP_{No}} - \frac{BP_{OL}}{BP_{No}} \quad (6.1)$$

where BP is the average tremor band power while the patient was receiving closed-loop (BP_{CL}), open-loop(BP_{OL}), or no stimulation(BP_{No}).

In order to compare how an algorithm’s delivered stimulation would impact the device’s battery life, we can compare the stimulation power between the open-loop and closed-loop systems with the assumption that the electrode-tissue impedance is constant for the duration of the evaluation. With this assumption, the stimulation amplitude squared (V_{CL}^2) can be used to determine a normalized stimulation power value during the closed-loop trial. By then summing the instantaneous power across the trial and dividing by the total closed-loop trial duration (T), a normalized stimulation power average can be obtained. The algorithm’s power reduction is then determined by dividing the average closed-loop stimulation power by the average open-loop stimulation power (V_{OL}^2) as shown:

$$Pwr = 1 - \frac{\sum V_{CL}(t)^2}{T * V_{OL}^2} \quad (6.2)$$

These two factors can be combined to obtain a single value that represents the trade-off that an algorithm brings to a patient between stimulation power and symptoms. A system

performance metric that can be used to examine the trade-off between stimulation power and tremor mitigation is defined by:

$$M = \frac{Pwr}{100 * Trem} \quad (6.3)$$

where M represents the percent power reduction the closed-loop algorithm delivers for every one percent increase of tremor. Thus, a larger result indicates a higher performance algorithm.

6.4.2 Discussion

In the chapters that follow, I will use this metric to evaluate how closed-loop DBS systems treat patient symptoms. By combining the performance scoring into a single value that indicates the tremor/stimulation trade-off, we also make it easier for future developers of closed-loop systems to benchmark their algorithms. In the future, such metrics will also be useful for presenting algorithm efficiency directly to the clinicians evaluating closed-loop systems for their patient for easy comparison of control options. Higher scores indicate that a system is capable of more efficient treatment of the patient's symptoms. Additionally, by normalizing the parameters used to the untreated tremor level and open-loop stimulation power, we are able to evaluate how a given algorithm performs broadly across patients whose symptoms and open-loop settings are different.

In the future there may be the need for additional terms in the metric as we learn more about engineering closed-loop neurostimulation systems. This may include power consumption from non-stimulation components, such as telemetry, or additional symptom metrics. However, the metric is designed such that it is easily extensible to include additional terms and weighting by adding terms as desired.

Chapter 7

CLOSED-LOOP DBS PROTOTYPES

Before deploying experimental systems on humans, it is imperative that we build robust system prototypes that can be tested to ensure that they will respond reliably in the field. For this reason, I have spent much of my time designing, testing, and iterating benchtop prototypes that demonstrate various closed-loop DBS system concepts without needing a patient in the loop. One difficulty with this however, is that without a model of how stimulation effects sensed parameters, it is impossible to predict the closed-loop response that patients will have to these systems. However, at the minimum, we can ensure system component performance in such a way that patients will be safe during closed-loop experimentation. I have based my prototype systems for evaluation around a generic closed-loop DBS system shown in Figure 7.1. The block diagram illustrates not just the implant, control algorithm, and patient, but also the various sensor data sources discussed in earlier chapters that are available for use when designing a closed-loop system.

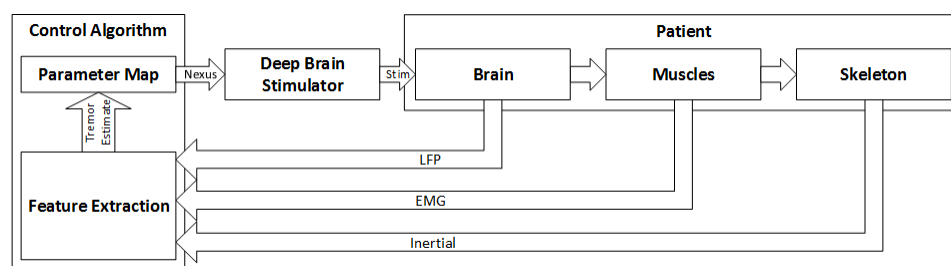


Figure 7.1: **Generic Closed-Loop Deep Brain Stimulation:** A system diagram showing various signal sources informing stimulation parameter adjustment to create a closed-loop DBS system

This generic system consists of computer performing signal processing on sensed data from the patient including local-field potentials from the brain, electromyography from the limb

muscles, and inertial data showing the physical movement of the skeletal system. The aim of this digital signal processing is to create a real-time estimate of the tremor. This tremor estimation would then be used to derive new stimulation parameters for the stimulator to reduce the experienced symptoms.

It is important to consider and the design process and validate performance for closed-loop DBS systems before they are used on patients. Patient time is valuable and their safety needs to be held as a top priority. These considerations lead us to perform substantial proof-of-concept development of example systems that could be used to validate a system without a patient in the loop. While the resulting stimulation and performance of such out-of-the-loop systems are not indicative of final closed-loop performance, they can still give insight into how the engineering tools and algorithms perform at interpreting data and modulating stimulation based on sensed features. This chapter details several examples of proof-of-concept work I performed before working with actual patients.

The first system uses EEG data collected from a healthy individual to trigger stimulation in an unimplanted deep brain stimulator. This system demonstrates an online implementation where data collection, processing, and stimulation parameter adjustment are all occurring simultaneously in real-time. The second prototype is for a bidirectional neuroprosthetic that uses an unimplanted Acliva PC+S as both a sensor and actuator. In this case, stimulation is modulated based on the bandpower estimate of a generated waveform from a signal generator. These two proof of concepts illustrate the validation of each of the system components that were done in preparation for the human trials covered in upcoming chapters.

7.1 On-line Movement Intentions for Real-Time Stimulation

In this section, I demonstrate a prototype system where electroencephalography (EEG) was used as a minimally invasive method to prototype the use of sensed movement indicators to trigger electrical stimulation from a DBS implant. While this is a benchtop experiment using a healthy subject, this system functions in real-time using implantable hardware. This

work represents an important proof-of-concept for developing closed-loop DBS systems that utilize movement intention to trigger stimulation. This work was originally published at the IEEE NER 2015 Conference [49].

Electroencephalography (EEG) is the measuring of the small amplitude electrical signals on the surface of the scalp generated by the brain. It is a well established fact that it is possible to predict periods of limb movement by using EEG [50]. This is accomplished by monitoring the area directly over the area of the motor cortex where limb movement processing occurs. When a patient moves their limb, there is a general desynchronization in the contralateral (opposite side of the brain from the limb) motor cortex [51]. A drop in alpha and beta band power can be measured as the movement-processing neurons begin firing more stochastically as a voluntary movement is executed. Interestingly, imagined movement also has this same desynchronization effect [52].

Even while experiencing tremor, ET patients exhibit this motor cortex desynchronization during movement [53]. Since a patient who suffers from kinetic tremor only experiences symptoms when they perform volitional movements, it is feasible to use intentions measured through EEG as a prediction for when deep brain stimulation should be triggered.

7.1.1 Demonstration System

A block diagram of our experimental prototype is illustrated in figure 7.2. EEG data is being collected from a healthy subject while wearing an inertial motion tracker on the right arm. This inertial data is logged and for allows precise monitoring of when the patient is moving their limb. The EEG data is processed in order to make control decisions as to when the stimulation should be turned on or off. These control decisions are used to update stimulation parameters are sent to the Axtiva PC+S through the Nexus-D. Finally the output stimulation waveform is logged through an analog-to-digital converter connected to the same desktop computer. This extensive system logging allows for substantial post-experimental analysis of overall performance.

To sense movement intention with EEG, I used the gTec Mobilab battery-powered bioam-

plifier. The device samples up to eight EEG channels at 256Hz to be recorded. By making use code provided with this device, the data was accessed in real-time through a desktop computer for our control algorithm. To sense motor intention of the right arm and hand, I placed electrodes as shown in figure 7.3. In order to reduce common-mode noise, a ring of electrodes is placed around the center electrode located at C3. The ring electrodes were then weighted by 1/4 and subtracted from the center electrode. Using the signals of the surrounding neighboring electrodes in this manner is a method for spatial filtering to increase EEG performance [54]. Due to the noisy nature of EEG, the subject kept the rest of their body at rest and their eyes closed and still for the duration of the experiment.

To process the data, I preformed a 1024-point FFT every 0.2 seconds. The spectral power was estimated by summing the FFT output bins corresponding to the 14-25Hz band. When the bandpower falls below a calibrated threshold, the stimulator is enabled and the electrical stimulation is ramped up to a therapeutic level. After the band power recovered

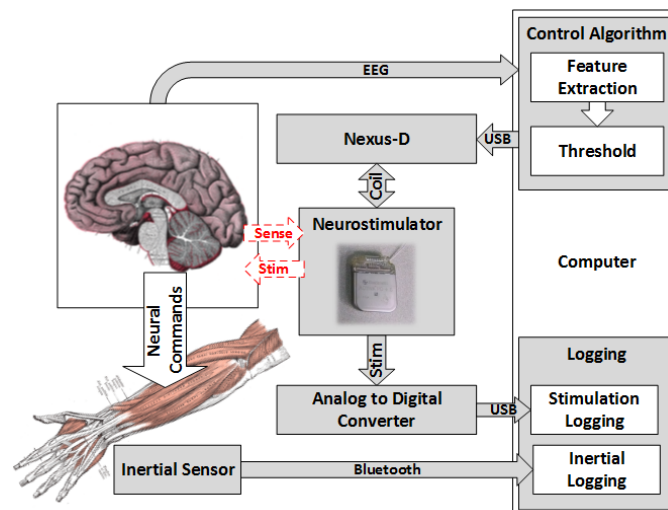


Figure 7.2: **Experimental Setup:** A system block diagram showing the connections between various components for this experiment. Grayed blocks are used in this proof-of-concept setup. Dashed lines indicate the ability for a future implanted system to perform sensing and stimulation directly without need of worn EEG.

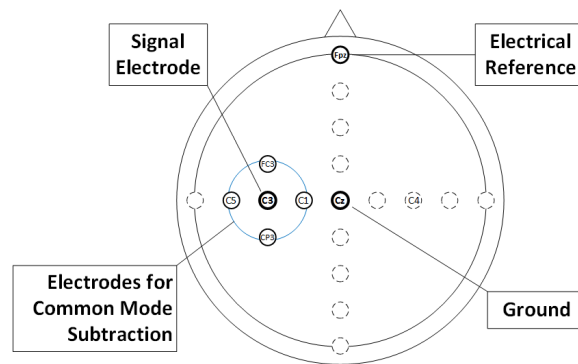


Figure 7.3: **EEG Electrode Positions:** Map of EEG electrodes used. Ground was placed at Cz in the middle of the head. Electrical reference is on the forehead at Fpz. Sensing of motor intention was done with an electrode placed at C3 with a ring of electrodes surrounding it for common-mode subtraction.

and remained above the threshold for two seconds, the stimulation was turned back off.

Once these control decisions have been made, they must be communicated to the implanted device. For this purpose, I once again selected to use the Medtronic Nexus-D. While the sensing ability of the PC+S will be useful for future work using neural signals to trigger stimulation, for these experiments I did not need to make use of this functionality. Using the Nexus-D, our host application running on a desktop PC has the ability to tune and adjust the stimulation parameters of the Activa PC/PC+S within bounds set up by a separate clinician programmer. This allows our program to control the timing of when and how stimulation is delivered..

During the trial run, the subject alternated between periods of rest and movement. The EEG movement intention was used to trigger stimulation in an unimplanted Activa PC+S. With no patient in the loop receiving the stimulation this is not representative of a truly closed-loop system. Instead it is an example of stimulation signals that would be sent while sensing this particular form of data.

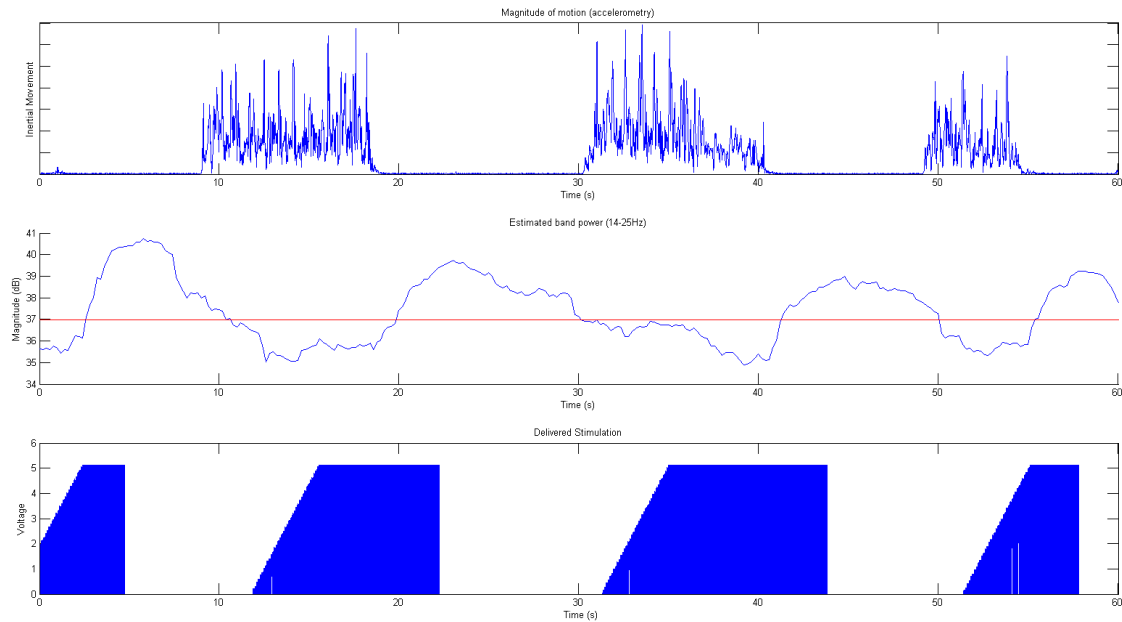


Figure 7.4: **EEG Prototype Stimulation Results:** *Top:* Magnitude of actual movement using worn inertial system. *Middle:* EEG 14-25Hz bandpower estimate. Representative of sensed movement intention. Horizontal line indicates threshold for enabling/disabling stimulation. *Bottom:* Recorded stimulation response from the neurostimulator. The ramping up of stimulation is standard practice due to the way patients perceive stimulation.

7.1.2 Results

The results of an experimental trial run are shown in figure 7.4. The top graph shows the recorded periods of movement using an inertial sensor on the arm being moved. Approximately every ten seconds the subject alternated between periods of limb movement and rest. The middle graph shows the 14-25Hz bandpower estimate from the EEG used to trigger stimulation. As expected, a drop in this bandpower estimate can be used to predict periods when the subject was moving. The tuned threshold used to enable or disable stimulation is shown as the horizontal line in this plot. Finally, the delivered stimulation is shown in the bottom plot. The stimulator is turned on in response to predicted movement and disabled

during periods of rest. The average total power used for stimulation for this experiment resulted in approximately 45% of the power used in an open-loop scenario, which is expected given the simulation conditions.

7.1.3 Discussion

The use of sensors to determine when and how deep-brain stimulation should be delivered has the potential to dramatically upon improve current implanted neurostimulation. By selectively stimulating the patient, the system will be able to extend the battery life of these devices, which will mean fewer battery-replacement surgery over the lifetime of patients. Additionally, for patients that experience side-effects from their stimulation, such a closed-loop system will potentially be able to limit these side-effects to only the time when stimulation is necessary.

There of course are limits to using EEG as a signal source for these closed-loop DBS systems. Most patients would not want to wear a EEG cap in their daily life, surface EEG is noisy due to the impedance of the scalp, and variations in electrode positions would mean the system would have to be calibrated too often to be practical. Instead, this system should be considered a proof of concept for using recorded cortical movement intentions. EEG movement-related signals collected on the scalp are similar to electrocorticography (ECoG) movement-related recordings taken from the surface of the brain [51]. The advantage of ECoG is that the recordings from the surface of the brain are far less noisy and much more stable over time.

The system demonstrated in this section is a proof of concept for experimental work with the use of implanted cortical electrodes as a signal source to determine movement intentions. These implanted cortical electrodes could be placed upon a specific location of the motor cortex directly and an implanted neurostimulator could make use of sensed desynchronization as a trigger for stimulation to treat kinetic tremor. In this sense, such a system would be non-volitional with the option of providing either static stimulation patterns or dynamic stimulation as demonstrated. While there may be concerns of an implanted

device’s ability to sense cortical movement intentions during stimulation due to electrical noise, detecting cortical signals during DBS stimulation has already been shown to be possible [55]. Additionally, if these intention signals are sensed by the same implanted device, there would be no need to communicate with an external computation device. This would allow further reductions in power by removing the high-power real-time telemetry requirements, and the energy cost of performing this sort of spectral analysis on chip has been shown to consume as little as $5\mu\text{W}$ per channel [56].

This proof of concept represents a first step towards the use of movement intentions to trigger deep brain stimulation for the suppression of kinetic tremor. The prototype system I have demonstrated fulfilled our design requirements for a closed-loop DBS system by being able to effectively identify periods of movement using scalp EEG and take action using an implantable neurostimulator. This EEG system was demonstrated in order to prepare for an eventual fully embedded system making use of cortical signals.

7.2 Real-Time Activa PC+S Sensing and Stim Validation

To demonstrate the capabilities of our Nexus C# API and our closed-loop neuromodulation systems I built an open ended test-bed consisting of an array of possible sensor types, all communicating with a single PC that manages a communication channel to an unimplanted neurostimulator. An overview of this prototype system is shown in Figure 7.5. The neurostimulator shown is the Medtronic Activa PC+S, which is capable of both stimulation and sensing from lead electrodes [9]. The Nexus-D system utilizing the modified patient programmer provided by Medtronic is being used to send a variety of commands to control the stimulation and access sensed biopotentials from the electrode sites. This prototyping platform allows for different control paradigms to be considered and tested by using the Nexus C# API. Online or offline sensor data can be streamed in near real-time to modulate stimulation parameters through a defined control algorithm. These systems were originally published as part of a conference paper at the IEEE Norbert Wiener Conference in 2014 [57].

In order to demonstrate a Nexus C# system that utilizes signals sensed by the neurostim-

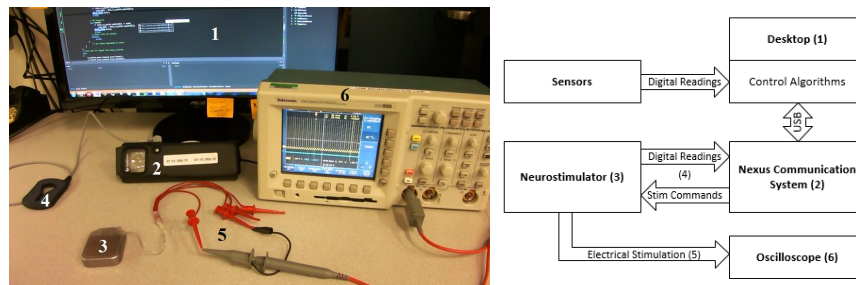


Figure 7.5: **Nexus C# API Demonstration Overview:** Sensors (not shown) send data to a desktop PC (1) running prototype control algorithms. The PC controls the USB connected Nexus System (2). The Nexus communicates to the neurostimulator (3) through a magnetic coil (4). The stimulators electrodes (5) are connected to an oscilloscope (6) to display the current output.

ulator, I used a signal generator connected across two of the four electrodes as a surrogate for a biopotential signal of interest. A noisy sweep function that rested for long periods at one hertz before rapidly ramping up to 80Hz before slowly ramping down was used as a stand-in for a biosignal of interest. The spectral power within a band centered around 80Hz was calculated and used to implement a proportional controller to actively adjust stimulation voltage.

7.2.1 Results

The response of the system to a 80Hz ramp is shown in the time-synchronized plots illustrated in Figure 7.6. It is important to note that the first plot is data recorded directly by the neurostimulator and streamed to the PC over the same channel that commands are sent over. Streaming both sensing data and commands over the shared communication channel is likely responsible for the lag seen in the time it takes for the stimulator to adjust parameters in response to our control actions.

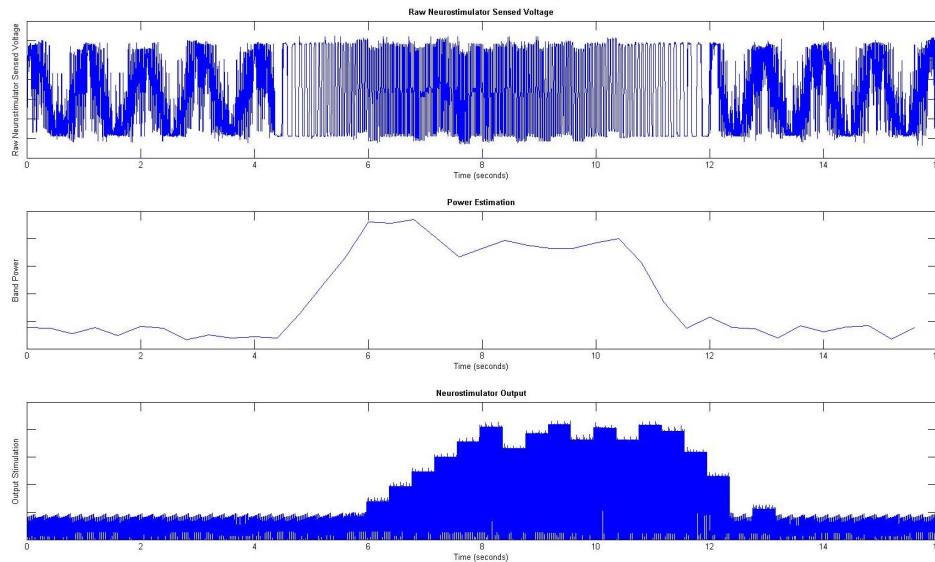


Figure 7.6: **Neurostimulator electrode spectral power mapped proportionally to stimulation voltage:** In the top plot, the raw signal generator output is shown. In this experiment, a dramatic ramping up of the sensed signal to 80Hz was used as our surrogate for a neural signal of interest. This ramping function begins here around $t = 4s$. The signal generator then held the output at a high frequency before slowly ramping back down to the steady state, which is achieved around $t = 12s$. The spectral power of the sensed signal is shown in the middle plot. This power estimation is proportionally mapped to the stimulation voltage level, plotted in the bottom graph.

7.2.2 Discussion

This proof of concept demonstrates our ability to make use of the Nexus-D and Activa PC+S to trigger stimulation in a patient based on data from implanted electrodes. Before making use of such implanted functionality, it is important to build benchtop prototypes to preserve patient safety and time. While actual neural data will look nothing like the tested waveform, the ability to sense spectral changes from the electrodes is the fundamental basis for future neurally closed-loop DBS systems as well as BCI. Additionally, work such as this is required

to design a fully implantable version of the movement intention based system discussed earlier in this chapter. The use of streamed neural data from chronically implanted electrodes is the cornerstone of two of the three aims of this thesis. This project accomplished the technical demonstration of designing a fully bidirectional neuroprosthetic system.

Conclusion

The prototype systems discussed in this chapter were designed in such a way to test each of the various system components required to design the bidirectional neuroprosthetics this thesis aims to implement. The implant interfaces, sensors, and control systems each need to be vigorously tested before interaction with patients. Stimulation limits need to be tested, communication protocols vetted, and real-time responsiveness validated in order to ensure patient safety in the future trials. However, since patients are incredibly variable, the code-base to develop these applications must be incredibly flexible to allow quick iterative prototyping on new algorithms. Through building these different benchtop prototypes, I gained confidence in the real-time performance, safety measures, and flexibility that was designed into the system at every level. From here, experiments with patients are the next step.

Chapter 8

WEARABLE CLOSED-LOOP DBS

In this chapter, I present work done to fulfill Aim 1 of this thesis: demonstrate power savings and investigate side-effect mitigation through wearable closed-loop DBS. Wearable sensors have the benefit of being easily rechargeable and replaceable at the cost of being forgotten or lost. The key advantage of wearable sensors is that they provide a gold-standard measurement for movement-disorder symptom strength. The tremor a patient experiences at a given moment can be easily estimated by measuring the movements of the limb directly. For the work with patients with Parkinson’s, we focus almost exclusively on the use of inertial sensors to trigger and modify DBS stimulation. With our Essential Tremor patient, we have tested the use of both inertial and EMG based systems.



Figure 8.1: A wearable closed-loop DBS system using wearable sensors, smartphone, NexDEX + Nexus-D, and the Activa PC+S.

8.1 Preliminary Wearable CLDBS for PD Rest Tremor

In this section I present a closed-loop DBS system capable of using wearable sensors that can sense tremor and respond by dynamically adjusting stimulation parameters of an implanted DBS device. This work was done in collaboration with Helen Bronte-Stewart’s Lab at Stanford. The Stanford team took care of all patient recruitment and clinical care while I engineered experimental systems to test the use of inertial sensors as a signal source for wearable closed-loop DBS.

In this study, several PD patient’s rest tremor is estimated through the use of inertial measurements taken from worn miniaturized accelerometers and gyroscopes that are mounted in a smart-watch. These tremor estimates are used to calculate updated stimulation amplitudes, which are then transmitted to an implanted Activa PC+S neurostimulator using the Nexus-D communication system by our custom software. As a preliminary demonstration of the wearable closed-loop DBS system, we present the results of several example control paradigms tested with our patients that dynamically modulate stimulation amplitude in response to the tremor intensity that a patient experiences at a given moment. The purpose of these tests is to demonstrate the real-time system’s ability to respond to sensed limb tremor and record the patient’s response to the stimulation. Finally, I conclude with a discussion of the ability of these systems to capture data that will be useful to further enhance clinical treatment options and advance our scientific understanding of the underlying neurological mechanisms that produce movement disorder symptoms.

8.1.1 Methods

First, I will describe the system components, signal processing, and control algorithms used these preliminary experiments. The patient demographics and experimental protocol for the human trials that were performed are then discussed. The basic structure of our closed-loop DBS system is shown in Figure 8.2. Existing implanted systems use an open-loop device to provide therapeutic stimulation. In our work, sensors of physiological symptoms are used to determine when and how this treatment is provided. The mapping of sensed data to stimulation parameter changes, in our case worn inertial measurements mapped to voltage amplitude settings, is handled by extracting symptom biomarkers through signal processing. A configurable control algorithm is then used to determine updated stimulation settings.

In each case, tremor is estimated through the use of a spectral analysis of inertial measurements taken from the LG Watch gyroscopes as described in 5.1. For these experiments, the overall system performance was limited by the slow communication rate through the Nexus-D. The IR serial communication link runs at 38,400 baud and the Nexus-D’s timeout

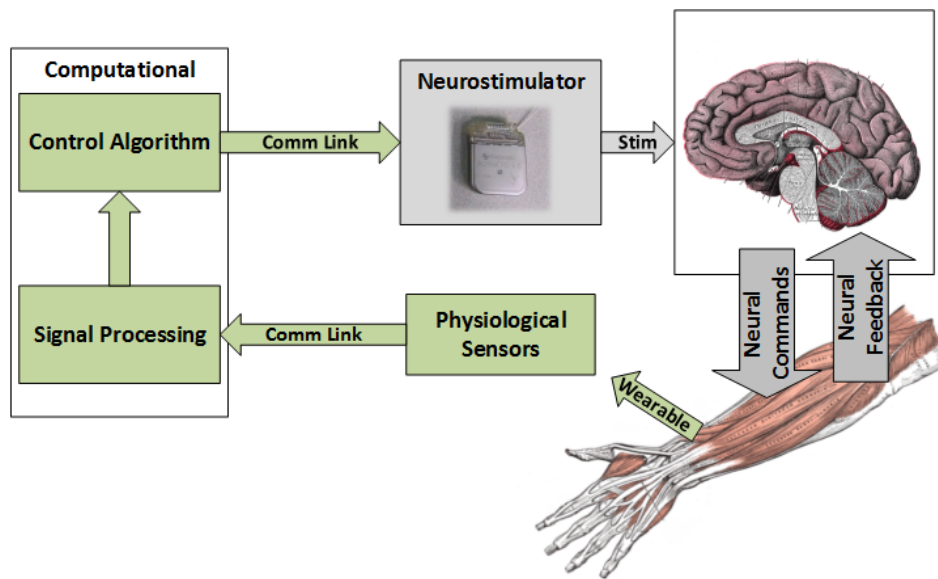


Figure 8.2: **Basic structure of our wearable closed-loop DBS System** While an open-loop system will stimulate the brain continuously to mitigate symptoms, in this closed-loop version the stimulation parameters are dynamically chosen based on sensed limb movements.

periods are at least 250ms for any given packet. Despite the long timeout period, most packets are executed and acknowledged in less than 100ms. In order to balance closed-loop system responsiveness against the limitations imposed by the Nexus-D communication system we selected 5Hz as our data processing rate. Every 200ms, the latest gyroscope data for the x, y, and z axes were shifted into buffers, multiplied by a Hann window, and then transformed into the frequency domain using a 128 long FFT. An estimate of tremor intensity is then calculated using the output spectral band power of the PD tremor frequency range, summed across all three axes of motion. These tremor estimates are used to calculate a new stimulation amplitude. The updated stimulation settings are then transmitted to an implanted Activa PC+S neurostimulator using the Nexus-D communication system.

Control Algorithms

We implemented two simple control algorithms to demonstrate the effectiveness of the experimental platform. The first of these was a threshold-based stimulation adjustment paradigm and the second made use of an additional dynamic baseline stimulation algorithm.

For the first threshold-based system, we used a calibrated threshold-based algorithm where the band power of the tremor was estimated and compared to two thresholds to determine what action the stimulator should take. When the tremor estimate was above the high threshold, the stimulation amplitude would be increased and stimulation amplitude would be decreased when the tremor estimate was below the low threshold. The separation between the two thresholds constituted a dead-band where no action would be taken to change the stimulation parameters.

To calculate the calibrated threshold, we calculate a rolling average of the tremor band

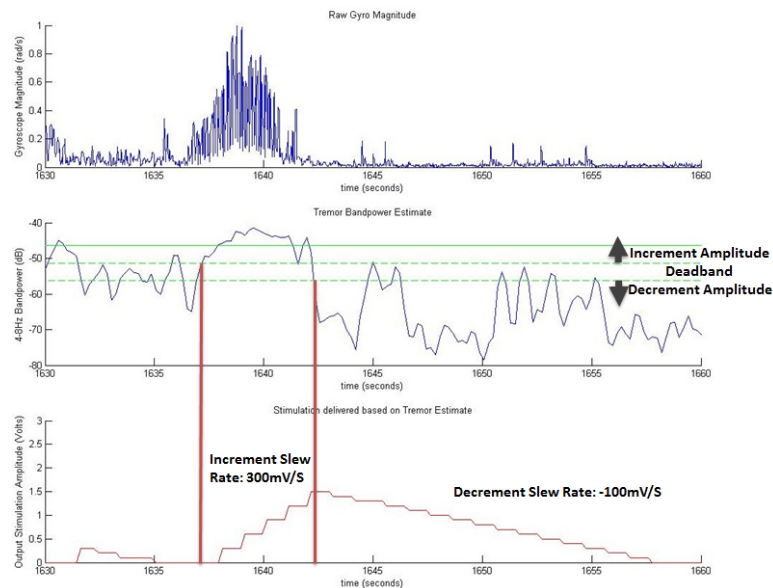


Figure 8.3: **Threshold-based System Overview:** A thirty second clip of a system using tremor thresholding to modulate stimulation. Top graph shows the raw magnitude of the gyroscope in degrees/second. Middle graph shows the tremor estimate during this time period and

power estimate over a ten second period where stimulation is off. When the calibration state is ended the latest rolling average value is used for the remainder of the experiment to determine the levels for the increment and decrement thresholds. For these trials the increment threshold was 30% of the untreated tremor band power and the decrement threshold was 15%. Different stimulation ramping rates were tested with a separate program and the patient reported if they experienced any unpleasant side-effects at different settings. The maximum value of stimulation was set to the clinically derived value of 2.5Volts. The system was ramped up at 0.3 volts/second and ramped down at 0.1 volts/second. The system ramped stimulation amplitude up much quicker than it would ramp it down in order quickly mitigate newly sensed tremor while adding some hysteresis in such a way that symptoms would not instantly rebound.

For the second system, which we refer to as our dynamic baseline algorithm, we separated our control paradigm into two feedback loops: one fast loop to mitigate tremor as quickly as possible, and a second much slower loop to adjust a baseline stimulation to slow the re-emergence of tremor. The system would make use of the same control logic involving dead-bands and thresholds based on a calibration period. However, instead of dropping to zero volts when there is no tremor, the system would drop to some intermediate value. If the patient has no tremor from that point on, this baseline stimulation would drop to zero, but over the course of minutes rather than seconds as performed in the previous setup. If the patient was continuously going in and out of tremor as they had been, the baseline stimulation would instead very slowly rise. This sort of experimental paradigm would potentially allow for both fast mitigation of tremor when we sense it, but also may be able to slow down or lessen the amplitude of reemerging tremor by settling at some non-zero stimulation setting. The system would still be more power efficient, but will hopefully treat the patient better without the oscillations between tremor and non-tremor state.

The baseline controller was implemented using a counter that was initialized to a starting stimulation value in mV, and then incremented or decremented by a configurable amount after every DSP FFT computation based on the state of the tremor estimation. When no

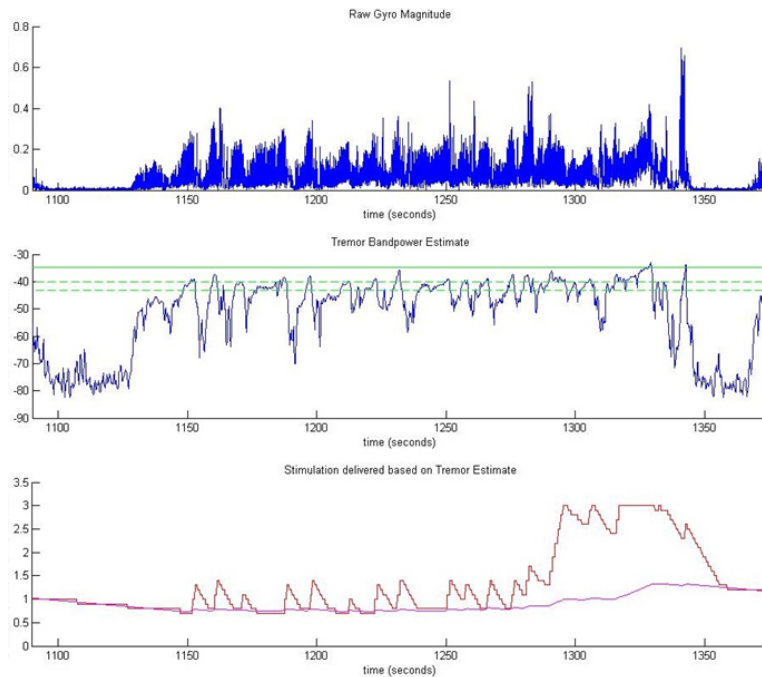


Figure 8.4: **Baseline System Overview:** A close-up of the system’s response when using a dynamic baseline: raw gyro on top (deg/s), tremor estimate (dB) in middle with thresholds, and output stimulation amplitude on bottom. Also shown on bottom plot is the baseline level which slowly responds to the amount of tremor a patient experiences over the duration of the experiment.

tremor is sensed, this value would then be rounded to the nearest 100mV and used as the stimulation level. Over time it would continue to slowly drop in power until tremor is sensed.

Experimental Application Development

Using the Nexus C# DLL that was covered earlier in this thesis (4.1), I developed our experimental code using C# in Microsoft Visual Studio 2013. C# and Visual Studio were chosen due to the ease of interfacing with our C# DLL and creating Windows Forms applications using the integrated tools that Visual Studio provides. The user interface (UI) that was developed is shown in Figure 8.5. It provides the ability for an experimenter to easily manage the experimental states described above through the use of buttons. The UI also includes

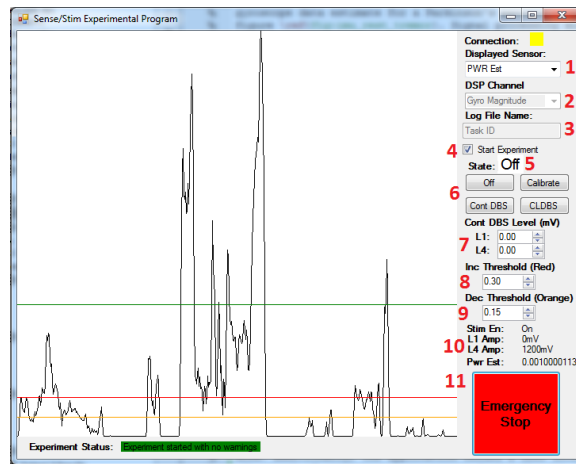


Figure 8.5: **Control Application UI:** This application graphically displays data and enables user interaction with the underlying real-time system. The user interface features include 1: Ability to show real-time data from various data sources; 2: Selection of gyroscope or accelerometer for tremor estimation; 3: custom logging file prefix; 4: experiment enable toggle; 5: system's current state; 6: system state selection; 7: continuous DBS level input; 8: Closed-Loop stimulation-increment threshold; 9: Closed-Loop stimulation-decrement threshold; 10: stimulation status; 11: Emergency stop button

the ability to display data from any inertial axis, FFT output, or the tremor estimations based on a spectral band power estimation. Performance of the program's real-time components were tested in benchtop scenarios over half-hour long sessions. Particular attention was paid to the logging capabilities and responsiveness of the system over the duration of the experiment. All data in the logs were timestamped with the CPU ticks (measured in 100nS) so that responsiveness and performance could be measured with high precision.

When the test algorithms were enabled, the 100Hz sampled inertial data from the LG G watch was streamed to the application over Bluetooth and processed as described above. Depending on the experimental state, the signal processing's output tremor estimate was then compared to tuned thresholds to determine a new stimulation setpoint for a parameter controller running in an independent thread. This parameter controller could then ramp the Activa PC+S output stimulation amplitude up or down to a given setpoint, over any

programmable amount of time. This stimulation slew rate was tunable on a per patient basis in case any unpleasant side-effects from the rate of stimulation change were experienced.

8.1.2 Experimental Evaluation

Human Subjects

All of these experiments took place in the Bronte-Stewart Lab at Stanford University in the presence of a clinical neurologist. The closed-loop DBS systems using inertial sensors were tested in PD patients implanted with the Activa PC+S. The patients had two DBS leads bilaterally implanted in the sensorimotor region of the STN. The leads were implanted using functional frameless stereotactic technique and multi-pass microelectrode recording (MER) [58]. Before trials, all subjects withheld long- and short-acting dopaminergic medication for more than 24 and 12 hours respectively prior to testing. All subjects signed a written consent for the study, which was both FDA and IRB approved. The pre-operative selection criteria, surgical technique, and assessment of subjects have been previously described [59] [58]. The experiments were performed at least 6 months after initial programming visit when the stimulation settings were considered clinically optimized. The stimulation therapy contacts determined by the clinician were used during testing. For all subjects the stimulation frequency was 140Hz and the pulse width was 60 microseconds. Prior to every experiment, a clinician determined safe voltage limits which are hard-coded into the implant through a separate clinical programmer.

Table 8.1 shows the age and disease duration for each subject tested with a control algorithm discussed in the results section. Each patient's motor symptom severity were clinically evaluated using the Unified Parkinson's Disease Rating Scale (UPDRS III). The lateralized UPDRS III scores were taken off medication and off DBS at initial programming visit. The patient's lateralized UPDRS III scores were also taken while off medication and on DBS before testing closed-loop algorithms.

| Subject | Age | Disease Duration | Implanted Time | Tested Limb | UPDRS Off DBS | UPDRS On DBS | Clinical Amplitude |
|-------------|-----|------------------|----------------|-------------|---------------|--------------|--------------------|
| Threshold 1 | 69 | 12 years | 10 months | RHand | 15 | 2 | 2.5 Volts |
| Baseline 1 | 63 | 2 years | 18 months | LFoot | 21 | 1 | 3 Volts |
| Baseline 2 | 72 | 9 years | 7 months | RHand | 15 | 6 | 2.6 Volts |

Table 8.1: **Subject Patient Demographics:** Subject ID refers to which experimental trial the subject participated in as described in the results section. Disease duration is when symptoms were first reported by the patient. Reported UPDRS scores for each patient are total lateral UPDRS III scores for the limb tested while off medication.

Experimental Procedure

During the experimental testing, we focused our efforts on one side of the body only. This was so that only one STN was stimulated in order to reduce possible experimental variables that may be introduced from performing bilateral stimulation. Subjects were resting in a sitting position with the contralateral hand on the contralateral leg and the ipsilateral arm placed on a pillow to isolate any transmission of ipsilateral side tremor to the inertial sensor. This position allowed one IMU sensor to capture the tremor of both contralateral limbs. The patient was asked not to perform any voluntary movement with the contralateral limbs, but was allowed to talk and involved in a conversation with the intention to keep his attention away from his rest tremor. Stimulation slew rates were tested before every trial to ensure that the patient would not experience any unpleasant side-effects from the maximum rate of stimulation change selected for the experiment.

There were four program states used during testing of these closed-loop algorithms with patients that composed a full experimental trial. First, the patient started in an off-state while the experimenter ensured that sensors and the Nexus-D were connected and functioning properly. The experimental system was then calibrated while the patient was experiencing tremor with no stimulation being delivered. This was done to tune the tested closed-loop

algorithm to a specific patient’s tremor level during no stimulation. For these experiments the calibrated value was derived from a rolling 10-second average of the tremor during the calibration period. The test algorithm’s closed-loop DBS state was then enabled. Finally, patient responses to continuous DBS were recorded in order to compare results between closed-loop and open-loop performance. Throughout the entire trial, all wearable data, state, spectral estimates, stimulation amplitude, and other experimental parameters were constantly logged to file.

8.1.3 Experimental Results

Threshold-based Stimulation Testing

In order to demonstrate the threshold-based algorithm described in the methods section, we took the opportunity to run two trials on a single patient. Each trial used a single wearable sensor on the wrist to trigger stimulation changes on the DBS lead used for clinical tremor suppression on that limb. We tested the system first on the right arm and then the left.

The right hand’s tremor response to the threshold-based closed-loop system (shown in Figure 8.6) oscillated between treated and untreated states. This is potentially due to the fact that system’s overall gain was too high, never allowing the tremor to settle within the dead-band. Instead, the stimulation would rapidly bring the tremor to zero, which the system would then respond to by lowering the stimulation amplitude. Tremor often would not resume until some variable time after the stimulation amplitude was zero volts, upon which it would then re-emerge to untreated levels very quickly. This large number of bursting re-emergences of tremor can be compared to the open loop case at 2.5V where the patient only experienced one small and short period of tremor near $t = 1300s$.

During open-loop 2.5V stimulation, the open-loop system reduced the average tremor band power to 0.45% of the tremor band power before the experiment began when there was no stimulation. Additionally, the patient had tremor above our calibrated threshold only 0.35% of the duration of open-loop stimulation. During closed-loop operation the average

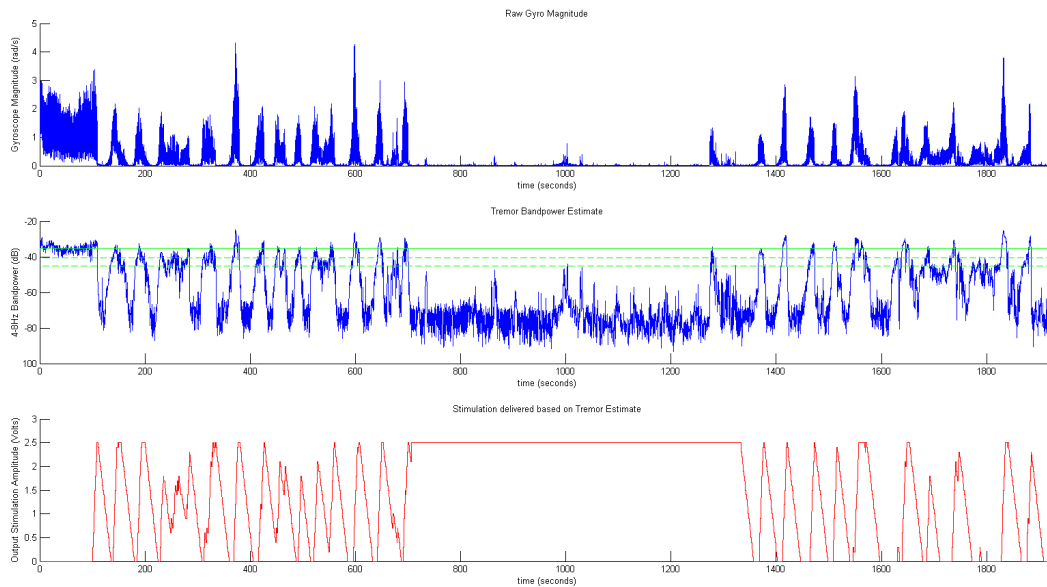


Figure 8.6: **Right Hand:** No stimulation before $t = 100$ s; closed-loop between 100s and 706s; open loop between 706s and 1332s; closed-loop after 1332s. *Top-* Three axis gyroscope sensing magnitude (deg/s). *Middle-* Tremor estimate in blue, calibrated no stimulation level in green, dead band thresholds in dashed green. *Bottom-* Delivered stimulation amplitude in volts.

tremor band power was 27.2% of the average no stimulation band power and the patient experienced tremor above our threshold for 19.8% of the total trial duration. The closed-loop paradigm in this experiment however, resulted in an average stimulation amplitude of 1.01 volts, which corresponds to a drop in stimulation power of 83.7%.

In contrast to the right hand, the left hand's tremor was far more intermittent, which can be seen clearly in Figure 8.7. This meant that after mitigating the tremor, it could often be minutes until the tremor re-emerged. While the open-loop system caused only one instance of tremor compared to the 5 in each closed-loop trial, the bursts of tremor were quickly mitigated for extended periods of time when compared to the our previous trial. There are periods of the closed-loop experiments where there is no reemergence of tremor for minutes at a time. This patient's tremor was reduced to 5.3% of the calibration tremor during 2.5V open-loop stimulation and was above our threshold for 2.8% of the open-loop test. The

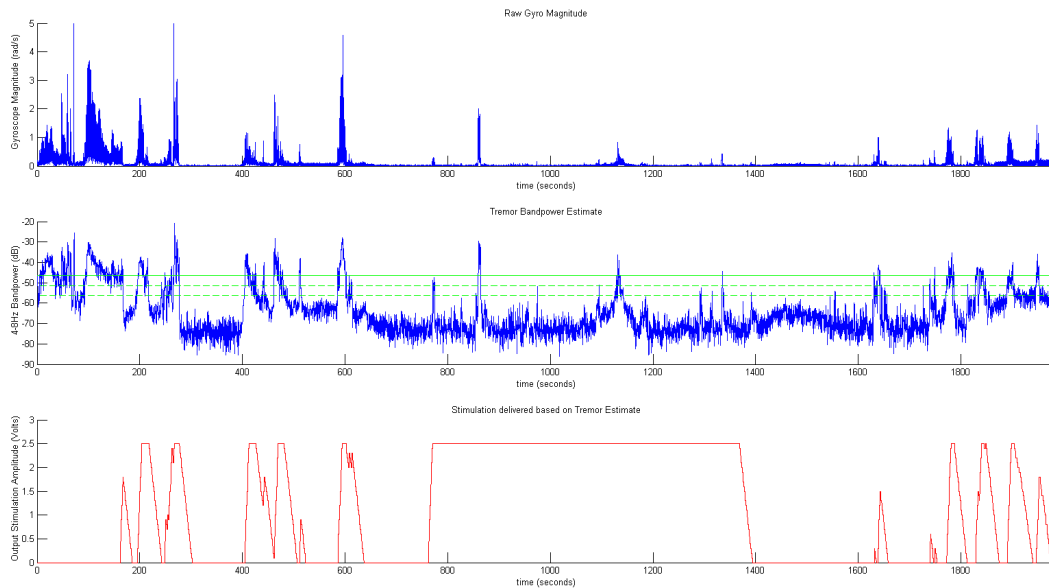


Figure 8.7: **Left Hand:** No stimulation before $t = 161$ s; closed-loop between 161s and 762s; open loop between 762s and 1390s; closed-loop after 1390s. *Top-* Three axis gyroscope sensing magnitude (deg/s). *Middle-* Tremor estimate in blue, calibrated no stimulation level in green, dead band thresholds in dashed green. *Bottom-* Delivered stimulation amplitude in volts.

closed-loop system was able to reduce the total tremor the patient experienced to 16.8% compared to the no stimulation case, and the patient's tremor was above our dead-band for 12.7% for the duration of the closed-loop trials. The average stimulation amplitude for the closed-loop system was 0.59 volts, a reduction of stimulation power by 94.4%.

Dynamic Baseline Stimulation Testing

For the baseline-adjustment closed-loop system, we had the opportunity to run this system on two patients and collect the real-time response of each patient to the system prototype. The voltage ramping rates and maximum levels were tested for the each patient in order to ensure that the patients did not experience unpleasant side-effects during the trials. In the first patient we tested the slew rate for the fast tremor response system and it was selected to be 0.3 volts per second for the incrementing rate and 0.1 volts per second for the

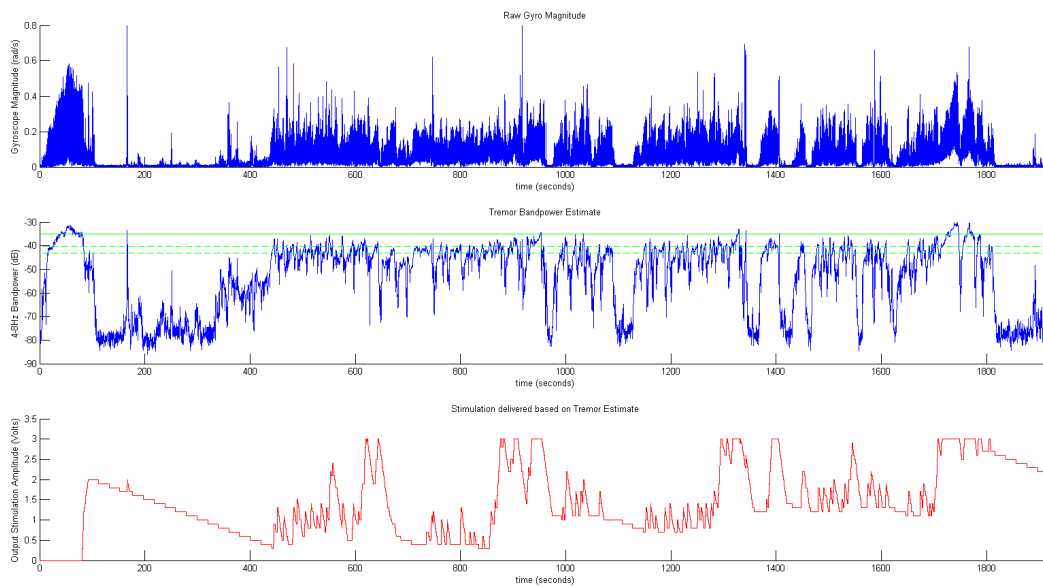


Figure 8.8: **Dynamic Baseline Trial 1:** No stimulation before $t = 80$ s; closed-loop after 80s. *Top-* Three axis gyroscope sensing magnitude (deg/s). *Middle-* Tremor estimate in blue, calibrated no stimulation level in green, dead band thresholds in dashed green. *Bottom-* Delivered stimulation amplitude in volts.

decrementing rate. The baseline stimulation was initialized at 2 volts and incrementing by 100mV every 4 seconds of continuous tremor and decrementing by 100mV every 20 seconds without tremor. The pre-trial parameter testing determined that the maximum stimulation level for this patient with no side-effects was 3V.

The first trial with this system demonstrated that the technical integration of the two amplitude controllers worked to specification. The baseline was continuously adjusted as tremor was estimated and the fast loop was used whenever the estimate was above the threshold. As shown in Figure 8.8, the response of the patient's tremor to the system was far less oscillatory and there were no longer the distinctive treated/untreated states that were present in the previous trials. Additionally, the tremor estimate was consistently less during the closed-loop paradigm than in the calibration period. The exception to this is at the end of the experimental trial near 2200 seconds. At this time, despite a high level of baseline stimulation, tremor strongly reemerged back to no-stimulation levels. On average the closed-

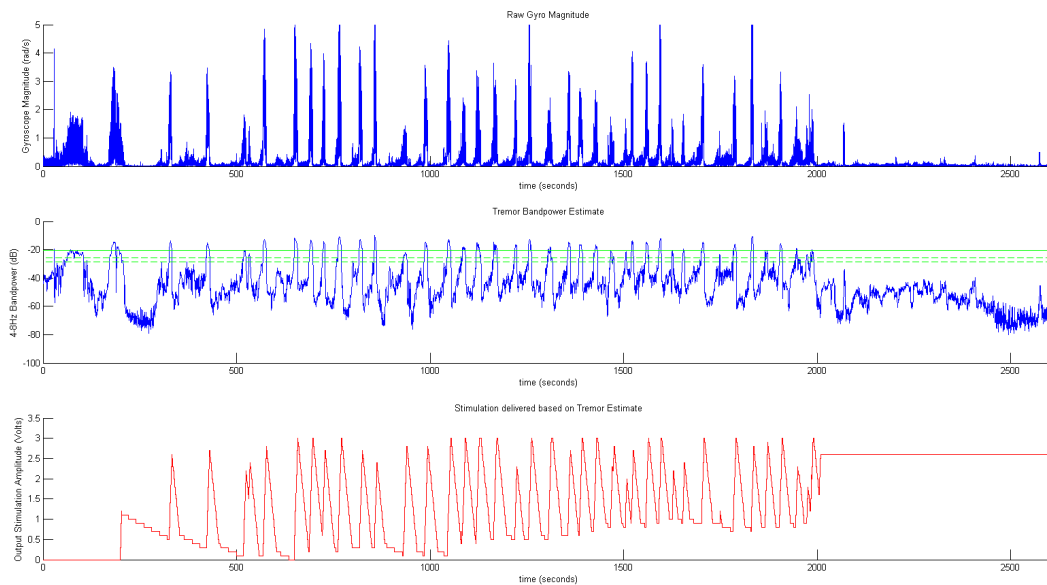


Figure 8.9: **Dynamic Baseline Trial 2:** No stimulation before $t = 200$ s; closed-loop stimulation between 200s and 2011s; open loop stimulation after 2011s. *Top-* Three axis gyroscope sensing magnitude (deg/s). *Middle-* Tremor estimate in blue, calibrated no stimulation level in green, dead band thresholds in dashed green. *Bottom-* Delivered stimulation amplitude in volts.

loop system was able to reduce the patient’s tremor to 19.4% of the no stimulation level, and the patient experienced tremor above our calibrated dead-band 14.0% of the duration of the trial. This system’s average stimulation level was 1.49 volts, which represents a reduction in stimulation power by 75%.

The second patient we tested with this system went through the similar stimulation parameter testing and calibration that the other patients were asked to perform. For the fast tremor mitigation loop, the stimulation amplitude slew rates were the same as the previous patient with 0.3 volts per second upward and 0.1 volts per second downward. The baseline controller used was the same as the first trial for Baseline-1: incrementing 100mV every 4 seconds of tremor and decrementing by 100mV every 20 seconds without tremor. This patient was given 30 minutes of closed-loop therapy before 10 minutes of open-loop stimulation at their clinical setting of 2.6 volts. In this case, the closed-loop system was

determined to be able to stimulate at above the clinical setting at a maximum of 3 volts due to the patient not reporting any side-effects at that level.

The results of the experiment with the second dynamic baseline adjustment are shown in Figure 8.9. Despite baseline seeming to reduce the oscillatory responses in the other patient, the results from this subject show a return to large oscillations between treated and untreated states. One difference between the two patients is the speed with which this patient responds to stimulation to mitigate tremor. While in the first dynamic baseline trial there were many times where stimulation would saturate to three volts for tens of seconds (and several instances of minutes at a time), in this trial the stimulation amplitude never remains at the peak value for more than five seconds at a time. Additionally, many of the peak tremor estimations are far above the tremor seen during the calibration period. Quantitatively, the open-loop stimulation resulted in 0.2% of the average band power of the no stimulation period, and there was no period of time that the tremor was above our calibrated dead-band. The patient's average tremor during the closed-loop experiment was 95% of the no stimulation tremor, but the tremor was limited to 16.2% of the trial duration. When it comes to power efficiency, the closed-loop system's average stimulation amplitude was 1.27 volts, which is a 76% drop in power over the open-loop case.

Compiled Quantified Results

Note that in all cases there is a qualitative decrease in average stimulation amplitude at a cost of an increase in tremor when comparing closed-loop to open-loop performance. Using the metric introduced in 6.4, the quantitative performance of the four trials are presented in a single table shown in table 8.2. For these example closed-loop algorithms, the stimulation power reduction ranged from 56% to 82%, while the tremor difference between closed-loop and open-loop ranged from 11% to 94% of the tremor while receiving no stimulation. The metric column for the trials illustrates the variation in system performance a single algorithm can have across patients or limbs. The best result was the use of the thresholding system on the left hand, where the system provided a 7.2% decrease in power for every 1% increase

in tremor. The baseline algorithm performed the worst for the second patient whose tremor regularly returned at a very high amplitude. For this patient, the system only provided a 0.7% decrease in power per percentage point of increased power.

8.1.4 Discussion

In this section I have presented an experimental closed-loop deep brain stimulation platform that makes use of wearable sensors to dynamically modulate stimulation parameters in response to sensed symptoms. To demonstrate the technical functionality of this system, two

| | Open-Loop Results | | | Closed-Loop Results | | | CLDBS Metrics | | |
|---------------|-----------------------|---|--------------|---------------------|---|--------------|---------------------|------------------------|--------------------|
| Patient Trial | Stim Amp (V_{OL}) | Tremor $\left(\frac{BP_{OL}}{BP_{No}}\right)$ | Tremor Time% | Avg Stim Amp | Tremor $\left(\frac{BP_{CL}}{BP_{No}}\right)$ | Tremor Time% | Stim Red. (Pwr) | Tremor Inc. ($Trem$) | Perf. Met. (M) |
| Th RH | 2.5V | 0.45% | 0.35% | 1.01V | 27.2% | 19.8% | 72.2% | 26.7% | 2.7% |
| Th LH | 2.5V | 5.31% | 2.75% | 0.59V | 16.8% | 12.7% | 82.6% | 11.5% | 7.2% |
| BL 1 | 3V | 0% | 0% | 1.49V | 19.4% | 13.0% | 56.9% | 19.4% | 2.9% |
| BL 2 | 2.6V | 0.28% | 0% | 1.27V | 95.1% | 16.2% | 66.4% | 94.8% | 0.7% |

Table 8.2: **Closed-Loop Performance Metrics:** “Stim Amp” is a constant for open-loop trials but is an average over the entire trial for closed-loop values. “Average Tremor” values are dividing the average tremor band power in the loop mode by the average tremor band power with no stim. “Tremor Time %” is the portion of trial where the tremor band power is above the threshold to increase stim. “Stim (Power) Red.” is the reduction in stim power across the closed-loop trial when compared to the open-loop stim trial. “Tremor Inc.” is the increase in tremor the closed-loop system results in compared to the open-loop case. The final closed-loop performance metric is based on equation 6.3. Note: BL1 open-loop tremor was not collected as part of the trial but the patient was clinically evaluated to have no tremor with DBS on.

simple control schemes were tested to treat the rest tremor of three patients with Parkinson's disease.

One key advantage of this platform is that it is versatile enough to allow for testing different signal processing and control algorithms. Additionally, while the simple preliminary systems that we have discussed in the results section were not able to completely eliminate tremor in any patients, they show the technical feasibility of exploring dynamic stimulation adjustment for future work. The real-time platform for Nexus-D and Activa PC+S applications allow for integration with other sensors as well as the simple adjustment of signal processing methods. Furthermore, we have the ability with this system to test more advanced control policies than the simple threshold based systems discussed. The ability to explore control algorithms and the neurological responses to these dynamic systems is a powerful tool for collecting data that will be required to model and understand the mechanisms of the diseases and symptoms that DBS treats. The data that these systems record contains a useful window into the underlying phenomena of both how the diseases manifest and how DBS treats them. Improving our scientific understanding of these systems through exploring system dynamics and control applications may shed light on how to better treat these diseases, and improve patient quality of life, in the future.

There also are many opportunities for future work on closed-loop DBS with wearable sensors to improve their clinical use in treating tremor. While the systems we produced only responded to tremor that the patient was already experiencing, it may be possible with other sensors or signal processing techniques to predict the onset of tremor based on body pose, patient intent, or neural signals. If a patient's tremor could be accurately predicted from behavior before symptoms arose then a wearable system would be able to preemptively increase stimulation amplitude to suppress symptoms before they arise. Such a system may have better results in a mixed-task trial where the patient alternates between rest and activity to more closely mimic everyday life. On the control algorithms side, the diversity of the possible control policies likely drive the need for system modeling based on the data being collected. Long-term data on the relationship between stimulation and symptoms

may allow for the development of patient-specific control policies based on some form of input-output modeling. Additionally, while we only adjusted stimulation amplitude in these experiments, we also have the ability to explore the effect of dynamically modulating pulse width or stimulation frequency.

8.1.5 Conclusion

To summarize, we have demonstrated closed-loop DBS systems that perform dynamic parameter adjustment using wearable inertial sensors. While the results of our four case studies vary, they should be considered a starting point for future investigations. These dynamically adjusted closed-loop systems are important tools for collecting data that will aid in learning more about the complicated neural system involved in PD. As we gain more knowledge about these neural systems, designing adaptive stimulation algorithms using external wearable sensors will become easier. Regardless, the ability to dynamically determine and update stimulation parameters in an implantable neuromodulation device is exciting due to the potential for improving clinical treatment of a wide variety of neurological disorders. Furthermore, observing how these dynamic closed-loop systems interact and modulate neurological disorder symptoms will also increase our scientific understanding of the neural mechanisms that give rise to these disorders.

8.2 Wearable CLDBS for Essential Kinetic Tremor

For ET patients who experience tremor during intentional movement, stimulation changes could be triggered based on sensors that either indicate tremor or identify volitional movement. Wearable inertial or electromyographic (EMG) sensors are both attractive options due to their ability to monitor a patient’s limb movements directly [57]. Another potential signal-source to determine when a patient will experience tremor is the motor cortex [49]. Beta-band desynchronization in the motor cortex has long been known to be associated with intentional movement of the limb, and these signals can be clearly observed using either electroencephalography (EEG) on the scalp [50] or with electrocorticography (ECoG) on the

brain surface [53]. Using either type of signal may allow systems to automatically determine when and how stimulation is needed, allowing the patient to experience side-effects only while actually using their arm. Additionally, such systems may allow an increased device battery life due to the reduced amount of stimulation they output.

This work was done at the University of Washington in collaboration with Andrew L. Ko, Margaret Thompson, and Tim Brown. To investigate the usefulness of both dynamic stimulation adjustment and cortical neural sensing in ET patients, Andrew Ko implanted a single ET patient with a stimulation lead in the ventralis intermedius nucleus of the thalamus (VIM), and a subdural electrode strip over the patients motor cortex, connected to an Activa PC+S DBS generator. This sensed data can be streamed to an external computer where it can be logged, control external devices, or trigger stimulation changes. In the following case report assembled by our collaborative team, we describe the patient’s clinical data, the surgical outcomes, and the results from several preliminary experimental sessions with the patient. I was responsible for experimental design, technical system integration, data analysis, and performing the experiment with our patient. The ability to deliver dynamic stimulation in a closed-loop fashion was demonstrated in this work using data gathered from wearable inertial and EMG sensors on the affected arm.

8.2.1 Patient History and Surgical Information

History and examination

A 58 year-old right-handed man presented to his neurologist with an action tremor noted for about four years. This tremor affects mainly his right upper and right lower extremity with minimal left-sided symptoms and no head or voice tremor. Tremor is not present at rest and worsens with intentional movement. He does not have any history suggestive of REM behavior disorder, constipation, postural dizziness, gait, or balance problems. He has had no exposure to dopamine antagonists. His tremor became more severe over two years, which significantly impacted the activities of his daily life (particularly when eating and drinking).

The patient does not drink alcohol and does not note that it improves tremor. The patient's family history is unknown as the patient was adopted. Propranolol did not have significant benefit, and a trial of primidone was not tolerated due to side effects.

On neurological examination, his affect and speech are normal. He scored 29/30 on the MoCA. He has no hypomimia or hypophonia. Cranial nerves 2-12 are intact. He has no motor or sensory deficits. He has no ataxia. Rapid alternating movements are normal and symmetric. Gait and arm swing are normal; he rises from a chair briskly without using his arms. He independently recovers with one step on the retropulsive pull test.

Pre-surgical evaluation

The patient had no head or voice tremor, and no tremor at rest. On the right side, his tremor was evaluated to be severe during action and while holding posture. On his left side he had minimal-to-no tremor. The Fahn-Tolosa Marin Tremor Rating Scale (TRS) was used to evaluate tremor severity preoperatively (Scores - Part A: 13; Part B: 10; Part C: 10). Preoperative gait and balance evaluations were performed, with no fall risk identified on the Berg Balance Test (55/56), Ten-meter Walk (1.6m/s) and Dynamic Gait Index (22/24). Pre- and peri-operative imaging revealed no concerning anatomic lesions. A DATscan showed no evidence of nigrostriatal degeneration. MR imaging obtained for operative planning included a 3T volumetric T1 MPRAGE sequence (1.5mm slice thickness, 512 x 512 matrix, FOV 250).

Operative procedure

Surgical treatment options were discussed with the patient and informed consent for implantation of DBS targeting the left Vim was obtained. Separately, in concordance with IRB and IDE regulations, research staff approached the patient and he was enrolled in this study.

The patient was brought to the OR and IV sedation was initiated. He was positioned supine, and the head was placed in 3-point fixation using a skull clamp and long Doro Radiolucent Transitional Members (Pro Med Instruments, GmbH, Freiburg, Germany) after infiltration of pin sites with local anesthetic. Bone fiducials (Medtronic, Inc., Minneapolis,

MN) were affixed to the skull and an intraoperative CT scan (1.25mm slice spacing, 512 x 512 matrix, FOV 250) was obtained using the Ceretom scanner (Neurologica, Inc., Danvers, MA). CT and MRI were merged using Framelink (Medtronic, Inc.) and an operative plan targeting the left Vim was created. Hand motor cortex was identified anatomically, and scalp overlying this target was marked in indelible marker.

Placement of the electrode was performed using the NexFrame (Medtronic, Inc.) frameless stereotactic system as previously described [12], with the following modifications. After securing the Stimloc (Medtronic, Inc.) burr hole cover to the skull and prior to placement of the NexFrame base, dura was opened widely in a cruciate fashion. A Resume II (Medtronic, Inc., Model 3587) electrode was introduced into the subdural space directed toward hand motor cortex. A channel was drilled into the Stimloc burr hole cover for egress of this electrode. The thalamic lead (Medtronic Inc., Model 3387) was then placed at target. An intraoperative CT was then obtained to confirm location of the thalamic electrode and cortical strip. Vector error to target was 0.3 mm for the thalamic electrode. Cortical electrodes were adjusted such that two contacts were over presumed hand motor cortex and two over hand sensory cortex. The patient was allowed to awaken for macroelectrode stimulation testing. He exhibited a robust microlesion effect with nearly complete extinction of tremor. Testing for side effects, with bipolar stimulation (Contact 0- 3+, 90 microseconds pulse-width, 130 Hz rate) showed no side effects up to an amplitude of 4.0 V, when transient paresthesias were noted. At 5.0 V he exhibited mild dysarthria. The patient was re-anesthetized, electrodes were secured and closure of soft tissues proceeded in standard fashion.

One week later, the patient underwent implantation of the Activa PC+S generator (Medtronic, Inc.) under general anesthesia without complication.

Postoperative course

At the patients first postoperative visit two weeks after generator implant, he continued to show micro-lesion effect but with minimal return of tremor. Monopolar mapping was performed, with no lasting side effects seen with stimulation up to 4.0 V (PW: 90 usec; rate:

130 Hz). Six weeks after surgery, he was programmed with the following settings: Electrode configuration, 2+ 1-; PW, 90 usec; Rate, 130 Hz; amplitude 3.7 V. When he returned 10 weeks postoperatively, he noted transient paresthesias when the system was turned on and off. He was re-programmed to his current settings, with an electrode configuration of 2+1-, PW of 90 usec, rate of 150 Hz and amplitude 2.5 V. His TRS scores with stimulation have been greatly improved (Part A: 1, Part B: 3).

8.2.2 Closed-Loop DBS with Wearable Inertial and EMG Sensors

To demonstrate CLDBS using this system, the patient was asked to move his hand from his lap and hold it in front of his nose. This task consistently evoked tremor in a stimulation-off state. We collected inertial and EMG data from the trembling limb while he performed this action, and used the sensed data to trigger stimulation changes in real-time. For the first system, we used the inertial sensor to deliver stimulation based on the presence of tremor. The system would increment or decrement stimulation based on the magnitude of the tremor band power between 4-8Hz. For the second system, we used EMG to trigger stimulation changes whenever the patient volitionally moved the limb. To accomplish this we attached four EMG electrodes to the patients arm (bicep, triceps, anterior forearm, posterior forearm) and triggered stimulation whenever the total EMG band power (4-50Hz) summed to a value larger than a calibrated threshold. The experimental results of the patients responses while using these systems is shown in Figure 8.10.

The plot is separated into four distinct system states: no stimulation, open loop stimulation, IMU tremor-modulated stimulation, and EMG movement-triggered stimulation. As can be noticed from the top gyroscope magnitude plot, there are large peaks whenever he started or stopped movement, which carry over into the middle 4-8Hz band power plot. These artifacts are due to the cross-band frequency components of initiating movement and the arm impacting the lap when the task was complete. In order to remove these artifacts and determine a quantified estimate of the actual tremor the patient was receiving, we multiplied the tremor band power by the proportion of the tremor band over the total band

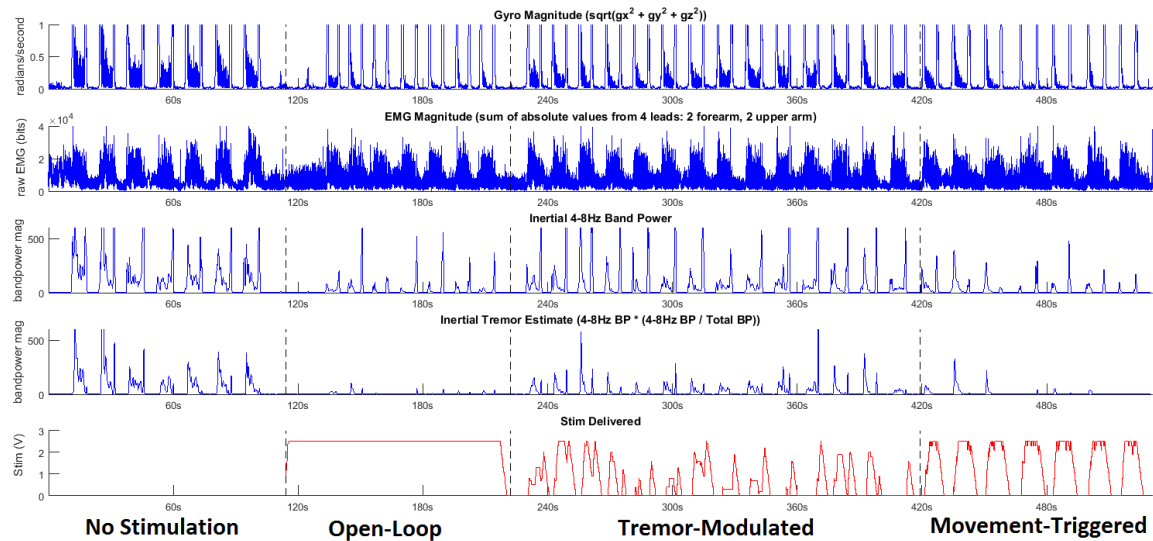


Figure 8.10: **Closed-Loop DBS Results:** Time-domain plots of experimental closed-loop DBS trial. *Top:* Gyroscope magnitude plot over the duration of the trial. Large peaks are movement initiation and impact events. *Second:* Magnitude of the raw EMG recorded through the trial, summed across four leads on upper limb. *Middle:* Gyroscope band power in the 4-8Hz frequency range. Note movement initiation/impact artifacts are still present. *Fourth:* Tremor intensity estimate taken by weighting the tremor band power by the proportion of the tremor band power of the total band power. Note still representative of tremor, but with smaller effects of initiation and impact. *Bottom:* Stimulation delivered to patient in each of the four states.

power. This takes advantage of the large cross band nature of the artifact and results in good removal of the initiation/impact events, as can be seen in the fourth plot.

With a quantified estimate of the tremor throughout the trial, we can then assess the amount of tremor the patient experiences while performing the limb movement in each of the four states. The quantifiable metrics of tremor and power usage during the open-loop, tremor-modulated, and movement-triggered trials are compiled into Table 8.3. The tremor experienced by the patient in each state is normalized to the open-loop tremor. The stimulation power difference is determined by comparing the closed-loop stimulation power with the open-loop settings. The final performance metric represents the trade-off

| | Open-Loop | | Closed-Loop | | CLDBS Metrics | | |
|--------------|-----------|------------------|--------------|------------------|-----------------|-------------|-------------|
| Control Mode | Stim Amp | Untreated Tremor | Avg Stim Amp | Untreated Tremor | Stim Power Red. | Tremor Inc. | Perf. Met. |
| Tremor | 2.5V | 5.3% | 0.7V | 41.6% | 84.5% | 36.2% | 2.3% |
| Movement | 2.5V | 5.3% | 1.4V | 13.5% | 53.2% | 8.2% | 6.5% |

Table 8.3: **Quantified Closed-Loop DBS Results:** “Stimulation Amplitude” is determined by taking the average stimulation amplitude over the entire time duration in a given state. “Untreated Tremor” values represent the percentage of the no stimulation tremor that the system cannot suppress. They are determined by dividing the average tremor band power in the each mode by the average tremor band power with no stimulation. “Stim Power Red.” represents the average stimulation power reduction that a closed-loop system provides over the open-loop case. “Tremor Inc.” represents the increased tremor that the closed-loop system provides compared to the open-loop system and normalized to the no stimulation case. The final “Performance Metric” is the proportional trade-off between stimulation power savings and increased tremor for the closed-loop system.

between power and additional tremor the patient would experience while using the closed-loop system when compared to the open-loop version as discussed in the previous section 6.4. While using the EMG-based movement sensing system, he experienced an additional 8.2% of tremor while decreasing power usage by 53%, which is a 2.3% gain of power efficiency for every 1% of additional tremor. With the tremor-modulated system, the patient experienced much higher power savings of 84.5% at the cost of significant (41.6%) additional tremor, resulting in 6.5% less power for every 1% increase in tremor.

8.2.3 Discussion

The results from our preliminary CLDBS trials indicate that the patients tremor can be reduced while receiving selective and dynamic stimulation. For this patient and these algorithms, the EMG-based movement-triggered system performed better during these trials

than the IMU tremor-modulated system. This is may be due to the inertial systems requirement that tremor be present in order to respond. Thus it is expected that there will be additional tremor when compared to the open-loop or EMG movement-triggered case. For the EMG movement-triggering system, it is important to note that the patient may make movements that do not result in tremor, but the system will still trigger stimulation. Thus, the EMG movement triggering algorithm may result in unneeded stimulation when used outside of the clinic. However, this may still provide a large enough reduction in stimulation power to be of benefit. Future work will examine the prediction of tremor and determining the optimal amount of stimulation to treat it in real-time.

It is also worth considering the patients perspective on the possibility of closed-loop DBS and the need for power conservation. During several conversations with him across several research visits, the patient was very interested in conserving his implanted battery for multiple reasons. At his first research visit, he was taken aback at how much the neurostimulator protrudes from his chest; he wondered if a system that conserves battery power could be built with a smaller battery and, thus, a thinner profile. At subsequent visits, he noted that he keeps his stimulator turned off 95 percent of the time: he only turns the stimulator on so that he can eat without tremor symptoms. When asked why he turns his stimulator off, he explained that he wanted to conserve his battery in the hopes of avoiding follow-up surgery. A closed-loop system would make it possible for the patient to conserve battery power without manual intervention. These conversations suggest that saving power is worth some additional tremor for some patients. It may be that future closed-loop systems may not need to reach the same level of tremor reduction as an open-loop system before being an attractive treatment option for some individuals.

8.3 Future Work: Improving Closed-Loop Performance

While the systems shown in this chapter were functioning proof-of-concepts, there is still significant room for improvement upon the results that have been shown. One avenue for investigation for improving closed-loop performance is the use of more sophisticated control

methods. The major barrier for developing high-performance controllers is the lack of knowledge about the system dynamics that give rise to these disorders. In particular, we do not have a model for the effect of stimulation on symptoms. Basically if we sense a particular level of symptoms, we have no way of knowing how much stimulation is needed to eliminate the tremor. Another problem is that even when tremor is not present, we do not we have techniques for predicting the onset of symptoms. In state-space control terms, we do not know the internal states that we need to consider, the internal dynamics of the states, the methods of observing those states, or the impact of our control actions upon the states. Until such models are produced, control will be limited to generic thresholding, proportional-integrative-derivative (PID) style control, or be entirely the product of empirically derived algorithms.

However, given the variable nature of the disorder across different patients, the assumption that a generic system model exists that works across patients is a long-shot. Given the difficulty in finding a model that works across all patients, then different approaches need to be taken to improve closed-loop performance. Instead of developing algorithms for the PD or ET populations at large, one potential method is to focus on developing tools for patient-specific controllers. A patient-specific controller may be tunable to the specific needs and dynamics of a given patient, and achieve higher performance than what would be achievable otherwise.

8.3.1 Ongoing Patient System-Identification Experiments

Fellow PhD student Andrew Haddock and I have spent some time discussing and developing methods for designing patient-specific controllers. The approach we are taking is to design system-identification experiments that hope to determine usable parameters in a patient's disorder dynamics that can be used for designing superior controllers. I have aided Andrew Haddock in developing our first system-ID experiments for PD rest tremor based off of the real-time DBS code that I have used elsewhere in this thesis. The system-ID experiment alternates between various stimulation levels in open-loop and monitors tremor in real-time

using the IMU watch. This will hopefully give insight into the stimulation-tremor relationship to deliver more appropriate stimulation in response to sensed tremor via wearables in the future.

Chapter 9

CHRONIC NEURAL SENSING AND BRAIN COMPUTER INTERFACES

The Activa PC+S provides us a unique platform to collect invasive neural data from cortical electrodes over a longer time duration than other previously used ECoG electrodes, allowing for recordings to be taken over months or years at a time. These neural signals may inform a closed-loop DBS system when stimulation is necessary, which would eliminate the need to communicate with external worn sensors, which is a considerable power draw.

In addition to using neural signals to investigate improvements to clinical DBS, we also intend to utilize the neural sensing functionality of the Activa PC+S and Nexus-D to demonstrate fully-implanted brain-computer interface (BCI) applications. In these cases, we will be asking patients to learn to modulate their brain signals to accomplish various goals. This work is being done to fulfill Aim 2 of this thesis: to demonstrate and evaluate a near-term fully implanted BCI. A chronic BCI has many potential clinical applications including providing the ability to communicate with locked-in patients, increase control over prosthetic limbs, and, as discussed earlier in 6.3, potentially provide a volitional control mechanism for DBS patients.

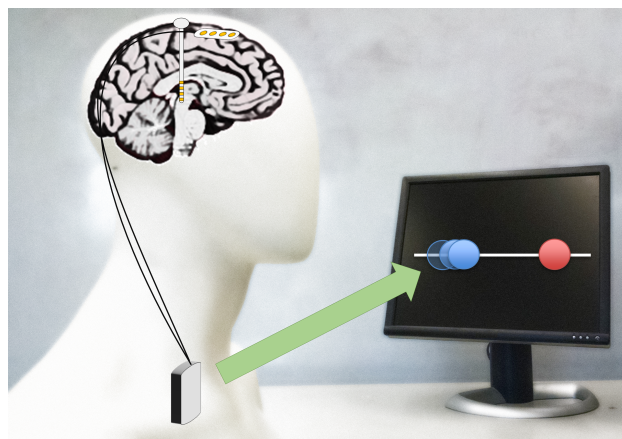


Figure 9.1: Neurostimulators may prove to be a gateway for the fully implanted BCI systems of the future

As an aside, it is important to point out that much of the BCI work done in this chapter is in collaboration with PhD Student Margaret Thompson. She and I were both responsible for designing the BCI tasks that were performed with our patient. On the technical side, she developed the patient-facing Unity implementation of the task while I was responsible for the acquiring data from the Axtiva PC+S and performing DSP to make cursor control decisions in real-time.

9.1 Sensing of Movement and Intention

Discussed throughout this thesis is the ongoing work to address current DBS shortcomings by developing a "closed-loop" system where sensors are used to estimate symptom intensity and adjust stimulation accordingly. For Essential Tremor patients who suffer from tremor during intentional movement, an important potential signal-source to determine when a patient will experience tremor is the motor cortex [49]. Beta-band desynchronization in the motor cortex has long been associated with intentional movement of the limb, and these signals can be clearly observed using either electroencephalography (EEG) on the scalp or with electrocorticography (ECoG) on the brain surface. This means that an indirect (as defined in 6.1) closed-loop DBS system for many ET patients may be able to make use of implanted ECoG electrodes on the motor cortex to determine when a patient is using their trembling limb, and trigger stimulation for the duration of the movement. With such a system, the patient would only experience side-effects while actually using their arm and may expect a longer battery life for their implanted device due to the reduced amount of stimulation they receive. However, before designing a neural closed-loop DBS algorithm (which will be discussed later in this thesis in 10) that makes use of these recordings, we first need to test our system's ability to sense the patient's neural markers of movement.

9.1.1 Task Description

In order to characterize the signals recorded from the cortical electrodes during periods of movement and intention, we designed a task where a computer prompted the user to move

their arm, hand, or to rest while we measured the limb activity using a worn accelerometer. We prompted the patient to alternate between movement and rest every 3 seconds in order to collect 20 trials of both arm and hand movement, and 40 trials of rest. The patient then repeated the same task while only imagining the movement, and the worn accelerometer was used to confirm that they did not accidentally perform overt movements.

9.1.2 Results

During both trials the Medtronic Nexus-D was used to stream data from the Activa PC+S to a laptop where it was time-stamped and logged. The Activa PC+S sensing lead was configured to record data sensed differentially from the hand M1 to S1 sampled at 422Hz. It

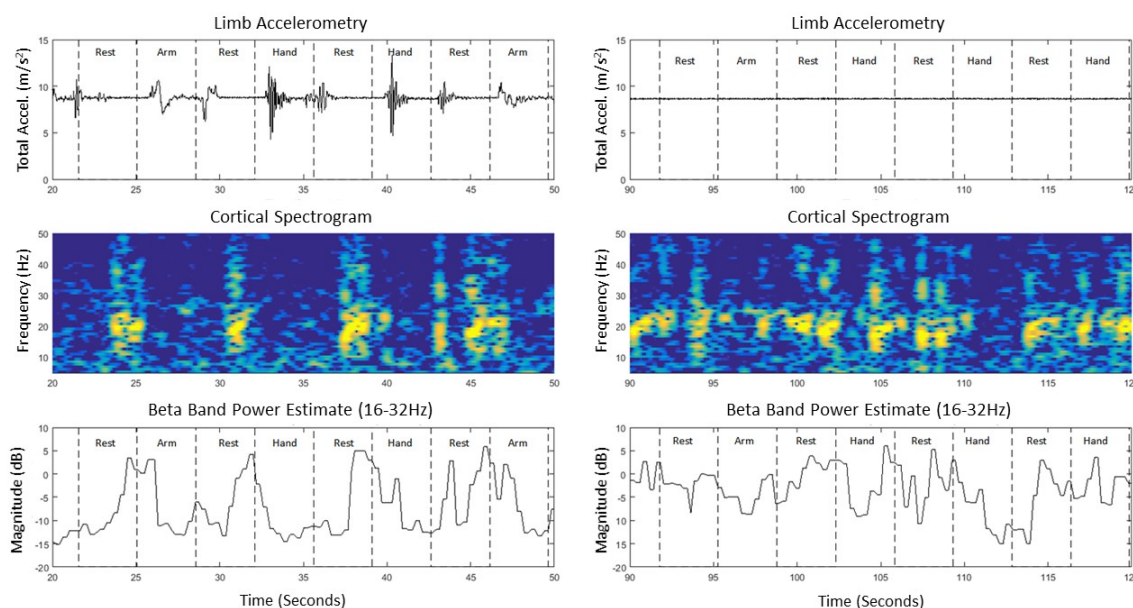


Figure 9.2: **Movement Prompting Results (Time-Domain)**: Example segments from experimental trials while the patient was performing prompted movements for either arm, hand, or rest. Overt movement trials are displayed on the left, imagined movement trials on the right. Prompted movements for each three second interval are indicated by text. *Top*: Limb accelerometry captured from wrist worn inertial sensor. *Middle*: Spectrogram of streamed ECoG data from M1 to S1 electrodes. *Bottom*: Real-time cortical beta band-power.

is important to note that the patient did not tremor while performing any of the prompted movements. Example time-series plots of the raw data collected from these trials are displayed in Figure 9.2 for both overt and imagined movement experiments.

We then segmented the data into periods based on the prompted action. The power-spectral density (PSD) was calculated for each prompted action using Welch's method with a 512 sample long Hann window with 80% overlap. The output PSD was then averaged with the other trials with the same prompted action to generate an average PSD for a given state. These average PSD plots are displayed in Figure 9.3 for both the overt and imagined movement tasks. Since the patient often took some time to react to the prompt and change their limbs state, the PSDs excluded the first second of every prompted action.

As can be seen in the overt movement PSD plot in Figure 9.3, the cortical signal's beta-

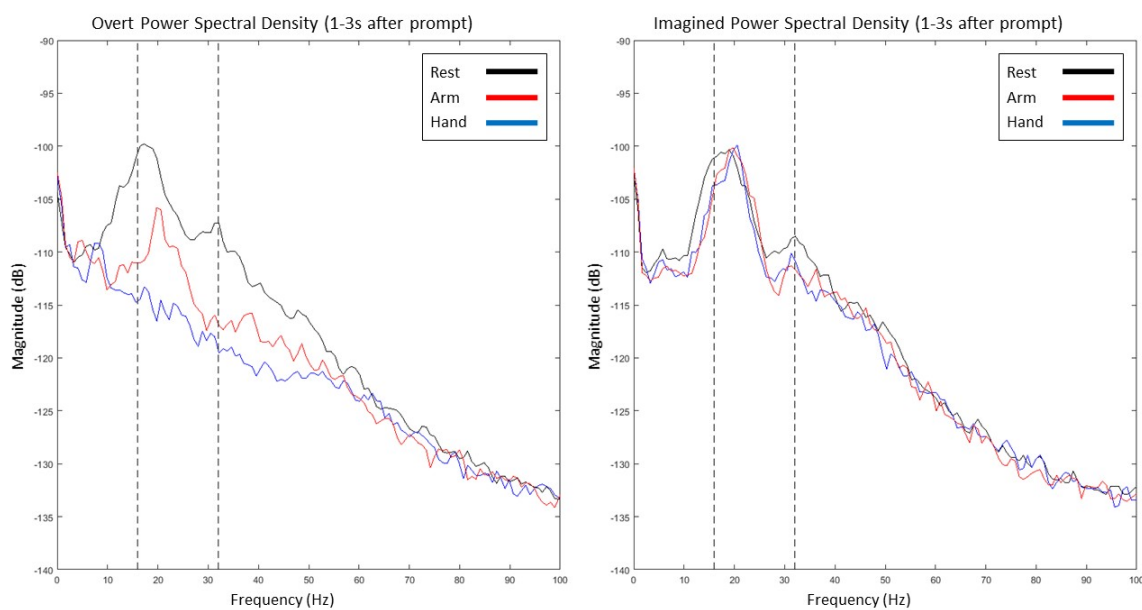


Figure 9.3: Movement Prompting Results (Average Power-Spectral Density): Average power-spectral density plot for each of the three prompted actions for both overt and imagined movement experiments. Dashed vertical lines indicate beta band (16-32Hz). Note beta-band desynchronization during overt movement as expected.

band is desynchronizing as expected whenever the patient moves their limb. Additionally, since the hand movements have a much lower beta band-power when compared to the arm, it suggests that our ECoG electrodes are accurately placed over hand motor cortex. During rest, the patient seems to have a beta peaks at both 20Hz and 32Hz. The beta-band power during overt arm and hand movements illustrates a broad drop in band-power across the entire band. However, for imagined movement, only a small band around the 32Hz peak lowered during the prompted imaginary actions.

It is also important when discussing a chronically implanted system to investigate how these signals change over time. By collecting cortically-sensed neural data during each of our sessions, we can examine if the system will provide a robust signal source for future closed-loop DBS projects. The results of this analysis are shown in Figure 9.4. In the figure, it can be seen that over each of the four sessions, spaced a month apart, the beta band desynchronization can be seen with overt movement.

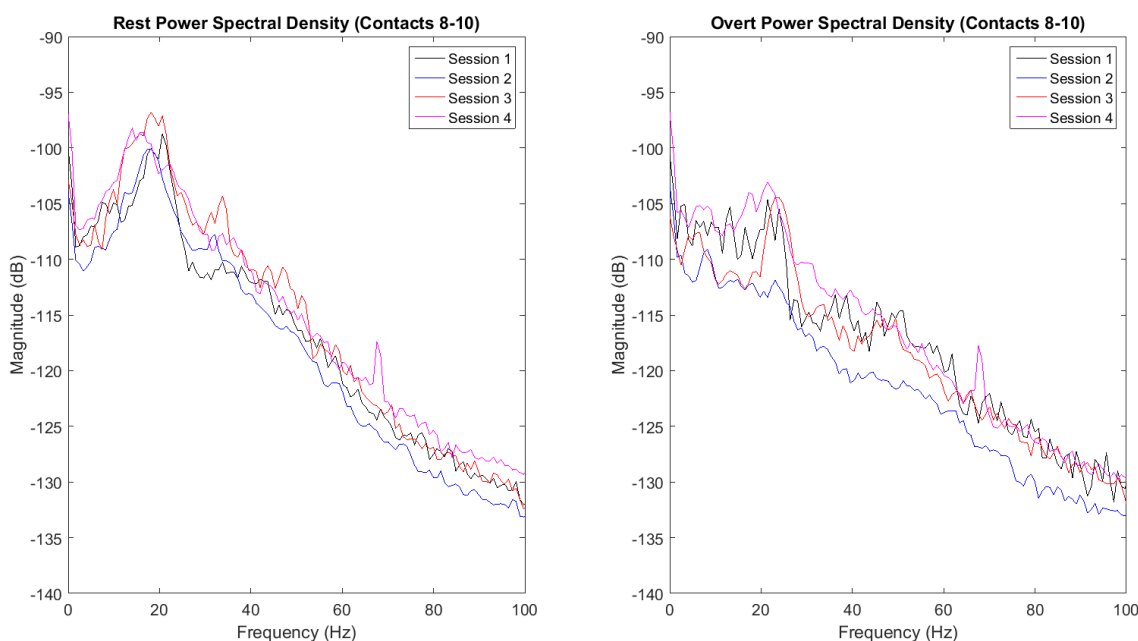


Figure 9.4: **Rest and Movement PSD Over Time:** Power Spectral Density during each of our monthly trials. On the left is "Rest", on the right is during overt movement of the limb. Dashed vertical lines indicate beta band (16-32Hz).

9.1.3 Discussion

This case study demonstrates that the Aactiva PC+S with cortical electrodes is a robust, fully-implanted platform to research improving neuromodulation technologies for movement disorder patients. Implanting an ET patient with both VIM and cortical electrodes opens up the ability to investigate the use of motor cortex signals for the purposes of creating a CLDBS systems. We have begun our preliminary research using this system to sense movement desynchronization as well as performing exploratory CLDBS experiments using wearable sensors to provide symptom feedback.

The results from our movement prompting task, shown in Figures 1 and 2, show that overt movements are clearly distinguishable from rest due to a broad movement related beta-band desynchronization. The fact the beta-band is so much lower in hand movement when compared to arm movement suggests that our electrodes are placed specifically over hand sensorimotor cortex. This patients imagined movements are however much harder to distinguish, with a smaller desynchronization only noticeable between 26Hz and 36Hz. This patient's beta band does not have the broad desynchronization during imagined movement, which has been seen in other literature [52]. The reason for this is unclear, but possibly arises from patient difficulty in imagining movement.

One exciting opportunity exists in merging the sensing work described here with the movement-triggered DBS work discussed in the previous chapter in section 8.2. In this case, the observed beta-band desynchronization during movement could be used to trigger stimulation changes in the patient. This will be similar to how we have used EMG to trigger stimulation on movement, with the possible advantage that an ECoG-triggered system being fully-implantable with no need to communicate with external components. It should be noted however, that the movements we performed with the patient did not actually trigger their tremor. This means that simply using movement as a trigger for DBS may still result in unnecessary stimulation for the patient. In future experiments we will have the patient perform prompted actions that we know cause tremor. Performing these future experiments

will allow us to search for more direct predictors of tremor in the collected neural data. This may allow for future systems to trigger stimulation not just on movement or intention, but instead when the specific movements have a high probability of causing tremor. This will further increase the power efficiency of future CLDBS paradigms due to the fact that transmitting across the skin barrier is incredibly power intensive for an implantable device.

9.2 Constant Velocity Cursor Task

However, ECoG data collected in the is not just useful for determining when a patient is moving their limb. ECoG is also an extremely important signal source for ongoing brain-computer interface research. Prior studies have allowed epilepsy patients to control devices and move cursors on screens by using cortical beta and gamma band signals collected from ECoG grid over motor cortex. While these studies have been promising and have been able to demonstrate that patients can learn to volitionally

modulate their brain signals to control these devices, the ECoG BCI studies are short in duration due to the fact that the grids can not be implanted chronically for months or years at a time.

9.2.1 Task Description

The first set of experiments will focus on demonstrating a patient's ability to perform common BCI tasks such as moving cursors on a screen. While ECoG BCI using devices similar to the cortical strip electrodes have been demonstrated, none have been performed in chronic sensing configurations such as this one. For the first experiments we have run, we replicated

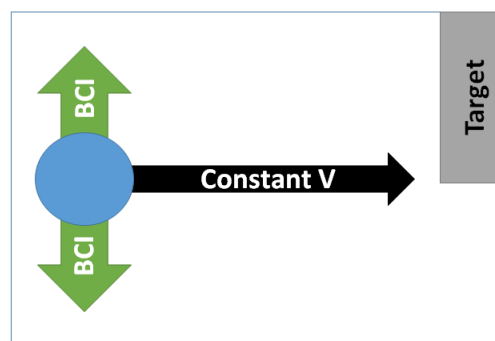


Figure 9.5: **BCI Task Overview:** Cortical band power within a selectable range drives the cursor up or down as the cursor crosses the screen towards a target.

prior work by building a task where the cursor moves across the screen left to right at a constant speed [54]. Targets are presented to the user for one second before the cursor appears and moves across the screen. Targets appear on either the bottom or top half on the right edge of the screen, and it is the patient’s task to modulate their neural signals to drive the cursor into the target. Each trial had ten up targets and nine down targets due to an indexing error, but in the future ten of each target will be presented per trial. It takes 4.8 seconds for the cursor to cross the screen, which means a total of twelve packets from the Aactiva PC+S will be used to determine the final cursor position. An overview of this trial is shown in Figure 9.5. This task has the benefit of being a set time duration so that trial lengths are predictable. Also, given that the target takes up half the screen, there is a minimum 50% chance of success for a given trial. This allows for easy chance analysis based on the number of success alone.

One difference between our work and prior work is that we have designed our tasks within the Unity Game Engine, as shown in 9.6. Unity is a multi-purpose game development engine that allows us to easily reconfigure BCI tasks or target geometry as needed. However, it is not a real-time environment with acceptable or predictable delays for BCI work directly. Our solution is to have a separate host application running on the computer that performs the real-time communication and digital signal processing required to run the BCI task, and then predictably update the cursor position through a socket connection to the task built in

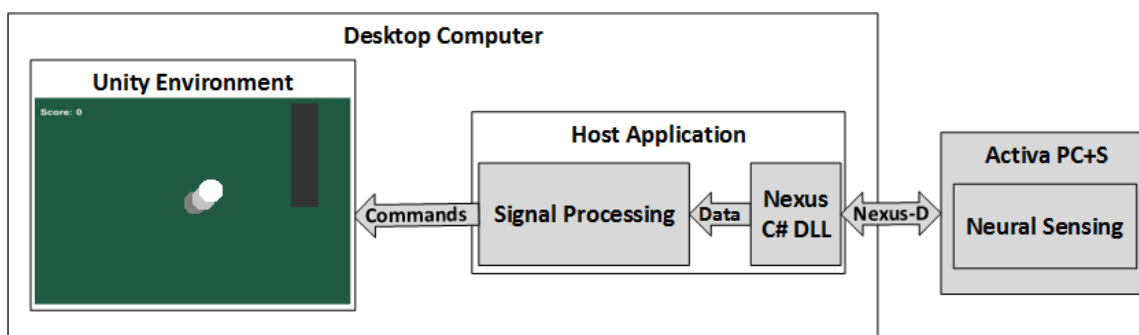


Figure 9.6: **Unity Based BCI System:** Aactiva PC+S communicates with a separate host application that is responsible for the real-time processing of data. Unity commands are sent from the host application to the Unity Game Engine to render cursor positions.

Unity. The Unity program then renders the cursor and targets and separately logs target locations and tasks successes. By having both programs running on the same computer and logging all data in reference to the computer's clock, the data is inherently synchronized to a single clock for easy data analysis after the task has completed.

9.2.2 Overt Movement BCI Training

Given our patient's difficulty with imagining movement while performing our neural sensing experiments, we chose to train the patient using overt movements to teach him the experimental trial. For this trial, the patient was asked to move his arm when the target was on the bottom side of the screen. The patient then had to rest when the target was on the top side of the screen.

We first had the patient perform a movement prompting task similar to what was performed earlier in the chapter, and identified that the largest movement-related desynchronization was occurring over the 10-20Hz frequency band. Then while he was performing this cursor task, we collected neural data from the Aactiva PC+S, and used this band to calculate a power estimate to move the cursor based on several tuned thresholds. The thresholds were tuned by taking the average beta band power measured during a pretrial rest and overt movement period. The final control threshold was then set at 25% of the difference between the overt and rest calibrated values. After several calibration runs to familiarize the patient with the task and demonstrate how it works, the patient then generated the trial run shown in Figure 9.7.

For this final run through the experiment, the patient had 100% success at reaching the movement targets, but only hit 60% of the up targets. Looking more closely at the trial results, it would appear that during movement trials the patient's beta band power was consistently below the threshold, but during rest the beta oscillated and frequently crossed the thresholds. This meant that for short periods, the cursor would move in the downward direction while resting, causing an increased error rate. This suggests that our calibrated value was too high, and that the threshold could have been set even closer to the

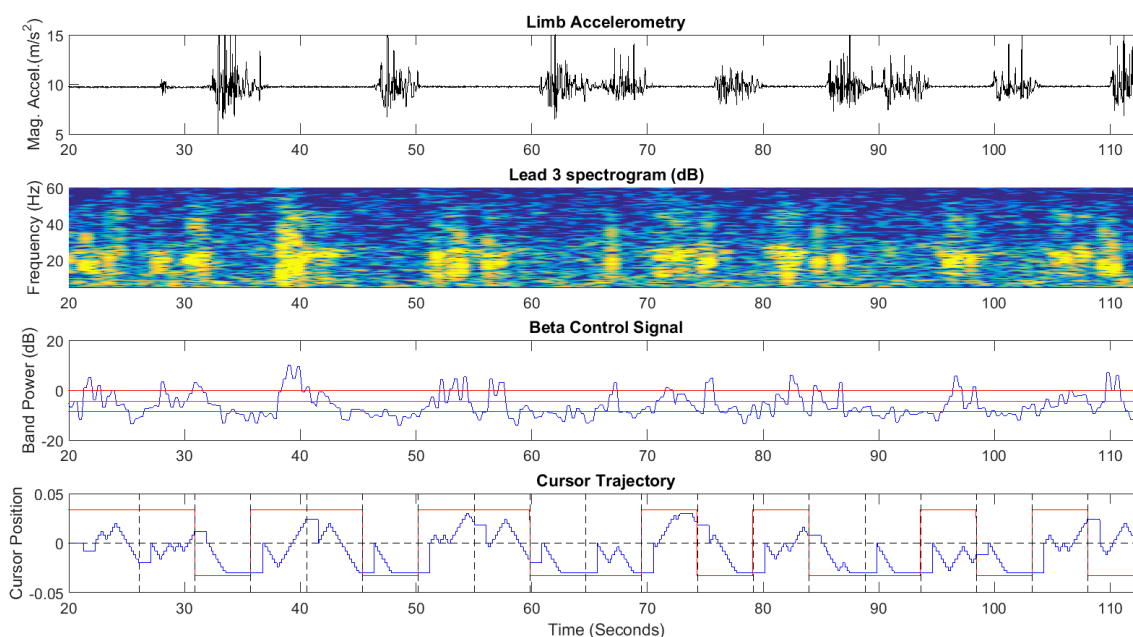


Figure 9.7: **Overt Cursor Task Results:** *Top-* shows limb accelerometry during the overt cursor task. Periods of movement are clearly illustrated by periods with high variation in the signal. *2nd from top-* spectrogram taken from the cortical strip electrodes during the overt trial. *3rd from top-* Beta band power estimate (10-20Hz) measured in dB. Red horizontal lines are calibrated thresholds used for control, magenta (middle) horizontal line indicates threshold for moving up versus down. *Bottom-* Cursor position over time. Red lines indicate the side of the screen that the target was, dashed vertical lines indicate each trial, and dashed horizontal line indicates the center point.

overt movement average beta. This would have reduced the tendency of the beta oscillations to have driven the cursor low in the rest periods.

Regardless, these results demonstrate the functionality of our sensing platform and BCI experimental task. This system will be used for future patients to familiarize them with how to perform the needed actions to move the cursor into the target using overt movements before asking them to perform imagined movement control of the cursor.

9.2.3 Imagined Movement BCI Trial Results

We have also performed BCI trials using imagined movement to move the cursor. Considering the difficulty in identifying imagined movement from the patient's cortical signals, it was

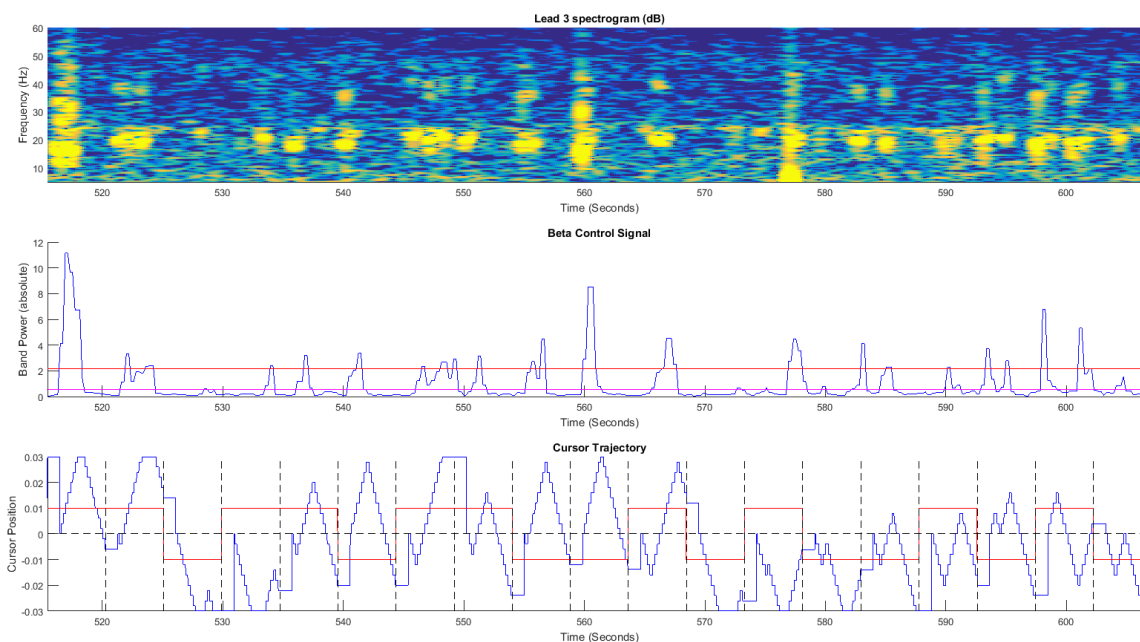


Figure 9.8: **Imagined Cursor Task Trial 1:** *Top-* spectrogram taken from the cortical strip electrodes during the overt trial. *Middle-* Beta band power estimate (16-32Hz) measured in dB. Red horizontal lines is the calibrated rest beta, magenta horizontal line indicates threshold for moving up versus down. *Bottom-* Cursor position over time. Red lines indicate the side of the screen that the target was, dashed vertical lines indicate each trial, and dashed horizontal line indicates the center point.

unclear how the patient would perform during these trials. For this system we calibrated a threshold based solely on 25% of rest beta, which was calculated using the 16-32Hz range. As before, we asked the patient to rest to move the cursor up and imagine moving his hand to move the cursor down. We had the patient perform the experiment a total of six times with five minute breaks between each trial. The first of these trials is shown in Figure 9.8.

For this first trial, the patient again succeeded at all of the down targets but only got four of the up resting targets. The compiled target success rates across each of the six trials is shown in Figure 9.9. The patient performed well on the downward targets with usually around 100-80% success. One exception is the third trial where they got 45% of the downward targets. Upward targets were around 40% successful, with the second trial an exception with 80% successful upward targets. In general the patient performed above chance when considering all targets, but only marginally so.

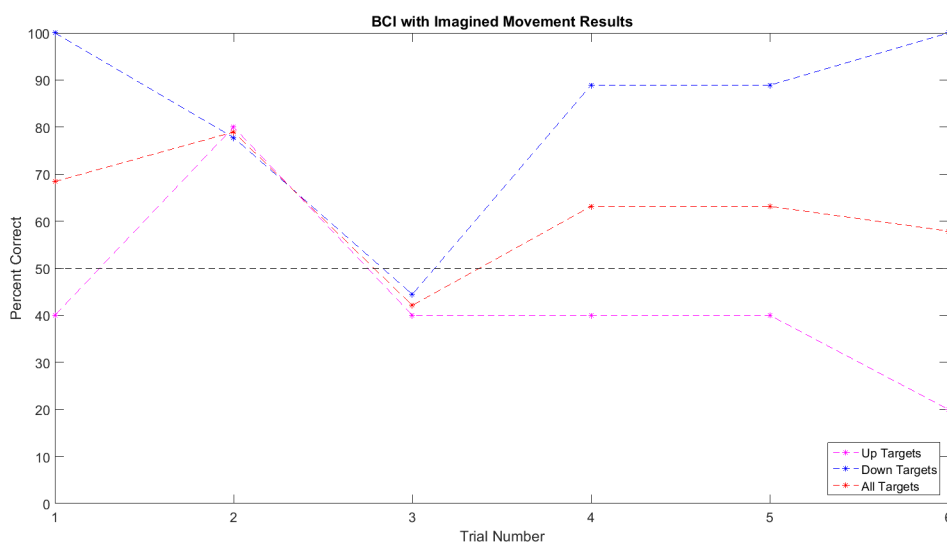


Figure 9.9: **Imagined Cursor Task Results:** plot indicates success at upward, downward, and all targets for each imagined movement based BCI trials. In general patient performed above chance as indicated by the “All Targets” line being above 50%.

9.2.4 Discussion

This section has discussed the design of a constant-velocity BCI task that has been built using a combination of our real-time Axtiva PC+S research platform and the Unity game engine. I have validated the system design and functionality using overt movement-related beta-band desynchronization to control a cursor. When the patient was asked to perform the task with imagined movements, he performed above chance, but showed little change over time. It is encouraging that he performed above chance, but up targets were potentially made difficult due to calibration and classification issues that will need to be addressed in future work.

As a note, it needs to be discussed that we had the patient perform the imagined trials before the overt trial. This was because it was not immediately obvious that he knew what he was expected to do during the imagined trials, and his performance was low enough that we decided to return to the cursor task with overt movement to train the patient the task dynamics. It could be that his imagined movement BCI performance will be quite different

the next time he performs the task. In future studies, we will always have the patient perform the overt task first as an intermediate training step before the imagined cursor task.

9.3 Future Work: Improving BCI Performance

While its very exciting that we have been able to design and integrate preliminary BCI tasks for use with the Aactiva PC+S, there are many avenues for improving the BCI performance in the future. There is a deep well of BCI literature that we can draw upon to design future classifiers for BCI tasks and our chronic platform gives a unique opportunity to compare how many different ECoG BCI algorithms work with our patients.

Another benefit of this chronic platform is the ability to investigate how BCI performance improves over much longer time-frames than previously available in epilepsy ECoG trials. We have already been able to demonstrate that our system can reliably sense movement-evoked beta desynchronization over a four month time period and counting. Since our implanted system is so long lasting, we hope to perform a continuing study into how well a patient can learn to use BCI by performing training and experiments over a multi-year time frame. In our current IDE application, we also hope to enable at-home BCI training to investigate how people learn to use a BCI at their own pace when using it every day.

It is also important to note however, that we have some unique opportunities to explore that have been unavailable to prior DBS research. In particular, thalamic signals have so far been unused for BCI purposes. Future work using LFPs to control cursors on screen may provide a new window by which to research BCI task performance and learning.

Finally, another avenue of research I am laying the groundwork for, is the inclusion of haptics into the BCI feedback loop. It could be that patients learn to use a BCI more effectively or quickly using the sense of touch than through visual feedback alone. If this is true, we may want to augment our BCI cursor tasks with a haptic pen or vibro-tactile feedback to give the person a sensation as they near the target. Ongoing work in our lab is focused on integrating haptic devices with Unity so that we can include them in future Unity-based BCI tasks.

Chapter 10

BIDIRECTIONAL NEUROPROSTHETICS

Previous chapters have covered closed-loop stimulation using sensors and using the Activa PC+S to sense neural signals separately. This final chapter covers the merger of the two, into the final aim of this thesis where signals collected by the implanted Activa PC+S are being used to trigger stimulation changes in the device.

I use the term “bidirectional neuroprosthetic” to describe these systems due to the fact that they have a fully integrated and input + output relationship with the patient’s brain. These systems have many advantages when compared to a wearable closed-loop DBS systems, but most important is the fact that future bidirectional neuroprosthetics may be able to selectively deliver stimulation and save power without the not need to rely on external communication systems to a large computational unit. Instead, by performing required signal processing on the device, the system can respond quickly without the delay prone and power-intensive communication across the skin barrier. These systems will likely also be more attractive to patients than a wearable-sensor driven closed-loop solution because they will not require wearing sensors which would draw attention and may not be able to be hidden under clothing.

However, these systems are more technically difficult to implement than work covered in previous chapters. The communication channel to the implanted device is a limited resource and sensing packets need to be carefully interleaved with stimulation updates so as to not lose data. Additionally, numerous stimulation artifacts in the neural sensor data need to be accounted for, as they should influence the control actions being decided by the real-time system.

10.1 *Beta-Modulated Stimulation in PD Patients*

There has been previous work discussed earlier in this thesis (see 3.3.2) where STN-sensed beta band power was used to trigger stimulation inter-operatively. The system they designed turned on the patient’s DBS when the beta band power sensed from nearby electrodes was above a threshold. This was based on the observation that DBS lowers the STN beta band power, and their results suggest that stimulating when beta is high can be more effective than open-loop DBS [45].

I worked with Helen-Bronte Stewart’s group at Stanford to replicate this form of system for testing in their PD patients. While the Activa PC+S allows us to perform these experiments out of the operating room, it does not have the same time resolution for stimulation or sensing that the bench-top equipment used in the prior work. As such, we had to make numerous adjustments to the control algorithm and system design. This section will review the system specifications, design, and test results based on a single patient’s trial.

10.1.1 *Methods*

For this system, we used the Activa PC+S and Nexus-D3 system to stream uncompressed data from the implanted DBS leads. This data is sent to a computer where a signal processing is performed, and stimulation updates are determined. These stimulation updates are then regularly sent to the Activa PC+S again using the Nexus-D3. We also had the patient wear the IMU watch so that we could evaluate how well the system suppressed rest tremor.

We calculated a beta-band power estimate at the STN site using the time-sampled data streamed from the Activa PC+S via the Nexus-E. Every time a new sensing packet is received, we performed an FFT on the data with a Hann window. Given that each sensing packet is 168-samples long, we used a 256 long FFT, and a 168 long Hann window with zero padding. The magnitude of the output spectral power was then summed across a patient-specific band. For this patient, we used the bins corresponding to the band 12-30Hz based on prior analysis of this patient’s beta peaks. This band power was then compared to an increment threshold

and decrement threshold. If the band-power was above the increment threshold then the stimulation output amplitude would step up, if below the decrement threshold it would step down, and no action would be taken if the band-power was in the dead-band in the middle.

There are several artifacts that need to be accounted for when designing a closed-loop DBS system. One of the obvious artifacts is the effect of each stimulation pulse wiping out the front-end of the analog-to-digital converter. This can be mitigated by configuring the sensing leads to differentially sense on either side of the stimulation contact. The differential-based sensing will then reduce the stimulation artifact by means of common-mode-reduction. Secondly, there seems to be an artifact when changing stimulation parameters. This can not be easily mitigated, and can potentially trigger false actions from our controller. To mitigate the affect of this artifact, we chose to have our system hold-off from making control decisions for a set period of time after every stimulation update. Because we do not know where exactly in a given sensing packet a stimulation update occurred, we had the system hold off from making new control decisions for two packets of Aactiva PC+S data, which corresponds to 800ms.

We have so far been able to test this system in a single PD patient with rest tremor. We first measured the patient's tremor and beta-band power with stimulation off for two minutes. Then we turned on the stimulator to the clinical setting of 3.2 volts for another two minutes. The average beta-band power in each of these states were used to calibrate the system control thresholds. The increment threshold was set to the middle point between the two thresholds, and the decrement threshold was set to the middle point between the increment and stim-on beta value. This results in a dead-band of 25% of the difference between stim-on and stim-off beta band power averages. We then enabled the closed-loop DBS for a half hour. During the trial, we logged all tremor data from the worn inertial sensor and Nexus-D3 sensor data to file for off-line analysis after the trial ended. When incrementing or decrementing, the system would change the stimulation amplitude by one volt for a given control action.

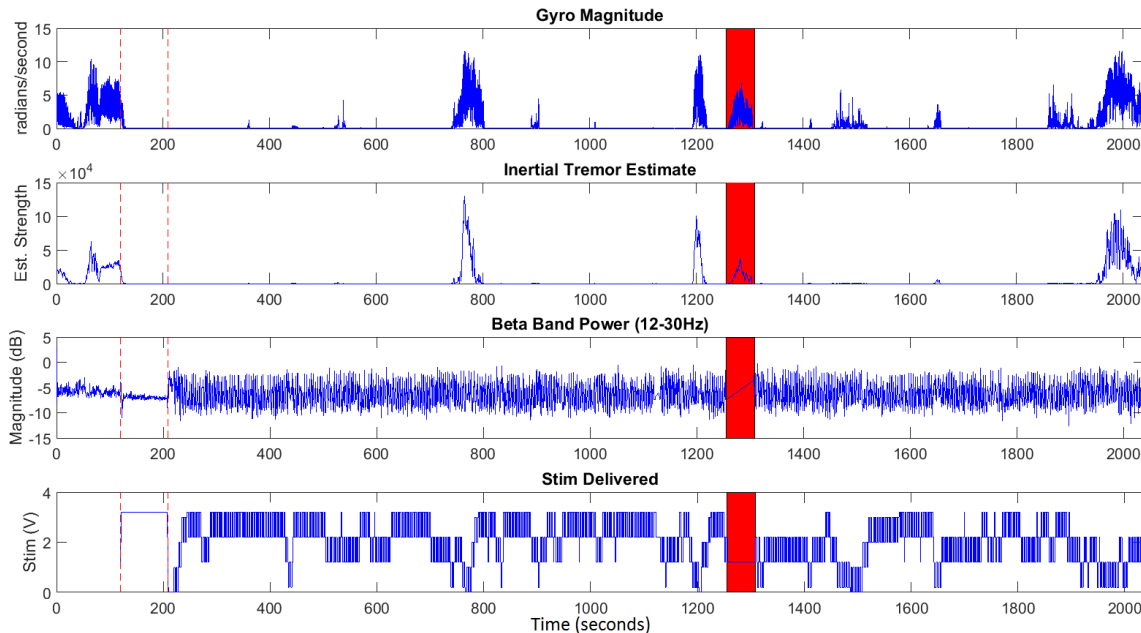


Figure 10.1: **STN Beta Modulated Stimulation Results:** Experimental results from the Beta-modulated CLDBS system. Note there was a period of communication drop-out indicated by red bar across the graphs. *Top:* Gyro Magnitude, tremor visible as periods of large variance. *Second from Top:* Estimate of tremor strength based on spectral band-power analysis of the gyroscope data. *Third from Top:* Real-time beta band-power measurement taken during the trial. *Bottom:* Stimulation delivered during the experiment.

10.1.2 Results

The time-plots of the patient trial are shown in Figure 10.1. It is important to note that there was a drop-out in communication shown in red. The no-stimulation period was the first 120seconds, followed by an open-loop stimulation at 3.2 volts. The patient then received the closed-loop DBS for the remainder of the trial. For large portions of the trial the patient's tremor was suppressed, but there were several time periods when the tremor re-emerged. However, each of these time periods were transient and were not sustained.

Using the performance metrics introduced earlier (in 6.4), we can break down this time-domain data into quantifiable values to examine how the system performed. These values are shown in Table 10.1. The open-loop and closed-loop tremor values are referenced to the

trial period when the patient received no-stimulation. However, one adjustment that was made when determining the open-loop DBS performance was to remove the first 20 seconds of the open-loop trial results to allow the patient’s system to change from the no-stimulation state to the open-loop state. This was because the patient had fairly high tremor when there was no stimulation present and it takes some time for the tremor to respond. Overall, the beta-modulated closed-loop DBS system reduced stimulation power by 55.1%, but resulted in an additional 24.6% of tremor for the patient. This results in a stim-tremor trade-off of 2.2%, which is in-line with the performance seen by the wearable methods presented in 8.1.

| Open-Loop | | Closed-Loop | | CLDBS Metrics | | |
|-------------|---------------------|--------------------|---------------------|-----------------------|----------------|-----------------------|
| Stim Amp | Untreated Tremor | Avg Stim Amp | Untreated Tremor | Stim Power Red. | Tremor Inc. | Perf. Met. |
| 3.2V | 0.0% | 2.0V | 24.6% | 55.1% | 24.6% | 2.2% |

Table 10.1: **Quantified Closed-Loop DBS Results:** “Stimulation Amplitude” is determined by taking the average stimulation amplitude over the entire time duration in a given state. “Untreated Tremor” values represent the percentage of the no stimulation tremor that the system cannot suppress. They are determined by dividing the average tremor band power in the each mode by the average tremor band power with no stimulation. “Stimulation Power Difference” represents the average stimulation power savings that a closed-loop system provides over the open-loop case. “Tremor Inc.” represents the increased tremor that the closed-loop system provides compared to the open-loop system and normalized to the no stimulation case. The final “Performance Metric” is the proportional trade-off between stimulation power savings and increased tremor for the closed-loop system.

10.1.3 Discussion

In this section I have presented results from our first trial using STN-sensed beta to modulate the stimulation amplitude for a PD patient in real-time. This system largely suppressed tremor with great benefits to the stimulation power required, but the patient still had a

few episodes of transient tremor. These results illustrate the both the potential benefit and difficulty in designing neural closed-loop DBS systems. On the one hand, no inconvenient wearables would be needed as a signal source. On the other, the numerous artifacts and communication bottlenecks imposed by our current system make it difficult to replicate the encouraging results illustrated in prior inter-operative work.

Another point of difficulty is the balancing act between system responsiveness and step resolution. Given that the system bottleneck is the rate at which we receive packets (2.5Hz), we have to be careful in deciding how large each stimulation step is for a given packet. If the step size is too large, then the output resolution is lowered. This may increase the chances of oscillations due to system overshooting or undershooting the amplitude that would be ideal for a given time. Alternatively, if the step-size is too small, then the system will lag behind the beta band-power oscillations that occur in the patient.

There is the additional issue in the experimental results where communication to the device was lost for a significant duration during the trial. This is indeed a risk for any system that requires a communication channel to external computational elements. However, future neural-DBS systems will allow for a custom controller to be embedded in the implant. Unlike a wearable closed-loop DBS system which needs a risky, secure, and robust communication link to the implant, an embedded controller mitigates the risk that the patient will have their therapy reduced in effectiveness due to poor communication quality.

In conclusion, this work demonstrates the fulfillment of the third aim of this thesis: to “demonstrate and evaluate a near-term bidirectional neuroprosthetic”. While there is still ample room for in-depth investigations into more sophisticated controllers and techniques, this section demonstrates the feasibility of future work by providing a prototype for the next step of the work.

10.2 Future Work: Cortical Sensing for Essential Tremor Patients

At the University of Washington, we will be making use of both the cortical strip electrodes and DBS electrodes to search for tremor indicators in essential tremor patients. This work

will require both an FDA IDE (Investigational Device Exemption) and an UW IRB. For the neural sensing portion of the Acliva PC+S work, the work flow will look very similar to our wearable sensing experiments. We will have patients do a series of movements while they wear IMU and EMG sensors. We will also include the logging implanted electrode LFP data from the Nexus system so we can correlate sensed tremors to identifiers in the neural data.

As has been discussed in Chapter 9 on neural sensing, one attractive signal source for a first attempt at neural closed-loop DBS is using movement-related beta band desynchronization collected from our ECoG strip on the motor cortex. This beta band desynchronization occurs whenever the patient uses his tremor-affected limb, and could be used to trigger therapy similar to the EMG movement-triggered stimulation discussed in 8.2. Our preliminary data suggest that such a system has a high likelihood of providing a desirable level of tremor suppression with significant power savings to the patient. While we have demonstrated the system functionality with a healthy individual's EEG and a benchtop Acliva PC+S (as discussed in 7.2), I have not been able to demonstrate this in our ET patient due to restrictions imposed on us by our current IDE and IRB process which will allow these experiments to take place next November.

10.2.1 Patient Volitional Control of DBS

One particularly exciting opportunity for future work is the merging of the neural sensing and preliminary BCI investigations into a cohesive experiment examining the possibility of BCI-triggered DBS. In such a system, the patient would volitionally control the stimulation parameters as they would a cursor on the screen. This would empower patients to make decisions as to how they want to manually balance their treatment, power, and side-effects as they go about their day. For example, with such a system our patient could preemptively turn their stimulation up to a higher value when they are about to perform an action that they know causes tremor (like drinking from a cup). While such a system would doubtlessly need significant training to use, the benefits to a patient may be more than a simple reduction in power or side-effects. Also to consider is the fact that BCI-triggered DBS would be a new

application of BCI technologies that so far have not seen wide-spread clinical use.

On the technical side, in order to demonstrate a volitional system we first need to train the patient to proficiency on the BCI tasks outlined in the previous chapter. Then, we will map the BCI task's cursor position to the stimulation output. By then controlling the cursor with visual feedback, the patient will be able to modulate their cortical signals based on their desired stimulation level. These sensed signals will then be mapped to control the stimulation amplitude, pulse width, or frequency. This would allow a patient themselves to predict or intervene when they need stimulation, or may simply be used as a feedback method to complement and modulate other portions of a closed-loop DBS system. This will mitigate concerns of side-effects and power usage by allowing a patient more control of the stimulation level so that they can choose for themselves how they want to balance therapy, side-effects and power usage. It may be the case that this eventually becomes a reflex, illustrating that the neuroprosthetic has truly integrated with the nervous system.

To prove that the stimulation parameters are being volitionally modulated, we will need to design a learning paradigm for the subjects. The difficulty lies in the fact that patients are often not able to feel their stimulation, so the lack of feedback may prove to be troublesome when operating a volitional system out of the clinic. In order to give patients feedback on the current settings of their device, it may in fact be advantageous to search for stimulation parameters that the patient can initially perceive. We could take advantage of a harmless sensation that would alternatively be deemed to be an unintended side-effect to provide feedback to the patient. An example of this could be using a paresthesia, a tingling of the skin. The patient could then perform closed-loop volitional control of the stimulation parameters by using the tingling sensation as feedback for to know what their current stimulation level is.

10.2.2 Embedding the Algorithm: Nexus-E

Another exciting opportunity we will make use of in the future is an upcoming update from Medtronic called the Nexus-E. This Nexus-E(embedded) allows us to send a patient home with

a neural-triggered closed-loop DBS system. Whereas the current Nexus-D(istributed) systems always needs a computer in the loop and the power-expensive communication channel to the externals, the Nexus-E performs all of the required functions for a simple closed-loop system internally. The system can change stimulation between one of two states (on/off, high amp/low amp, high freq stim/lower freq stim etc) based on a classifier. The inputs to the classifier are configured power estimates of each sensor channel, there is no classification options for using time-domain data. Each lead has up to two power channels that can be collected from any combination of the implanted leads. The system comes with a modified patient programmer that allows the patient to change their stimulation between open-loop or the closed-loop stimulation, so if they find the closed-loop insufficient they can revert themselves to open-loop.

As an example, one experiment would be to embed the beta triggered stimulation algorithm used with our PD patient in an experiment discussed earlier in this chapter. For this system, we could set up a power channels on our STN electrodes. The device could then be configured such that when the beta raises above a threshold, the system turns stimulation on to the maximum value. When the beta returns to the low, the system would then automatically turn stimulation down. This is just one example, and there are a multitude of signals, bands, and stimulation settings we could make use of with the Nexus-E. This may even allow us to send a patient home for an at-home study with volitional DBS. However, future studies will need to be sure that algorithms work sufficiently well before accepting the additional risk of sending a patient out with a potentially poorly tuned system. As such, we will be making sure to test any algorithm multiple times in the clinic before embedding the controller and sending the patient home with the experimental algorithm.

Chapter 11

CONCLUSION

This work has demonstrated potential closed-loop systems to improve the treatment of Essential Tremor and Parkinson’s Disease with DBS. The research platform I have designed will enable future studies in ambulatory patients, as various sensors, signal processing techniques, and control algorithms interface with the implanted hardware to feedback stimulation parameters in real-time. Basing this work around the implantable Activa PC+S and Nexus communication system has allowed us to also investigate neural sensing for closed-loop DBS purposes, but also for brain computer interface research as well. In terms of the research aims put forth at the beginning of this thesis, I have accomplished the following:

Aim 1: Demonstrate Closed-Loop DBS using Wearable Sensors. This aim was to show that by applying closed-loop control paradigms to essential tremor and Parkinson’s patients we can lower the average power of the stimulation while maintaining the same level of tremor mitigation as well. As explored in chapter 8, I have fulfilled this requirement by developing methods for worn inertial and EMG sensors to modulate stimulation in real-time in both ET and PD patients. These systems were then validated with an ET patient while working with Andrew Ko at UW and in PD patients in the Helen Bronte-Stewart Lab at Stanford. While the systems were not able to maintain the same level of tremor-mitigation as open-loop, they did provide dramatic power savings.

In the chapter I also discussed room for future improvement of CLDBS paradigms, namely patient-specific modeling for the purpose of developing individualized controllers to increase performance. This is working off of the observation that not only are individual patient’s symptoms dramatically different, but the patient response to closed-loop DBS algorithm could be dramatically different as well. In order to compare algorithm performance across

patients, I introduced a metric discussed in section 6.4, which I used to evaluate all of the tested algorithms.

Aim 2: Demonstrate Chronic Neural Sensing and BCI. Using the neural sensing capabilities of the Aactiva PC+S, I set out to design a system to allow patient control of a cursor in a one-dimensional target task. This was to demonstrate a fully-implanted research platform for long-term studies for investigating a patient’s ability to learn novel BCI tasks without risk of electrodes shifting or infection.

To fulfill this goal, I designed and performed preliminary cursor control trials with our ET patient. This work was covered in Chapter 9, where I discussed a prompting task to distinguish overt and imagined movement from rest, and a single degree of free cursor trial built in Unity. Through the use of these systems we were able to collect data from our chronic ECoG electrodes showing clear desynchronization during overt movements and validating the system-integration of our cursor task.

Additionally, I showed that the neural data we were collecting was stable over time, allowing for beta-band based identification of overt movements even four months after implantation. This shows promise for the future of using this platform to collect neural signals for long-term BCI use. Given the long duration of time we will have with this patient, future work will be able to cohesively examine different cursor mappings, calibration techniques, or classifiers in order to improve BCI performance. Future work will also have the opportunity to examine non-traditional signal sources, such as using the thalamic electrodes for BCI cursor control. The clinicians we are working with could even implant the cortical strip on locations other than the motor cortex, allowing for a wide variety of signals to be tested.

Aim 3: Demonstrate and evaluate a near-term bidirectional neuroprosthetic. The final aim was to merge the neural sensing with closed-loop stimulation to demonstrate a bidirectional neuroprosthetic for the use of improving DBS treatment of PD and ET patients. By modulating stimulation parameters in real-time based off of neural data, future closed-loop DBS systems will provide consistent benefit to the patient without the need for bulky communication equipment, external computation, or worn sensors.

To fulfill this aim, I designed a system for an experiment that was performed at Stanford in Helen Bronte-Stewart's lab. The system used a patient's STN beta recordings to dynamically modulate the output stimulation amplitude to treat rest tremor. While the system still resulted in more tremor than open-loop stimulation, this was limited to just a few periods of tremor in a thirty minute long trial. The stimulation power savings of the system was still above 50%, and for most of the trial the patient experienced no tremor.

The immediate next steps in this work is to extend the bidirectional neuroprosthetics work to our ET patient. Once IDE and IRB approval has been granted to accelerate this work, the team will use overt movement beta desynchronization to trigger stimulation whenever the patient uses his tremor-affected limb. Other work will focus on extending the ongoing BCI work to train the patient to volitionally modulate their stimulation settings without the need of an external patient programmer.

11.1 Significance of this Work

One of the main benefits of this work to future patients may be increased power savings for the implanted device. By increasing power efficiency, patients may be able to go longer before a battery replacement surgery and implantable devices may be manufacturer to smaller sizes due to lower battery capacity needs. Every system tested on patients so far has resulted in at least 50% stimulation power savings, and for many our patients these numbers are conservative due to the way the task were constructed. For our PD patients, we tested them in the worst-case scenario (constant rest) and still achieved admirable power savings. Our ET patient had a task that alternated evenly between movement and rest, so a 50% power savings is also acceptable given that he needed stimulation to be on half of the time.

Additionally, by being more selective with stimulation, we can reduce the side-effects for future patients. Side-effects of DBS are common, and our ET patient reports that he has more headaches with stimulation on. If stimulation was only delivered when he needed it, as demonstrated with our EMG-triggered and IMU proportional systems, he would have less headaches.

The significance of this work also extends to enabling future research into the nature of these disorders. The current mechanisms of PD, ET, and DBS are very poorly understood, and research tools like the one I have developed will hopefully yield data that will aid in the modeling of the disorder's neural dynamics, improve classification of symptom biomarkers, and gain a greater understanding of how and why these diseases progress the way that they do. But it is not just ET and PD patients that will benefit from the research with these platforms, but also patients with other disorders or conditions that may benefit from neural technologies as a whole. These fields require the development of bidirectional research systems that can be used to concurrently stimulate, sense, and interact dynamically with the underlying neural tissue. The methods, considerations, and system design issues explored in this thesis have applications far beyond the neurological movement disorder field traditionally associated with DBS.

Exploring other neural engineering fields may also lend to exciting opportunities for improving DBS. As discussed earlier, there is an exciting possibility of merging BCI technologies with the bidirectional DBS work that I have demonstrated. Such a system would allow a patient to modulating their neural signals in order to volitionally control their own therapy by changing the output stimulation parameters. This has the benefit of allowing patients to maintain their autonomy by balancing their power usage, side-effects, and symptoms in real-time. Alternatively, a chronic BCI may be implemented with an Aactiva PC+S and two cortical strips, potentially giving locked-in patients a means of communicating with the outside world or prosthetic users a robust long term neural interface. Another opportunity is to make use of the cortical electrodes as they were originally intended as a spinal electrode. The sensing and stimulation of the spine may aid in rehabilitation for spinal cord injury patients, or aid in the reanimation of their limbs.

11.2 The Importance of Neural Security and Privacy

One of the most important factors to consider whenever connecting a medical device to a networked enabled device is security. This is especially important if the device is being

connected to a desktop computer or smartphone. In general, there are two immediate patient harms that need to be considered and mitigated when it comes to a “smart” DBS system. Firstly, patient over-stimulation needs to be considered, as these systems are more than capable of delivering enough charge to burn the nervous tissue that is interfaced with. Secondly, and uniquely to the closed-loop case, there is the risk of under-stimulation, or delivering not enough therapy in a time when the patient’s safety depends on receiving therapy. Finally, another important concern that needs addressing are the privacy issues surrounding connecting a neural device to a networked device.

11.2.1 Over-Stimulation

The Medtronic Activa PC+S has a couple of very attractive features that mitigate some safety concerns when it comes to over-stimulation. Most importantly is the fact that a clinical programmer can dictate which range of stimulation values can be used by our closed-loop system. It is important to note that this clinical programmer device is different from the modified patient programmer device we are using for our communication system. In our system, a clinician will determine the range of parameters we are allowed to use by examining the effect of various stimulation types on the patient. The clinical programmer device then hard-codes these safety limits into the implanted device itself. The implanted Activa PC+S does not allow any stimulation parameter to go beyond these specified limits. However, one shortcoming of this approach is that it does not take into account the fact that sudden changes in stimulation can cause patient discomfort. It will be important to address these issues in the future work while translating these systems from the lab into clinical care.

11.2.2 Under-Stimulation

There is also the possibility that turning off the stimulation at an inopportune time, such as when a patient is driving, could leave the patient vulnerable to harm. This is not a problem that exists in open-loop devices, as the device does not turn itself on or off without patient involvement with the external programmer. Instead, this is purely a problem in a closed-loop

device, where even a very small classifier false-negative rate may cause a problem at just the wrong time. Alternatively, in the case where the device has enabled external communication to a wearable sensor or computational device, like a smartphone, it may be possible that a malicious application “denies” therapy by actively keeping the stimulation off against the patient’s wishes. In an even worse case, such a malicious application could use other information, like the knowledge that the patient is driving, to turn off the stimulation in a particularly dangerous situation. The sudden lack of mobility or dexterity in such a situation may result in harms to the patient that need to be avoided in the design phase.

11.2.3 Privacy

A legitimate concern with any neural sensing system is that there is likely private patient information contained within the raw neural signals [60]. In preparation for addressing potential privacy concerns in this project we have been collaborating with Tamara Bonaci to identify potential issues in brain-computer interfaces [61]. This collaboration has resulted in an IRB-approved experiment being designed and built to demonstrate a potential privacy attack with a BCI application. While this experiment is ongoing and no results have been published yet, preliminary analysis done by Tamara suggest that BCIs indeed pose a privacy risk and can leak personal information. It likely would be beneficial for future implanted systems that stream neural data out of the body to include measures to protect patient privacy, but the exact methods to do so are still unexplored.

11.3 The Role of Ethics in Closed-Loop DBS Design

Often the barriers to medical devices becoming clinically used are often not technological but are instead often instead due to how society accepts new technology. In particular, I am interested in both the ethical issues that arise when considering the BCI-triggered DBS methods discussed throughout this thesis, where a patient can volitionally modulate their own stimulation settings using BCI techniques. This interest in non-technical barriers to the technologies proposed in this thesis lead to a collaboration with two students outside of my

discipline: philosophy student Timothy Brown and legal student Patrick Moore. Our discussions focused primarily on the issues surrounding volitional control and the applicability of these systems to individuals operating outside of the clinic in society.

In regards to the ethics of this new technology, I see closed-loop neurostimulation systems as a clear benefit over current static systems. For one, neurostimulators can interact with a patient's nervous system in such a way that can cause unpleasant side-effects. For these patients, selectively stimulating can often directly correspond to less time experiencing side-effects. Additionally, by conserving stimulation power to only the time needed, we can increase the time between battery-replacement surgeries. Reducing the need for surgery is a very direct reduction of physical harm for these patients. However, with bidirectional neuroprosthetics under the volitional control of the patient, I believe the ethical benefits are more than simply preventing patient harm. Instead I would like to consider patient well-being, which can be harder to quantify than most engineering considerations like power efficiency.

We have to consider the fact that our systems are playing an integral role in balancing and stabilizing a patient's brain, which to many is considered to be their innermost self. The impact of DBS on personality and personal autonomy has been a past cause for ethical debate around the treatment [62] [63], but the fact remains that for the patients who undergo DBS surgery there is of course no other option as the disease progresses. Still as our technological capacities have grown we, as a society, have consistently had to revisit how we treat patients. In the past, it was acceptable to treat patients with PD and ET by physically removing or killing tissue deep within the brain. This caused permanent and often dramatic side-effects in addition to not always being effective. With the rise of DBS, stimulation methods have become the method of choice because of all side-effects cease when stimulation is stopped and the stimulation is tunable on a per-patient and per-visit basis. While this works, it effectively puts the balancing act between therapy and side-effects in the hands of clinicians, with intermittent patient feedback playing a role in minor adjustments.

In the future, a BCI-enabled neuroprosthetics may have the ability to give patients

moment-to-moment control of their side-effects and control of their therapy. For any given moment they will be able to choose for themselves if they want to tremor while speaking better or if they need to turn on their stimulation to move even if it means they can not speak as well. This has the potential of dramatically improving the lives of patients by giving them back control of not just their bodies, but also their minds. This is potentially empowering technology that can enable patients to live with a higher quality of life than current systems.

Empowering individuals to have control over their own stimulation levels may restore their own personal responsibility for their actions. It is a known fact that a common side-effect of DBS for PD patients can often result in lower inhibition, which often manifests as gambling problems. If PD patients can instead modulate their DBS level to return to a more normal state of mind before making decisions, they then probably have a responsibility to do so.

However, while there are potential ethical advantages of such systems, there are equally just as many questions that they raise. Most PD and ET patients are elderly and many may not be able to learn to use a system as I have described so far. In this case, the clinician can of course use a device without neurological control, so perhaps it is their responsibility to determine if a patient is capable of making decisions about their stimulation. They already, in fact, do this for manual patient programmers. These manual patient programmers can be used to turn the device off while sleeping, but are too awkward and difficult to use on a moment-by-moment basis.

However, what happens if a clinician gives a patient volitional brain control of their own stimulation but the patient can not handle or appropriately use it? What if they then get in a car accident? Legally speaking is this any different than a patient with dementia getting into a car accident? What happens when a PD patient fails to modulate their stimulation level because they have already lost their inhibition? These are the sorts of questions we addressed through regular discussion. The results of this philosophical discussion, questions, and analysis of volitional bidirectional neuroprosthetics eventually coalesced into a paper that our group submitted to We Robot 2015 Conference on Robotics, Law and Policy [64].

In this paper, we discussed several hypothetical cases that could arise from BCI-triggered DBS technologies, focusing on the story of a hypothetical patient. The discussions are also being reworked for an upcoming IEEE Ethics submission by Tim Brown, which will focus more exclusively on the ethical considerations of these sort of devices and systems.

11.4 Final Thoughts

In conclusion, while I have fulfilled all of the aims that this thesis was meant to accomplish, there is an inordinate amount of future work. Neural prosthetics is a new field, and closed-loop neurostimulation systems are very new, with little prior work to build off of. While that has given me the benefit of being able to design exploratory systems and research platforms to aid in future work, it is also at times frustrating that we can do so little when it comes to proper control of symptoms. System dynamics are unknown and every patient is so unique that generalized methods will likely be the exception instead of the rule.

This is of course, what makes this work all the more important. In a field such as neuroprosthetics, collaboration across disciplines, clinics, and researchers is important because collaboration acts as a multiplier on the contributions an individual can make. I have tried to include this focus on collaboration in my approach to this thesis by focusing on platform development and enabling the research occurring at UW, Stanford, and UCSF.

AFTERWORD

As I move on to the next stage of my career, I hope to bring this focus on setting up collaborations with me so that I can continue to act as a force-multiplier for fascinating research happening in the neural engineering field. Ultimately, I see this is as the most effective way to aid researchers to improve the treatment of patients with neurological movement disorders. The continued advancement in our neural engineering capabilities is exciting not just to improve the lives of ET and PD patients though, but will instead drive forward the empowerment of individuals across a wide array of disorders and disabilities. It is tremendously exciting to work in this new and dynamic field with such potential to change the daily life of so many people, and I look forward to continuing my neural-engineering work.

BIBLIOGRAPHY

- [1] Günther Deuschl, Carmen Schade-Brittinger, Paul Krack, Jens Volkmann, Helmut Schäfer, Kai Bötzel, Christine Daniels, Angela Deutschländer, Ulrich Dillmann, Wilhelm Eisner, et al. A randomized trial of deep-brain stimulation for parkinson's disease. *New England Journal of Medicine*, 355(9):896–908, 2006.
- [2] Olof Sydow, S Thobois, F Alesch, and JD Speelman. Multicentre european study of thalamic stimulation in essential tremor: a six year follow up. *Journal of Neurology, Neurosurgery & Psychiatry*, 74(10):1387–1391, 2003.
- [3] Eliana Della Flora, Caryn L Perera, Alun L Cameron, and Guy J Maddern. Deep brain stimulation for essential tremor: a systematic review. *Movement Disorders*, 25(11):1550–1559, 2010.
- [4] Marie Vidailhet, Laurent Vercueil, Jean-Luc Houeto, Pierre Krystkowiak, Alim-Louis Benabid, Philippe Cornu, Christelle Lagrange, Sophie Tézenas du Montcel, Didier Dormont, Sylvie Grand, et al. Bilateral deep-brain stimulation of the globus pallidus in primary generalized dystonia. *New England Journal of Medicine*, 352(5):459–467, 2005.
- [5] Alexandre Gironell and Jaime Kulisevsky. Review: Diagnosis and management of essential tremor and dystonic tremor. *Therapeutic Advances in Neurological Disorders*, 2(4):215–222, 2009.
- [6] Joel S Perlmutter and Jonathan W Mink. Deep brain stimulation. *Annu. Rev. Neurosci.*, 29:229–257, 2006.
- [7] Alexis M Kuncel, Scott E Cooper, Barbara R Wolgamuth, Merlise A Clyde, Scott A Snyder, Erwin B Montgomery, Ali R Rezai, and Warren M Grill. Clinical response to varying the stimulus parameters in deep brain stimulation for essential tremor. *Movement disorders*, 21(11):1920–1928, 2006.
- [8] Adam O Hebb, Jun Jason Zhang, Mohammad H Mahoor, Christos Tsiokos, Charles Matlack, Howard Jay Chizeck, and Nader Pouratian. Creating the feedback loop: Closed-loop neurostimulation. *Neurosurgery Clinics of North America*, 25(1):187–204, 2014.

- [9] Medtronic. New Medtronic Deep Brain Stimulation System the First to Sense and Record Brain Activity While Delivering Therapy. <http://newsroom.medtronic.com/phoenix.zhtml?c=251324&p=irol-newsArticle&id=1845602>, 2013. Online; accessed March-2014.
- [10] Wolfgang Eberle, Julien Penders, and R Firat Yazicioglu. Closing the loop for deep brain stimulation implants enables personalized healthcare for parkinson’s disease patients. In *Annual International Conference of the IEEE Engineering in Medicine and Biology Society (EMBC)*, pages 1556–1558. IEEE, 2011.
- [11] Takamitsu Yamamoto, Yoichi Katayama, Junichi Ushiba, Hiroko Yoshino, Toshiki Obuchi, Kazutaka Kobayashi, Hideki Oshima, and Chikashi Fukaya. On-demand control system for deep brain stimulation for treatment of intention tremor. *Neuromodulation: Technology at the Neural Interface*, 16(3):230–235, 2013.
- [12] Alim L Benabid, P Pollak, D Hoffmann, C Gervason, M Hommel, JE Perret, J De Rougemont, and DM Gao. Long-term suppression of tremor by chronic stimulation of the ventral intermediate thalamic nucleus. *The Lancet*, 337(8738):403–406, 1991.
- [13] Svjetlana Miocinovic, Suvarchala Somayajula, Shilpa Chitnis, and Jerrold L Vitek. History, applications, and mechanisms of deep brain stimulation. *JAMA neurology*, 70(2):163–171, 2013.
- [14] David E Vaillancourt, Molly M Sturman, L Verhagen Metman, RAE Bakay, and DM Corcos. Deep brain stimulation of the vim thalamic nucleus modifies several features of essential tremor. *Neurology*, 61(7):919–925, 2003.
- [15] Medtronic. System Eligibility, Battery Longevity: Neurostimulation systems for deep brain stimulation. http://professional.medtronic.com/wcm/groups/mdtcom_sg/@mdt/@neuro/documents/documents/dbs-sys-longevity.pdf, 2010. Online; accessed July, 2014.
- [16] Julián Benito-León and Elan D Louis. Clinical update: diagnosis and treatment of essential tremor. *The Lancet*, 369(9568):1152–1154, 2007.
- [17] JP Hubble, KL Busenbark, R Pahwa, K Lyons, and WC Koller. Clinical expression of essential tremor: effects of gender and age. *Movement disorders*, 12(6):969–972, 1997.
- [18] Elan D Louis, Ruth Ottman, and W Allen Hauser. How common is the most common adult movement disorder? estimates of the prevalence of essential tremor throughout the world. *Movement disorders*, 13(1):5–10, 1998.

- [19] CM Tanner, SM Goldman, KE Lyons, DA Aston, JW Tetrud, MD Welsh, JW Langston, and WC Koller. Essential tremor in twins an assessment of genetic vs environmental determinants of etiology. *Neurology*, 57(8):1389–1391, 2001.
- [20] Elan D Louis. Etiology of essential tremor: should we be searching for environmental causes? *Movement disorders*, 16(5):822–829, 2001.
- [21] Rodger J Elble. Central mechanisms of tremor. *Journal of clinical neurophysiology*, 13(2):133–144, 1996.
- [22] Jan Raethjen, Michael Lindemann, Holger Schmaljohann, Roland Wenzelburger, Gerd Pfister, and Günther Deuschl. Multiple oscillators are causing parkinsonian and essential tremor. *Movement disorders*, 15(1):84–94, 2000.
- [23] Stefan F Bucher, Klaus C Seelos, Richard C Dodel, Maximilian Reiser, and Wolfgang H Oertel. Activation mapping in essential tremor with functional magnetic resonance imaging. *Annals of neurology*, 41(1):32–40, 1997.
- [24] Arif Dalvi and Michael G Mercury. Essential tremor not just a shake. *Disease-a-Month*, 57(3):127–134, 2011.
- [25] Elan D Louis. Essential tremor. *New England Journal of Medicine*, 345(12):887–891, 2001.
- [26] P Richard Schuurman, D Andries Bosch, Patrick MM Bossuyt, Gouke J Bonsel, Eus JW van Someren, Rob MA de Bie, Maruschka P Merkus, and Johannes D Speelman. A comparison of continuous thalamic stimulation and thalamotomy for suppression of severe tremor. *New England Journal of Medicine*, 342(7):461–468, 2000.
- [27] Simon Little and Peter Brown. What brain signals are suitable for feedback control of deep brain stimulation in parkinson’s disease? *Annals of the New York Academy of Sciences*, 1265(1):9–24, 2012.
- [28] Lonneke ML de Lau and Monique Breteler. Epidemiology of parkinson’s disease. *The Lancet Neurology*, 5(6):525–535, 2006.
- [29] Diane Whitmer, Camille De Solages, Bruce Hill, Hong Yu, Jaimie M Henderson, and Helen Bronte-Stewart. High frequency deep brain stimulation attenuates subthalamic and cortical rhythms in parkinson’s disease. *Frontiers in human neuroscience*, 6, 2012.

- [30] Stephen K Van Den Eeden, Caroline M Tanner, Allan L Bernstein, Robin D Fross, Amethyst Leimpeter, Daniel A Bloch, and Lorene M Nelson. Incidence of parkinsons disease: variation by age, gender, and race/ethnicity. *American journal of epidemiology*, 157(11):1015–1022, 2003.
- [31] Anette Schrag, Marjan Jahanshahi, and Niall Quinn. How does parkinson’s disease affect quality of life? a comparison with quality of life in the general population. *Movement Disorders*, 15(6):1112–1118, 2000.
- [32] Joseph Jankovic. Parkinsons disease: clinical features and diagnosis. *Journal of Neurology, Neurosurgery & Psychiatry*, 79(4):368–376, 2008.
- [33] Douglas J Gelb, Eugene Oliver, and Sid Gilman. Diagnostic criteria for parkinson disease. *Archives of neurology*, 56(1):33–39, 1999.
- [34] William Dauer and Serge Przedborski. Parkinson’s disease: mechanisms and models. *Neuron*, 39(6):889–909, 2003.
- [35] Alastair JJ Wood and Donald B Calne. Treatment of parkinson’s disease. *New England Journal of Medicine*, 329(14):1021–1027, 1993.
- [36] Werner Poewe, Angelo Antonini, Jan CM Zijlmans, Pierre R Burkhard, and François Vingerhoets. Levodopa in the treatment of parkinsons disease: an old drug still going strong. *Clinical interventions in aging*, 5:229, 2010.
- [37] Neeraj Kumar, Jay A Van Gerpen, James H Bower, and J Eric Ahlskog. Levodopa-dyskinesia incidence by age of parkinson’s disease onset. *Movement disorders*, 20(3):342–344, 2005.
- [38] Alim Louis Benabid. Deep brain stimulation for parkinsons disease. *Current opinion in neurobiology*, 13(6):696–706, 2003.
- [39] Pierre Pollak, Valérie Fraix, Paul Krack, Elena Moro, Alexandre Mendes, Stephan Chabardes, Adnan Koudsie, and Alim-Louis Benabid. Treatment results: Parkinson’s disease. *Movement Disorders*, 17(S3):S75–S83, 2002.
- [40] Y Chen, HW Hao, YX Hu, and LM Li. Wireless wrist-wearable wake/sleep identification device for closed-loop deep brain stimulation. *Electronics Letters*, 49(7):452–453, 2013.
- [41] Ishita Basu, Daniel Graupe, Daniela Tuninetti, Pitamber Shukla, Konstantin V Slavin, Leo Verhagen Metman, and Daniel M Corcos. Pathological tremor prediction using surface electromyogram and acceleration: potential use in ‘on-off’ demand driven deep brain stimulator design. *Journal of Neural Engineering*, 10(3):036019, 2013.

- [42] AG Rouse, SR Stanslaski, Peng Cong, RM Jensen, Pedram Afshar, Dave Ullestad, R Gupta, GF Molnar, DW Moran, and TJ Denison. A chronic generalized bi-directional brain–machine interface. *Journal of neural engineering*, 8(3):036018, 2011.
- [43] Boris Rosin, Maya Slovik, Rea Mitelman, Michal Rivlin-Etzion, Suzanne N Haber, Zvi Israel, Eilon Vaadia, and Hagai Bergman. Closed-loop deep brain stimulation is superior in ameliorating parkinsonism. *Neuron*, 72(2):370–384, 2011.
- [44] Pedram Afshar, Ankit Khambhati, Scott Stanslaski, David Carlson, Randy Jensen, Dave Linde, Siddharth Dani, Maciej Lazarewicz, Peng Cong, Jon Giftakis, et al. A translational platform for prototyping closed-loop neuromodulation systems. *Frontiers in neural circuits*, 6:117, 2012.
- [45] Simon Little, Alex Pogosyan, Spencer Neal, Baltazar Zavala, Ludvic Zrinzo, Marwan Hariz, Thomas Foltynie, Patricia Limousin, Keyoumars Ashkan, James FitzGerald, et al. Adaptive deep brain stimulation in advanced parkinson disease. *Annals of neurology*, 74(3):449–457, 2013.
- [46] Sabato Santaniello, Giovanni Fiengo, Luigi Glielmo, and Warren M Grill. Closed-loop control of deep brain stimulation: a simulation study. *IEEE Transactions on Neural Systems and Rehabilitation Engineering*, 19(1):15–24, 2011.
- [47] LG Electronics. Technical specifications of the LG G Watch. <http://www.lg.com/us/smart-watches/lg-W100-g-watch/technical-specifications>, 2014. Online; accessed June-2015.
- [48] Mahsa Malekmohammadi, Jeffrey Herron, Anca Velisar, Zack Blumenfeld, Megan Trager, Howard Jay Chizeck, and Helen Bronte-Stewart. Kinematic adaptive deep brain stimulation for resting tremor in parkinsons disease. *Movement Disorders*, 2016.
- [49] Jeffrey Herron, Tim Denison, and Howard Jay Chizeck. Closed-loop dbs with movement intention. In *7th International IEEE/EMBS Conference on Neural Engineering*, pages 844–847. IEEE, 2015.
- [50] G Pfurtscheller and A Berghold. Patterns of cortical activation during planning of voluntary movement. *Electroencephalography and clinical neurophysiology*, 72(3):250–258, 1989.
- [51] Camilo Toro, Günther Deuschl, Robert Thatcher, Susumu Sato, Conrad Kufta, and Mark Hallett. Event-related desynchronization and movement-related cortical potentials on the ecog and eeg. *Electroencephalography and Clinical Neurophysiology/Evoked Potentials Section*, 93(5):380–389, 1994.

- [52] Herbert Ramoser, Johannes Muller-Gerking, and Gert Pfurtscheller. Optimal spatial filtering of single trial eeg during imagined hand movement. *IEEE Transactions on Rehabilitation Engineering*, 8(4):441–446, 2000.
- [53] Andrea L Crowell, Elena S Ryapolova-Webb, Jill L Ostrem, Nicholas B Galifianakis, Shoichi Shimamoto, Daniel A Lim, and Philip A Starr. Oscillations in sensorimotor cortex in movement disorders: an electrocorticography study. *Brain*, page awr332, 2012.
- [54] Dennis J McFarland, Lynn M McCane, Stephen V David, and Jonathan R Wolpaw. Spatial filter selection for eeg-based communication. *Electroencephalography and clinical Neurophysiology*, 103(3):386–394, 1997.
- [55] Scott Stanslaski, Pedram Afshar, Peng Cong, Jon Giftakis, Paul Stypulkowski, Dave Carlson, Dave Linde, Dave Ullestad, A-T Avestruz, and Timothy Denison. Design and validation of a fully implantable, chronic, closed-loop neuromodulation device with concurrent sensing and stimulation. *IEEE Transactions on Neural Systems and Rehabilitation Engineering*, 20(4):410–421, 2012.
- [56] A-T Avestruz, Wesley Santa, Dave Carlson, Randy Jensen, Scott Stanslaski, Alan Helfenstine, and Tim Denison. A 5 w/channel spectral analysis ic for chronic bidirectional brain-machine interfaces. *IEEE Journal of Solid-State Circuits*, 43(12):3006–3024, 2008.
- [57] Jeffrey Herron and Howard Jay Chizeck. Prototype closed-loop deep brain stimulation systems inspired by norbert wiener. In *IEEE Conference on Norbert Wiener in the 21st Century*, pages 1–6. IEEE, 2014.
- [58] Helen Brontë-Stewart, Stephanie Louie, Sara Batya, and Jaimie M Henderson. Clinical motor outcome of bilateral subthalamic nucleus deep-brain stimulation for parkinson’s disease using image-guided frameless stereotaxy. *Neurosurgery*, 67(4):1088–1093, 2010.
- [59] Helen Bronte-Stewart, Crista Barberini, Mandy Miller Koop, Bruce C Hill, Jaimie M Henderson, and Brett Wingeier. The stn beta-band profile in parkinson’s disease is stationary and shows prolonged attenuation after deep brain stimulation. *Experimental neurology*, 215(1):20–28, 2009.
- [60] Tamara Bonaci, Ryan Calo, and Howard Jay Chizeck. App stores for the brain: Privacy & security in brain-computer interfaces. In *IEEE International Symposium on Ethics in Engineering, Science, and Technology*, 2014.

- [61] Tamara Bonaci, Jeffrey Herron, Charlie Matlack, and Howard Jay Chizeck. Securing the exocortex: A twenty-first century cybernetics challenge. In *IEEE Conference on Norbert Wiener in the 21st Century*, 2014.
- [62] Laura Klaming and Pim Haselager. Did my brain implant make me do it? questions raised by dbs regarding psychological continuity, responsibility for action and mental competence. *Neuroethics*, 6(3):527–539, 2013.
- [63] Felicitas Kraemer. Authenticity or autonomy? when deep brain stimulation causes a dilemma. *Journal of medical ethics*, pages medethics–2011, 2013.
- [64] Patrick Moore, Tim Brown, Jeffrey Herron, Margaret Thompson, Tamara Bonaci, Sara Goering, and Howard Jay Chizeck. Personal responsibility in the age of user-controller neuroprosthetics. In *We Robot 2015 Conference on Robotics, Law & Policy*, 2015.